

Response to Interactive comment by Anonymous Referee #1

Comments from the referee are printed in black. **Authors' responses are printed in red.**

The authors perform a set of numerical experiments to investigate the shape of the transit time distribution for a watershed under different catchment and climate characteristics. They focused mainly the role of soil depth, soil hydraulic conductivity, antecedent soil moisture content and subsequent precipitation amount, but other runs explored also soil porosity, bedrock hydraulic conductivity, depth dependence of the soil hydraulic conductivity and precipitation frequency. The ambitious goal of the article is to relate the shape (i.e., parameters) of common probability density functions (the AD, Gamma, and Beta distributions) to the variability of catchment and climate characteristics.

Exactly.

The paper is well written, with a simple structure that makes it easy to follow. Of course, they authors could not explore the role of all parameters, but the analysis is yet very inclusive overall. All the details that necessary to reproduce the work are explained in detail, and the presentation and discussion of the results are comprehensive.

We want to thank referee #1 for the assessment of our manuscript and a thoughtful review that led to a significant improvement of the study.

However, I have both some major and minor questions that I would ask the authors.

The major question is mostly conceptual. The authors aim at finding general results about the TTD shape variability across locations with different characteristics. I like their systematic approach as an attempt to quantify this variability, e.g. by linking alpha to F. However, I am not surprised that they could only partly achieve their goal.

The issue is that the authors assume a given distribution (e.g., the gamma) for each run. This is analogous to assume that the discharge depends only on the residence time of the water, and not on the water storage. In other words, the authors do not move away from the assumptions behind the instantaneous unit hydrograph approach. From a mathematical standpoint, other authors introduced this assumption by stating that the storage selection function or the loss function (e.g., Botter, 2011; Calabrese and Porporato, 2015) depend on only the residence time (or age). This, however, is the simplest scenario and the farthest from reality. It is very likely, in fact, that if the authors injected the tracer later in the simulation, the TTDs would again differ.

As an example, a more realistic assumption would be to somewhat include a dependence of the TTDs on the overall water storage, or some proxy for it. I think it would be very instructive to explore the dependence of time dependent TTDs parameters on the time dependent water storage. As I mentioned earlier, I still believe that their analysis is very insightful. It is only that,

in my opinion, this work could be even more impactful. I wonder whether the authors have comments on this.

This is a very valid point that we hope to address by examining the influence of antecedent moisture content on the shape of TTDs. We believe that the antecedent moisture content of the soil is a proxy for the water storage of the catchment (the bedrock is almost permanently fully saturated). We agree that a tracer injection at a different point in time would cause the TTD shape to differ (depending to a much higher degree on the current antecedent soil moisture content than on the pattern of following precipitation). In section 3.2 (figure 6, panel in the upper left corner) we analyze the dependence of time dependent TTD parameters on the time dependent water storage. You can see that, e.g., for situations when the water storage is high, K_S has a higher influence on TTDs than when water storage is low, while the relative influence of P_{sub} is larger when the initial water storage is low. In the revised manuscript we have clarified Figure 6 and improve its discussion in the text.

I also have some minor questions/comments.

-It seems that boundary conditions, mainly I am referring to the shape of control volume, may have a big effect on TTDs, perhaps that could partly overwhelm the effect of the parameters studied by the authors. Have the authors tested this (e.g., with a non-elliptical shape)?

Again, a valid point that we had not tested yet. Catchment shape was one of the properties we also thought could potentially influence the TTD shape but chose to investigate at a later point in a different study (like, e.g., catchment size or slope). However, after your remarks we decided to try out two additional catchment shapes to get an idea whether it would have a significant impact on the results. So we tested one catchment with the center of gravity located farther away from the outlet and another catchment with the center of gravity located closer to the outlet (catchment size and slope staying the same in all cases). We found that changing the catchment shape had substantially less influence on the TTD shape than we expected. We have added this analysis to the manuscript.

-I don't agree with repeating the one year precipitation time series in loop 32 times. First, it is not realistic, and second it might cause some statistical bias. Why not using a Poisson generator throughout the analysis? It would certainly be more consistent. On a different note, there are numerous references that introduced Poisson rainfall/storm. One of the first was Cox and Isham (1988).

Thanks for the additional reference, we have added it to the manuscript. In order to erase your worries about looping the time series we did what you suggested and created a 33 year time series with a Poisson generator. The resulting TTDs did not differ significantly from the ones we derived from the looped time series. We have added a comment on this to the manuscript and a figure to the supplement.

-The authors believe that a truncated Gamma or a lognormal distribution may work better over the all range of ages. Why not trying it?

Ok, following your suggestion we conducted this analysis. The truncated lognormal distribution did indeed capture almost all of the TTD shapes better. Additionally we also tested the regular (i.e. not truncated) lognormal distribution and found that it is a better representation for the shape of TTDs in catchments with high K_s than the advection-dispersion distribution. To reflect the results of these new analyses we modified our results and discussion sections accordingly in the revised manuscript.

Hoping that these comments may help improve the manuscript, I suggest major revisions.
Thanks again for the valuable input that helped to improve our paper.

Botter, Gianluca, Enrico Bertuzzo, and Andrea Rinaldo. "Catchment residence and travel time distributions: The master equation." *Geophysical Research Letters* 38.11 (2011).

Calabrese, Salvatore, and Amilcare Porporato. "Linking age, survival, and transit time distributions." *Water Resources Research* 51.10 (2015): 8316-8330.

Cox, David Roxbee, and Valerie Isham. "A simple spatial-temporal model of rainfall." *Proceedings of the Royal Society of London. A. Mathematical and Physical Sciences* 415.1849 (1988): 317-328.

Response to Interactive comment by Anonymous Referee #2

Comments from the referee are printed in black. **Authors' responses are printed in red.**

The manuscript presents and discusses an interesting analysis based on virtual (numerical) experiments on the TTD in small catchments / hillslopes. The work is interesting and well done and it touches a relevant topic, namely the identification of the leading components and parameters in the definition of TTDs. The approach is rather "classic" in the sense that the analysis is somewhat based on the concept of time invariant TTD, while recent approaches have shown the importance of other metric, like e.g. the backward TT distributions, for a comprehensive description of water age and contaminant dynamics. Still, the analysis is useful and instructive.

We want to thank referee #2 for the assessment of our manuscript and a detailed and thoughtful review that led to a significant improvement of the study. We would like to point out that in our opinion the concept of 'time variability' is implemented in this study since factors causing time variability of TTDs are either changes in catchment storage (e.g. antecedent soil moisture) or changes in atmospheric forcing (like precipitation amount). Of course, there are also other/more factors causing time variability we have not explored yet (e.g. erosion, vegetation, different precipitation patterns).

Perhaps the manuscript is too long and involved at times, with plenty of text (with some verbosity) and figures. See for instance the long Conclusion section (and it is the first time I see a subsection there...). I think that this might be detrimental to the work as the reader can easily get lost in the many details and miss the important aspects. Thus, I suggest further distilling the principal results, moving the details that are not important for the storyline in the supplementary material and concentrate on the main results that the Authors want to convey. This would strengthen the message of the work and its diffusion.

A very valid observation. We have struggled with exactly the problem the referee describes. In the revised manuscript we have condensed the conclusion, restructured the results and discussion sections and moved more of the details to the supplement.

With so many fine details, I miss a description of the physical processes, as observed in the model runs, which determine the TTD. What is the impact of subsurface stormflow? Saturated and unsaturated flows? Groundwater? This is important in order to explain the impact of the parameters examined.

We have tried to always include explanations of the physical processes that play a role in shaping the TTDs for the different scenarios. Apparently that effort was insufficient in certain places. We have added more details on the description of the physical processes in the results and discussion sections of the revised manuscript.

In the following a few specific comments.

- Line 38. I would also cite the pioneer works by Niemi (1977) and Nauman (Residence time distribution theory for unsteady stirred tank reactors, Chemical Engineering Science, 1969).
Thanks for the additional references. It is very hard to get a comprehensive overview of the pioneering work. Niemi is already cited, we have added Nauman (1969).

- Line 55-57. Here the introduction moves to the field of groundwater hydrology, where the issue of the BTC tailing (power-law or not) has been the subject of intense discussions in the last 2 decades or so; this short text and citation does not even scratch the surface and it looks quite superficial here.
In order to avoid the surface scratching, we have done more research on groundwater breakthrough curves and added more references.

- Line 57: The sentence of the “great” underestimation of mass is very much debatable, in most cases it’s a tiny fraction of the total mass. It may be important for risk assessment of highly toxic compounds, but uncertainty is anyway very large there.
Agreed 100%. We have made clear that it might not be relevant from a mass balance perspective (but possibly when conducting a risk assessment).

- mTT: please define it (I guess it’s mean TT)
You are correct. We define it at the first mention (line 64).

- Line 94-95. This sentence is repeated in other parts of the manuscript. By definition such approach cannot “completely” erase differences. The question is whether the approximation is good enough for applications. The study by Ali et al (A comparison of travel-time based catchment transport models, with application to numerical experiments, JoH 2014) shows that in many cases it does the job, also considering the several sources of uncertainty, including for instance the estimation of ET (not done here).
We have added the reference to Ali et al. (2014) and discuss your point.

- Lines 137-139. Unfortunately the effective hydraulic conductivity cannot replace the dispersive effects of the distributed macropores because it only impacts the mean velocity. I would delete this sentence as it is not needed: the exclusion of such component is legitimate and meaningful in my view because of the important role of macrodispersion in the TTD determination.
Thank you for the constructive comment. We have proceeded as suggested.

- Line 159. vertical or hortogonal to the slope? I guess the latter.
It is indeed vertical and not orthogonal to the slope (but that makes only a small difference).

- Line 163. 5m of dispersivity is quite a lot, even more so for the vertical one. Why the choice? In this case the inclusion of D_{free} looks irrelevant.
The longitudinal dispersivity and lateral dispersivity were estimated with regard to the length scale of the model catchment (100 m). $\alpha_L \approx 5$ m were estimated using the relation between the

longitudinal dispersivity and length scale described in Gelhar et al., 1992 and Schulze-Makuch, 2005 (regression $\alpha = 0.085 \cdot L^{0.81}$). We agree that the free-solution diffusion is significantly smaller than the dispersion and could have been neglected. We have clarified this in the manuscript adding the references [Gelhar et al., 1992] and [Schulze-Makuch, 2005].

References:

Gelhar, L.W., Welty, C., Rehfeldt, K.R., 1992. A critical review of data on field-scale dispersion in aquifers. *Water Resources Research* 28 (7), 1955–1974.

Schulze-Makuch, D. (2005). Longitudinal dispersivity data and implications for scaling behavior. *Groundwater*, 43(3), 443-456.

- Lines 174-175. What head is provided in the boundary condition? Where is the water table located? This is quite important.

Thanks for catching that. I thought I would have written it somewhere. We have added information on the location of the head (it is equal to the surface elevation).

- Line 204. What is the “subsequent precipitation amount”?

Clarified (essentially a measure of the amount of precipitation after the delivery of the tracer).

- Line 214. I guess that mm/a means mm/y

Yes, HESS officially prefers this abbreviation.

- Line 214. Please provide more details on the rainfall time series, e.g. regime, climate etc. As a matter of fact TTD depends also on the rainfall regime, not only the total rainfall per year (e.g. Botter et al 2010).

We agree it is correct that the TTD also depends on the distribution of rainfall. We investigate the influence of different precipitation event frequencies. The precipitation time series we used has the following properties: Average interarrival time: 2.64 days; Average event duration: 3.17 days. The climate in the north west of Germany can be described as maritime temperate (Cfb in the Köppen classification) Maximum precipitation falls usually in June (65 mm), minimum in February (28 mm). We have added this information to the manuscript.

- Line 338. I don't like the definition, I would rather speak of “The Inverse Gaussian distribution, with parameters D , ..., that is a particular solution of the Advection Dispersion Equation”. AD is misleading, as ADE can have several different solutions.

We would like to follow your suggestion. We have reformulate the description in the following way:

1) The inverse Gaussian distribution with dispersion parameter D (dimensionless) and mean mTT (d) that is a particular solution of the advection dispersion equation (Eq. 6):

- Line 401. This discussion is based on log-log plots, which many times are misleading. The convergence of curves at large time can be an artifact of the plots.

It is correct that log-log plot can make large differences at large times appear smaller. However, they also exaggerate small differences at short times. In this particular case we are interested more in the short time differences because we expect the largest differences at the beginning of the TTDs. At late times, differences are averaged out more and more.

- Line 408-409. Differences seems larger to me. Again, the log-log plot does not help. We double-checked the numbers and they are correct. The fact that the differences seem larger is probably due to the very high resolution of the log-log plot for short and very short times.

- Section 3.3. Some of the (interesting) conclusions here are very similar to those of Fiori et al (Stochastic analysis of transport in hillslopes: Travel time distribution and source zone dispersion, WRR 2009) which I think is important for this work. There, the different parts of the Gamma distribution pertains to different mechanisms and parameters (soil, bedrock, etc.). The main difference is that they identify the important role of KBr in the behavior of the tail, which is the exponential part of the Gamma, which in turn is related to groundwater discharge. The aquifer volume, which depends on water table, thickness and slope, has an important role here. Thank you for pointing us to this reference. It is indeed a very interesting study that we were not aware of yet. In the revised manuscript have included it.

- Line 490. I don't see the power law. We are aware of the fact that straight lines in log-log plots are necessary for identifying power laws but insufficient as evidence. So you are right, we cannot be sure whether they are actually power laws just from this graphical analysis. Therefore we have changed our focus away from the power-law towards the characteristic break in the slope where the tail part begins.

- Line 510. How is the fitting done? What inference methods? How one can say that a distribution performs better than another? Any statistical test? In Section 2.4.3 (Fitting) we describe the procedure. It was done by the least squares method on the cumulative distributions.

- Line 668. I don't agree with this analysis, the presumed power-law tail covers less than one logscale. Also, identification of power law tails is not simple (see e.g. Pedretti and Bianchi, Reproducing tailing in breakthrough curves: Are statistical models equally representative and predictive? AWR 2018), the emergence of a (short) straight line in a log-log plot may not be enough. At any rate, I would not say that the inadequacy of the distributions in fitting the TTD is because of the tail, that by the way involves a tiny fraction of the mass, which is magnified by the log-log representation. I think that the issue of powerlaw tails is too much emphasized here. We agree with your comment. We have changed our description of the TTD tail behavior (now we just describe the fact that the tails begin with a sudden break in the slope of the TTD and continue from there on as straight lines on a log-log plot). It's also clear that the tails are not relevant in terms of the total mass balance and will hardly be noticed for most solutes – with the exception of highly toxic pollutants. We have made sure to stress this in the revised manuscript.

- Section 4.2. This part is not entirely convincing, I can't see the validity of the prediction based on F. By the way the latter does not include other relevant ingredients, like e.g. KBr.

We understand your concerns. This section is not meant to represent to full and complete truth about TTD shapes. It is rather an attempt to find some structure in the way TTD shapes change with certain parameters, an attempt to explore overarching principles. Many of the potential shape-controlling parameters are still excluded from this analysis (like KBr). We have tried to put more emphasis on this interpretation of our results in the revised manuscript.

- Line 750. Again, the method cannot erase "all" differences, but perhaps is adequate for many applications.

Agreed. We have added this remark to the revised manuscript.

- Conclusion section. It is too long, one cannot see immediately the main results of the work. It's a pity because there is a lot of interesting material, that however needs to be better distilled and conveyed.

There is definitely room for improvement in the conclusion section. We agree with your criticism and we have done our best to condense, restructure and clarify the conclusions in the revised manuscript. To this end we moved a lot of text from the conclusion to the results and discussion sections.

- Line 754-755. "...it is possible to predict the change using the dimensionless flow path number F.". At the third line of the Conclusion section this seems the major conclusion of the work. Is it so? It does not seem like after reading the text.

This can indeed be considered the main conclusion of our work. We have made sure that this outcome is conveyed better in the revised conclusion section.

Response to Interactive comment by Anonymous Referee #3

Comments from the referee are printed in black. Authors' responses are printed in red.

This is an interesting paper that describes the relationships between transit time distributions and catchment characteristics. This manuscript is a modeling study for which the authors use a state-of-the-art 3 dimensional saturated unsaturated zone and surface water model. They vary several catchment characteristics and evaluate how this affects the transit time distribution. Moreover they characterize catchment behavior and transittimes using characteristic numbers such as the flowpath number F. The manuscript is well written and mostly easy to read, literature is extensively cited. Maybe the manuscript is long and could be shortened in some sections to gain more impact(17 figures and 9 tables are hard to take in).

Thank you for reading and evaluating our manuscript. We fully agree that it is long and that it would benefit from further condensing certain sections. We have already shortened it considerably in the past and have made another effort to achieve this.

Having noted this, I must also admit that it is clear that a lot of time, effort and attention has been put into this manuscript. The many variables that have been tested make the results section a bit of a struggle to read and fully digest. The discussion and conclusions do highlight the most important findings effectively. The conclusion could even be further shortened.

Thank you also for acknowledging the effort we put into this research. It started small but grew into this large study comprising more and more of the relevant catchment and climate properties. Still, it is far from being complete (there are still more parameters to test and analyze). We have make another effort to streamline the results section better in the revised manuscript and to shorten the conclusion to the most important take-away messages (moving more of the less important findings to the supplement).

I have no major objections to this manuscript and think it could be published with minor revisions. I do wonder why the authors decided to present all their analyses on the transient traveltime distributions instead of the cumulative outflow as mention in section 4.3, which in my opinion would give a results that is less dependent on the precise rainfall sequence?

The decision to plot the TT probabilities against the actual transit time instead of the cumulative outflow is mainly based on the desire to work with TTDs that are 'real' in order to get an impression of how they would look like and change their shape in real-world catchments. Also, we could not have investigated the influence of precipitation frequency or the influence of different precipitation patterns/sequences with the cumulative outflow method.

Most interestingly I found that an advection-diffusion based model (mostly darcaïn) does only under strict conditions yield TTD's that can be described accurately with advection-dispersion TTDs. Therefore a gamma-distribution is not only an effect of preferential flow paths and dual porosity, but also of flowpath-storage relationships as indicated with the flowpath number.

Thank you for pointing this out. Actually, based on another reviewers comment we additionally tested lognormal and truncated lognormal distributions to fit the modeled TTDs. We found that the lognormal distributions capture the TTD shapes in many cases better than the AD distributions.

Minor comments Figure 11: why does panel D have curved lines while all the others are straight. If you look closely, you can see that the lines in panel A are also slightly curved. This is due to the fact that both P_{sub} and θ_{ant} have three different modes (large, medium, small and wet, intermediate, dry) while D_{soil} and K_S have both only two modes.

Figure 6. I think the order of the legend does not correspond with the panels. But this figure is really hard to understand. For example the center front panel shows “no condition”, but still it causes a decrease in traveltime. (y axis). So the decrease is relative to what? All the different colors and linetypes make it hard to understand.

Agreed. This is a very complex figure that is hard to understand. We have made another effort to make it clearer and simpler (also adding more explanation in the text and in the caption). We double-checked and all the different colors and line types are indeed correct (also the order in the legends).

Figure 9 and 10: Fig 9 I don't understand why the alpha-plot has no dashed symbols and the D-plot has no solid symbols. This also doesn't seem to match with fig. 10 that has both dashed and solid symbols?

This correct observation is due to the fact that we recommend using gamma distributions for catchments with low hydraulic conductivity (solid) and Log-normal distributions for catchments with high hydraulic conductivity (dashed). In figure 10 we show relationships for all (low and high K_S) scenarios.

Line 685: not fully sure what you mean to say with “-but only taking”. I suggest to replace it with “and use”

Good suggestion. We have modified this section anyways due to the new results we received from the fitting of the lognormal distributions.

Line 701. Available storage > storage change. Here I miss the timescale. Do you refer to yearly storage change?

The timescale is the combined average interevent and event duration (~5 days). A much shorter time scale – compared to the yearly storage change – that makes F more variable/responsive in time. We have added this information to the manuscript.

Line 701 more water than it can remove (yearly or daily or hourly?) I think you need some kind of characteristic timescale here to define these definition (probably closely related to flowpath number F?) similar in figure 9.

Yes, we have added the characteristic time scale (combined average interevent and event duration) to the description.

Line 760 “where” or “when”?

When sounds indeed better. Thanks.

On the shape of forward transit time distributions in low-order catchments

Ingo Heidbüchel¹, Jie Yang¹, Andreas Musolff¹, Peter Troch², Ty Ferré², Jan H. Fleckenstein¹

¹Department of Hydrogeology, Helmholtz Centre for Environmental Research – UFZ, Leipzig, 04318, Germany

²Department of Hydrology and Atmospheric Sciences, University of Arizona, Tucson, 85721, USA

Correspondence to: Ingo Heidbüchel (ingo.heidbuechel@ufz.de)

Abstract. Transit time distributions (TTDs) integrate information on timing, amount, storage, mixing and flow paths of water and thus characterize hydrologic and hydrochemical catchment response unlike any other descriptor. Here, we simulate the shape of TTDs in an idealized low-order catchment investigating whether it changes systematically with certain catchment and climate properties. To this end, we used a physically-based, spatially-explicit 3-D model, injected tracer with a precipitation event and recorded the resulting TTDs at the outlet of a small (~6000 m²) catchment for different scenarios. We found that the TTDs can be subdivided into four parts: 1) early part – controlled by soil hydraulic conductivity and antecedent soil moisture content, 2) middle part – transition zone with no clear pattern or control, 3) later part – influenced by soil hydraulic conductivity and subsequent precipitation amount and 4) very late tail of the breakthrough curve – governed by bedrock hydraulic conductivity. The modeled TTD shapes can be predicted using a dimensionless number: higher initial peaks are observed if the inflow of water to a catchment is not equal to its capacity to discharge water via subsurface flow paths, lower initial peaks are connected to increasing available storage. In most cases the modeled TTDs were humped with non-zero initial values and varying weights of the tails. Therefore, none of the best-fit theoretical probability functions could exactly describe the entire TTD shape. Still, we found that generally the Gamma and the ~~Log-normal Advection-Dispersion~~ distribution work better for scenarios of low and high soil hydraulic conductivity, respectively.

1. Introduction

Transit time distributions (TTDs) characterize hydrologic catchment behavior unlike any other function or descriptor. They integrate information on timing, amount, storage, mixing and flow paths of water and can be modified to predict reactive solute transport (van der Velde et al., 2010; Harman et al., 2011; Musolff et al., 2017; Lutz et al., 2017). If observed in a time series, TTDs bridge the gap between hydrologic response (celerity) and hydrologic transport (velocity) in catchments by linking them via the change in water storage and the varying contributions of old (pre-event) and young (event) water to streamflow (Heidbüchel et al., 2012). TTDs are time and space-variant and hence no TTD of any individual precipitation event completely resembles another one. Therefore, in order to effectively utilize TTDs for the prediction of, e.g., the effects of pollution events or water availability, it is necessary to find ways to understand and systematically describe the shape and scale of TTDs so that they are applicable in different locations and at different times. In this paper we look for first order principles that describe

30 how the shape and scale of TTDs change, both spatially and temporally. This way we hope to improve our understanding of
31 the dominant factors affecting hydrologic transport and response behavior at the catchment scale.

32 1.1. Initial use of theoretical probability distributions

33 Since the concept of TTDs was introduced, many studies have reported on their potential shapes and sought ways to describe
34 them with different mathematical models like, e.g., the piston-flow and exponential models (Begemann and Libby, 1957;
35 Eriksson, 1958; Nauman, 1969), the advection-dispersion model (Nir, 1964; Małozzewski and Zuber, 1982) and the two
36 parallel linear reservoirs model (Małozzewski et al., 1983; Stockinger et al., 2014). Dinçer et al. (1970) were the first to
37 combine TTDs for individual precipitation events via the now commonly used convolution integral.

38 Early studies reported that the outflow from entire catchments is characterized best with the exponential model (Rodhe et al.,
39 1996; McGuire et al., 2005). However, neither the advection-dispersion nor the exponential model is able to capture the
40 observed heavy tails of the solute signals in the streamflow (Kirchner et al., 2000). Instead, the more heavy-tailed TTDs
41 created by advection and dispersion of spatially distributed rainfall inputs traveling toward the stream can be modeled with
42 TTDs resembling Gamma distributions (Kirchner et al., 2001). Likewise, tracer time series from many catchments exhibit
43 fractal 1/f scaling, which is consistent with Gamma TTDs with shape parameter $\alpha \approx 0.5$ (Kirchner, 2016). Gamma distributions
44 are quite flexible and can take on very different shapes when α is changed: $\alpha < 1$, highly skewed distributions with initial
45 maximum and heavier (i.e. sub-exponential) tails; $\alpha = 1$, exponential distribution; $\alpha > 1$, less skewed, "humped" distributions
46 with initial value of 0, a mode and lighter tails (see Fig. S9 in the supplement for examples). Gamma distributions can be
47 stretched or compressed with a scale parameter (β) and their mean is the product of α and β . Thus when using Gamma
48 distributions for the determination of mean transit times (mTTs), it is necessary to choose the correct shape parameter α to
49 avoid problems of equifinality.

50 1.2. General observations on the shape of TTDs

51 General observations on TTD shapes from the application of conceptual and physically-based models we know include that
52 individual TTDs for individual precipitation events are highly irregular and that they can rapidly change in time for
53 successive precipitation events (van der Velde et al., 2010; Rinaldo et al., 2011; Heidbüchel et al., 2012; Harman and Kim,
54 2014). If the early part of TTDs (mainly controlled by unsaturated transport in the soil layer) resembles a power law while the
55 subsoil is responsible for the exponential tailing, the combination of those two parts can result in TTD shapes that are similar
56 to Gamma distributions (Fiori et al., 2009). In the field of groundwater hydrology there have been intense discussions on the
57 tailing of break through curves (e.g. on the issue of whether they follow a power-law or not) (Haggerty et al., 2000; Becker
58 and Shapiro, 2003; Zhang et al., 2007; Pedretti et al., 2013; Fiori and Becker, 2015; Pedretti and Bianchi, 2018). For radial
59 flow to a well Pedretti et al. (2013) simulated that given strong contrasts of hydraulic conductivity between aquifer layers,
60 TTDs tend to have power law tails with unit slope that breaks down at very late times. If disregarded, these heavy tails can
61 constitute a significant problem when using TTDs to predict solute transport because the legacy of contamination can be

Kommentiert [IHh1]: - Line 38. I would also cite the pioneer works by Niemi (1977) and Nauman (Residence time distribution theory for unsteady stirred tank reactors, Chemical Engineering Science, 1969).
Answer: Thanks for the additional references. It is very hard to get a comprehensive overview of the pioneering work. Niemi is already cited, we have added Nauman.

Kommentiert [IHh2]: - Line 57: The sentence of the "great" underestimation of mass is very much debatable, in most cases it's a tiny fraction of the total mass. It may be important for risk assessment of highly toxic compounds, but uncertainty is anyway very large there.
Answer: Agreed 100%. We have made clear that it might not be relevant from a mass balance perspective (but possibly when conducting a risk assessment).

Kommentiert [IHh3]: - Line 55-57. Here the introduction moves to the field of groundwater hydrology, where the issue of the BTC tailing (power-law or not) has been the subject of intense discussions in the last 2 decades or so; this short text and citation does not even scratch the surface and it looks quite superficial here.
Answer: In order to avoid the surface scratching, we have done some more research on groundwater breakthrough curves and added more references.

62 ~~greatly underestimated (not so much from a total mass balance perspective but when providing risk assessments for highly~~
63 ~~toxic pollutants reaching further into the future). Hence, a~~ truncation of heavy TTD tails should be avoided, ~~especially. Also,~~
64 ~~when computing using transfer function models the computed mean transit times (mTTs) since they are~~ highly sensitive to
65 the shape of the chosen transfer function (Seeger and Weiler, 2014) ~~with the poorly identifiable tails greatly influencing the~~
66 ~~mTT estimates.~~ Further complicating matters are special cases of bimodal TTDs that can be caused by varying contributions
67 from fast and slow storages (McMillan et al., 2012) or from urban and rural areas (Soulsby et al., 2015). Apart from individual
68 catchment and event properties, mixing assumptions also affect TTD modeling since certain TTD shapes are inherently linked
69 to specific mixing assumptions (e.g. a well-mixed system is best represented by an exponential distribution, partial mixing can
70 be approximated with Gamma distributions and no mixing with the piston-flow model) (van der Velde et al., 2015).

71 1.3. Controls on shape variations

72 A number of studies reported on the best-fit shape of Gamma distributions generally ranging from α 0.01 to 0.90 (Hrachowitz
73 et al., 2009; Godsey et al., 2010; Berghuijs and Kirchner, 2017; Birkel et al., 2016) which indicates L-shaped distributions
74 with high initial values and heavier tails. Several studies found that α values decrease with increasing wetness conditions (e.g.,
75 Birkel et al., 2012; Tetzlaff et al., 2014) causing higher initial values and heavier tails. However, the opposite was observed in
76 a boreal headwater catchment (Peralta-Tapia et al., 2016) where α ranged between 0.43 and 0.76 for all years except the wettest
77 year ($\alpha = 0.98$). In the Scottish highlands α showed little temporal variability (and therefore no relation to precipitation
78 intensity) but was closely related to catchment landscape organization – especially soil parameters and drainage density –
79 where a high percentage of responsive soils and a high drainage density resulted in small values of α (Hrachowitz et al., 2010).
80 Conceptual and physically-based models have also been used to investigate the (temporally variable) shapes of TTDs. Haitjema
81 (1995) found that the TTD of groundwater can resemble an exponential distribution while Kollet and Maxwell (2008) and
82 Cardenas and Jiang (2010) derived a power-law form and fractal behavior adding macrodispersion and systematic
83 heterogeneity to the domain in the form of depth-decreasing poromechanical properties. Increasing the vertical gradient of
84 conductivity decay in the soil decreased the shape parameter α (from 0.95 for homogeneous conditions down to a value of 0.5
85 for extreme gradients) in a study by Ameli et al. (2016). Somewhat surprisingly, the level of “unstructured” heterogeneity
86 within the soil and the bedrock was found to only have a weak influence on the shape of TTDs (Fiori and Russo, 2008) since
87 the dispersion is predominantly ruled by the distribution of flow path lengths within a catchment. Antecedent moisture
88 conditions and event characteristics influenced catchment TTDs at short timescales while land use affected both short and long
89 timescales (Weiler et al., 2003; Roa-Garcia and Weiler, 2010). TTD shapes appeared highly sensitive to catchment wetness
90 history and available storage, mixing mechanisms and flow path connectivity (Hrachowitz et al., 2013).

91 Kim et al. (2016) recorded actual TTDs in a sloping lysimeter and reported that their shapes varied both with storage state and
92 the history of inflows and outflows. They argued that “the observed time variability [...] can be decomposed into two parts:
93 [1] ‘internal’ [...] – associated with changes in the arrangement of, and partitioning between, flow pathways; and [2] ‘external’
94 [...] – driven by fluctuations in the flow rate along all flow pathways”. ~~From these partly contradictory findings, it is clear that~~

95 relating best-fit values for the shape parameter α of the Gamma distribution to catchment or precipitation event properties does
96 not yield a consistent picture yet. Moreover, the shape of TTDs is also dependent on the resolution of time series data (sampling
97 frequency). While α can decrease with longer sampling intervals (since the nonlinearity of the flow system is overestimated
98 when sampling becomes more infrequent (Hrachowitz et al., 2011)), higher α values can also result from lowering the sampling
99 frequency in both input (precipitation) and output (streamflow) (Timbe et al., 2015).

100 Replacing transit time with flow-weighted time or cumulative outflow (Niemi, 1977; Nyström, 1985) erased a substantial
101 amount of the TTD shape variation associated with the external variability. However, since a change in the inflow often causes
102 both fluctuations along and also a rearrangement between the flow pathways (i.e. internal variability), flow-weighted time
103 approaches are not able to completely erase the influence of changes in the inflow rate. Still, Ali et al. (2014) providing a
104 comprehensive assessment of different transit time based catchment transport models (where they compare several time-
105 invariant to time-variable methods) conclude that applying a flow-weighted time approach can indeed yield adequate results
106 for predicting transport.

107 From these partly contradictory findings, it is clear that relating best fit values for the shape parameter α of the Gamma
108 distribution to catchment or precipitation event properties does not yield a consistent picture yet. Moreover, the shape of TTDs
109 is also dependent on the resolution of time series data (sampling frequency). While α can decrease with longer sampling
110 intervals (since the nonlinearity of the flow system is overestimated when sampling becomes more infrequent (Hrachowitz et
111 al., 2011)), higher α values can also result from lowering the sampling frequency in both input (precipitation) and output
112 (streamflow) (Timbe et al., 2015).

113 1.4. TTD theory

114 To summarize, soil hydraulic conductivity, antecedent moisture conditions (storage state), soil thickness and precipitation
115 amount and intensity are amongst the most frequently cited factors that influence the shape of TTDs. Obviously, there is not
116 one single property that controls the TTD shape. Instead, the interplay of several catchment and event characteristics results
117 in the unique shape of every single TTD. One approach to deal with this problem of multicausality is the use of dimensionless
118 numbers. Heidbüchel et al. (2013) introduced the flow path number F which combines several catchment, climate and event
119 properties into one index relating flows in and out of the catchment to the available subsurface storage. It was originally
120 designed to monitor the exceedance of certain storage thresholds for the activation of different dominant flow paths
121 (groundwater flow, interflow, overland flow) at the catchment scale but can also help to categorize and predict TTD shapes.
122 Moreover, from continuous time series of TTDs one can mathematically derive residence time distributions (describing the
123 age distribution of water stored in the catchment), storage selection functions (describing the selection preference of the
124 catchment discharge for younger or older stored water) (Botter et al., 2010; 2011; van der Velde et al., 2012; Benettin et al.,
125 2015; Harman, 2015; Pangle et al., 2017; Danesh-Yazdi et al., 2018; Yang et al., 2018) and master transit time distributions
126 (MTTDs) (representing the flow-weighted average of all TTDs of a catchment) (Heidbüchel et al., 2012; Sprenger et al., 2016;
127 Benettin et al., 2017) which all can take on different shapes depending on climate and catchment properties, just like the

Kommentiert [IH4]: - Line 94-95. This sentence is repeated in other parts of the manuscript. By definition such approach cannot "completely" erase differences. The question is whether the approximation is good enough for applications. The study by Ali et al (A comparison of travel-time based catchment transport models, with application to numerical experiments, JoH 2014) shows that in many cases it does the job, also considering the several sources of uncertainty, including for instance the estimation of ET (not done here). Answer: We have added the reference to Ali et al. (2014) and discuss your point.

128 individual TTDs. Hence the results presented in this paper can also provide insights into the use of these descriptors of
129 catchment hydrologic processes.

130
131 Since McGuire and McDonnell (2006) stated a lack of theoretical work on the actual shapes of TTDs, quite a diverse range of
132 research has been conducted to approach this problem from different angles and has yielded fragments of important knowledge.
133 However, what is still missing is a coherent framework that enables us to structure our understanding of the nature of TTDs
134 so that it eventually becomes applicable to real world hydrologic problems. Already in 2010, McDonnell et al. had asked how
135 the shape of TTDs could be generalized and how it would vary with ambient conditions, from time to time and from place to
136 place. This study sets out to provide such a coherent framework which – although not exhaustive (or entirely correct for that
137 matter) – will provide us with testable hypotheses on how shape and scale of TTDs change spatially and temporally. As
138 Hrachowitz et al. (2016) put it: “an explicit formulation of transport processes, based on the concept of transit times has the
139 potential to improve the understanding of the integrated system dynamics [...] and to provide a stronger link between [...] hydrological and water quality models”.

141 ~~Moreover, from continuous time series of TTDs one can mathematically derive residence time distributions (describing the~~
142 ~~age distribution of water stored in the catchment), storage selection functions (describing the selection preference of the~~
143 ~~catchment discharge for younger or older stored water) (Botter et al., 2010; van der Velde et al., 2012; Benettin et al., 2015;~~
144 ~~Harman, 2015; Pangle et al., 2017; Danesh-Yazdi et al., 2018; Yang et al., 2018) and master transit time distributions (MTTDs)~~
145 ~~(representing the flow-weighted average of all TTDs of a catchment) (Heidbüchel et al., 2012; Sprenger et al., 2016; Benettin~~
146 ~~et al., 2017) which all can take on different shapes depending on climate and catchment properties, just like the individual~~
147 ~~TTDs. Hence the results presented in this paper can also provide insights into the use of these descriptors of catchment~~
148 ~~hydrologic processes.~~

149 1.5. Our approach

150 In this study we will make use of a physically-based, spatially-explicit, 3-D model to systematically simulate how different
151 catchment properties and climate characteristics and also their interplay control the shape of forward TTDs. We test which
152 TTD shapes are most appropriate for capturing hydrologic and hydrochemical catchment response at different locations and
153 for specific points in time. Furthermore we will try to interpret the results in the most general way possible, so that the theory
154 can be extended to other potential controls of the TTD shape in the future. Our modeling does not explicitly include preferential
155 flow within the soil and bedrock (like, e.g., macropores or fractures), therefore our TTDs mostly represent systems where
156 water is transported via overland flow coupled with subsurface matrix flow. Still, the exclusion of these components can be
157 considered legitimate and the results meaningful because of the important role that macrodispersion plays in shaping TTDs
158 (Fiori et al., 2009) on the smaller scale the hydrologic effect of evenly distributed macropores can be represented by and
159 reproduced with the concept of effective hydraulic conductivity. Hence, we consider our results the base for further

160 investigations approaching ever more realistic representations of the many hydrological processes taking place at the catchment
161 scale.

162 2. Methods

163 We used HydroGeoSphere (HGS), a 3-D numerical model describing fully coupled surface-subsurface, variably saturated flow
164 and advective-dispersive solute transport (Therrien et al., 2010). Groundwater flow in the 3-D subsurface is simulated with
165 Richards' equation and Darcy's law, surface runoff in the 2-D surface domain with Manning's equation and the diffusive-
166 wave approximation of the Saint-Venant equations. The classical advection-dispersion equation for solute transport is solved
167 in all domains. The surface and subsurface domains are numerically coupled using a dual node approach, allowing for the
168 interaction of water and solutes between the surface and subsurface. The general functionality of HGS and its adequacy for
169 solving analytical benchmark tests has been proven in several model intercomparison studies (Maxwell et al., 2014; Kollet et
170 al., 2017) and its solute transport routines have been verified against laboratory (Chapman et al., 2012) and field measurements
171 (Sudicky et al., 2010; Liggett et al., 2015; Gilfedder et al., 2019). Since our modeling approach entails only-subsurface flow
172 only in porous media (no explicit fractures or macropores are included), the resulting TTDs have to be considered a special
173 subset of distributions lacking some of the dynamics we can expect in real-world catchments while still providing a sound
174 basis for further investigations (like, e.g., adding more complex interaction dynamics along the flow pathways).

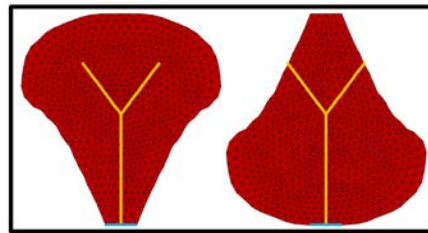
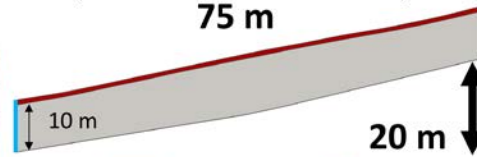
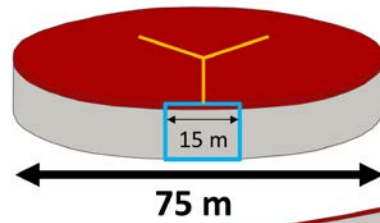
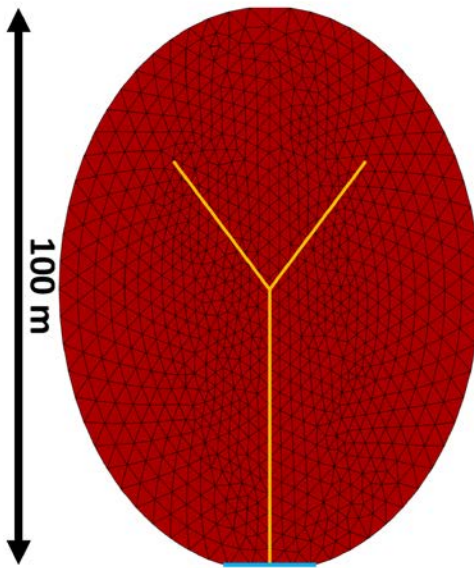
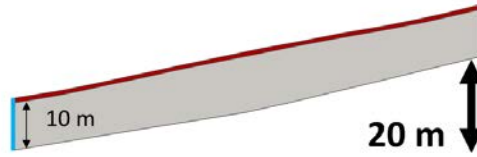
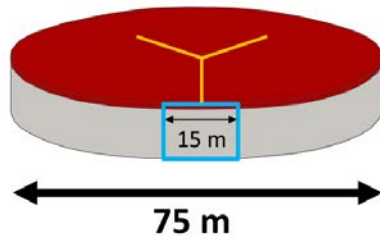
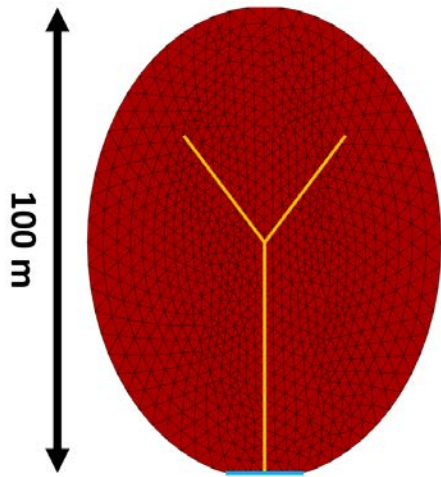
175 2.1. Model setup

176 A small zero-order catchment was set up, 100 m long, 75 m wide (~6000 m²) with an average slope of 20 % towards the outlet
177 and elliptical in shape (Fig. 1). The catchment converges slightly towards the center creating a gradient that concentrates flow.
178 The bedrock is 10 m thick and has a saturated hydraulic conductivity of $K_{Br,x} = K_{Br,y} = 10^{-5} \text{ m day}^{-1}$ (horizontal) and $K_{Br,z} = 10^{-6}$
179 m day^{-1} (vertical). The soil layer is isotropic, of uniform thickness and has a higher hydraulic conductivity. All other
180 parameters are uniform across the entire model domain (based on values typically found in many catchments in Central
181 Europe): porosity $n = 0.39 \text{ m}^3 \text{ m}^{-3}$, van Genuchten parameters alpha $\alpha_{vG} = 0.5 \text{ m}^{-1}$, beta $\beta_{vG} = 1.6$, saturated water content $\theta_s =$
182 $0.39 \text{ m}^3 \text{ m}^{-3}$, residual water content $\theta_r = 0.05 \text{ m}^3 \text{ m}^{-3}$, and pore-connectivity parameter $I_p = 0.5$; and longitudinal and transverse
183 dispersivity $\alpha_L = 5 \text{ m}$ and $\alpha_T = 0.5 \text{ m}$, respectively, free-solution diffusion coefficient $D_{free} = 8.64 \cdot 10^{-5} \text{ m}^2 \text{ day}^{-1}$. The magnitude
184 for α_L was estimated with regard to the length of the model catchment (100 m) using the relationship described in Gelhar et al.
185 (1992) and Schulze-Makuch (2005). Both bedrock and soil are exclusively porous media without any potential preferential
186 flow paths like macropores or rock fractures.

Kommentiert [IHh5]: - Lines 137-139. Unfortunately the effective hydraulic conductivity cannot replace the dispersive effects of the distributed macropores because it only impacts the mean velocity. I would delete this sentence as it is not needed: the exclusion of such component is legitimate and meaningful in my view because of the important role of macrodispersion in the TTD determination.
Answer: Thank you for the constructive comment. We have proceeded as suggested.

Kommentiert [IHh6]: - Line 159. vertical or horizontal to the slope? I guess the latter.
Answer: It is indeed vertical and not orthogonal to the slope (but that makes only a small difference).

Kommentiert [IHh7]: - Line 163. 5m of dispersivity is quite a lot, even more so for the vertical one. Why the choice? In this case the inclusion of Dfree looks irrelevant.
Answer: The longitudinal dispersivity and lateral dispersivity were estimated with regard to the length scale of the model catchment (100 m). $\alpha_L = 5 \text{ m}$ were estimated using the relation between the longitudinal dispersivity and length scale described in Gelhar et al., 1992 and Schulze-Makuch, 2005 (regression $\alpha = 0.085 \cdot L^{0.61}$). We agree that the free-solution diffusion is significantly smaller than the dispersion and could have been neglected. We have clarified this in the manuscript adding the references [Gelhar et al., 1992] and [Schulze-Makuch, 2005].
References:
Gelhar, L.W., Welty, C., Rehfeldt, K.R., 1992. A critical review of data on field-scale dispersion in aquifers. Water Resources Research 28 (7), 1955–1974.
Schulze-Makuch, D. (2005). Longitudinal dispersivity data and implications for scaling behavior. Groundwater, 43(3), 443-456.



190 Figure 1: 3-D model domain and shape of the virtual catchment from top (left), front (upper right) and side (lower middle right).
191 The blue square indicates the outflow boundary with constant head condition. The red layer represents the soil which has a much
192 higher hydraulic conductivity than the underlying bedrock (grey). The orange lines indicate the zone of convergence (but no explicit
193 channel). The two additional catchment shapes (top-heavy and bottom-heavy) we tested in section 2.2.1 are shown in the black box.

194 2.1.1. Boundary conditions

195 Both the bottom and the sides of the domain were impermeable boundaries. A constant head boundary condition (equal to the
196 surface elevation) was assigned to the lower front edge of the subsurface domain (nodes in the blue square in Fig. 1), allowing
197 outflow from both the bedrock and the soil. A critical depth boundary was assigned to the lower edge of the surface domain
198 (on top of above the constant head boundary) to allow for overland flow out of the catchment. The surface of the catchment
199 received spatially uniform precipitation. We used a recorded time series of precipitation from the north-east of Germany
200 (maritime temperate climate: Cfb in the Köppen climate classification) amounting to 690 mm a^{-1} (Fig. 2a). The time series
201 was 1 year long and repeated 32 more times to cover the entire modeling period which lasted a total of 33 years. We made
202 sure that the looping of the precipitation time series would not cause any unwanted artifacts in the resulting TTDs (see Text
203 S1 and Figure S1 in the supplement). Neither evaporation nor transpiration was considered during the simulations. This means
204 that all precipitation we applied was effective precipitation that would eventually discharge at the catchment outlet. The
205 addition of the process of evapotranspiration is planned in a follow-up modeling study to investigate what influence it exerts
206 on catchment TTDs. The tracer was applied uniformly over the entire catchment during a precipitation event that lasted one
207 hour, had an intensity of 0.1 mm h^{-1} and a tracer concentration of 1 kg m^{-3} . This resulted in a total applied tracer mass of 0.589
208 ~~kg-over the entire catchment.~~

Kommentiert [IHh8]: - Lines 174-175. What head is provided in the boundary condition? Where is the water table located? This is quite important.

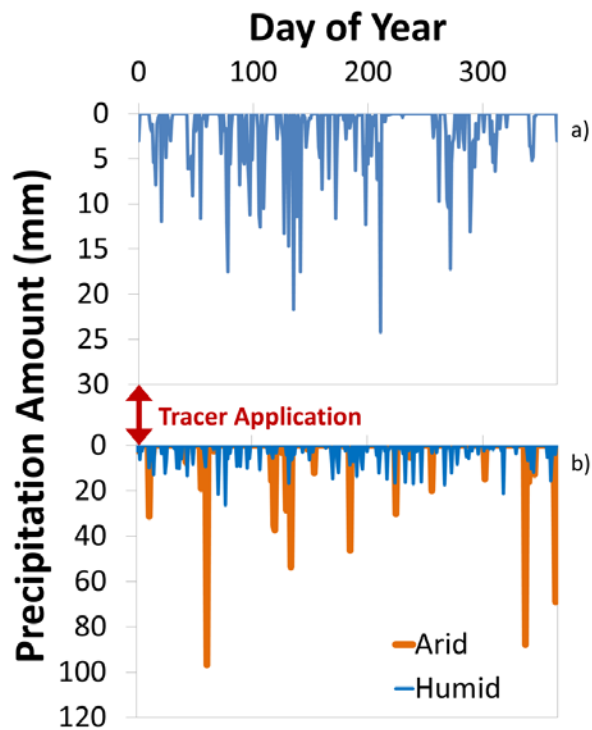
Answer: Thanks for catching that. I thought I would have written it somewhere. We have added information on the location of the head (it is equal to the surface elevation).

Kommentiert [IHh9]: - Line 214. I guess that mm/a means mm/y

Answer: Yes, HESS officially prefers this abbreviation.

- Line 214. Please provide more details on the rainfall time series, e.g. regime, climate etc. As a matter of fact TTD depends also on the rainfall regime, not only the total rainfall per year (e.g. Botter et al 2010).

Answer: We agree it is correct that the TTD also depends on the distribution of rainfall. We investigate the influence of different precipitation event frequencies. The precipitation time series we used has the following properties: Average interarrival time: 2.64 days; Average event duration: 3.17 days. The climate in the north west of Germany can be described as maritime temperate (Cfb in the Köppen classification) Maximum precipitation falls usually in June (65 mm), minimum in February (28 mm). We have added this information to the manuscript.



210
 211 **Figure 2:** a) One-year time series of subsequent precipitation (looped 33 times for the entire modeling period and rescaled for smaller
 212 or larger subsequent precipitation amounts). Tracer application took place during the first hour of the model runs. b) Time series
 213 of subsequent precipitation for a high-frequency scenario (humid) and a low-frequency scenario (arid). The total precipitation
 214 amount is the same for both scenarios.

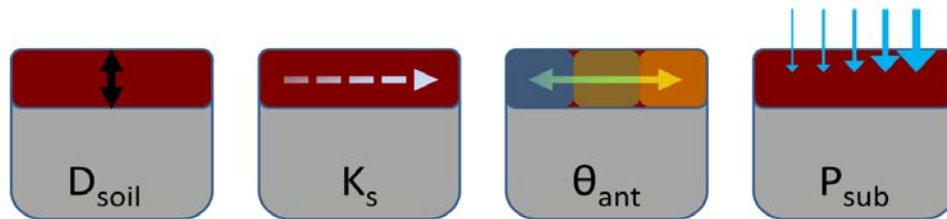
215 **2.1.2. Initial conditions**

216 The model runs were initialized with three different antecedent soil moisture conditions θ_{ant} – a dry one ($\theta_{ant} = 22.0\%$;
 217 corresponding to an average effective saturation of the soil layer $S_{eff} \approx 50\%$), an intermediate one ($\theta_{ant} = 28.8\%$; $S_{eff} \approx$
 218 70%) and a wet one ($\theta_{ant} = 35.6\%$; $S_{eff} \approx 90\%$). To obtain realistic distributions of soil moisture, we first ran the model starting
 219 with full saturation and without any precipitation input and let the soils drain until the average effective saturation reached the
 220 states for our initial conditions. We recorded these conditions and used them as initial conditions of the virtual experiment
 221 runs. In general, the soil remained wetter close to the outlet in the lower part of the catchment and became drier in the upper
 222 part of the catchment. Note that the process of evapotranspiration was excluded from the modeling so that the lowest achievable

223 saturation was essentially defined by the field capacity. An average effective saturation S_{eff} of approximately 50 % was the
 224 lowest that could be achieved by draining the soil layer since the lower part stayed highly saturated due to the constant head
 225 boundary condition being equal to the surface elevation at the outlet. The upper parts of the catchment, however, were initiated
 226 with much lower S_{eff} values (≈ 30 % in the dry scenarios). That means that although an S_{eff} value of 50 % seems to be quite
 227 high, it actually represents an overall dry state of the catchment soil. Throughout the modeling runs the dry initial condition
 228 did not occur again as that would have taken 13 years of drainage without any precipitation for the scenarios with high soil
 229 hydraulic conductivity K_S and almost 1500 years for the scenarios with low K_S . The inclusion of evapotranspiration would,
 230 however, speed up the drying process of the soil and hence make these initial conditions more realistic.

231 2.2. Model scenarios

232 To investigate how different catchment and climate properties influence the shape of forward TTDs we systematically varied
 233 four characteristic properties from high to low values and looked at the resulting TTD shapes of all the possible combinations
 234 (for a total number of 36 scenarios). The properties we focused on were soil depth (D_{soil}), saturated soil hydraulic conductivity
 235 (K_S), antecedent soil moisture content (θ_{ant}) and subsequent precipitation amount (P_{sub} , essentially a measure of the amount of
 236 precipitation that falls after the delivery of the traced event) (Fig. 32).



238
 239 **Figure 32:** The four properties that were varied to explore their influence on the shape and scale of TTDs: soil depth D_{soil} , saturated
 240 soil hydraulic conductivity K_S , antecedent soil moisture θ_{ant} and subsequent precipitation amount P_{sub} . The bedrock hydraulic
 241 conductivity K_B was kept constant for all of these base-case scenarios.

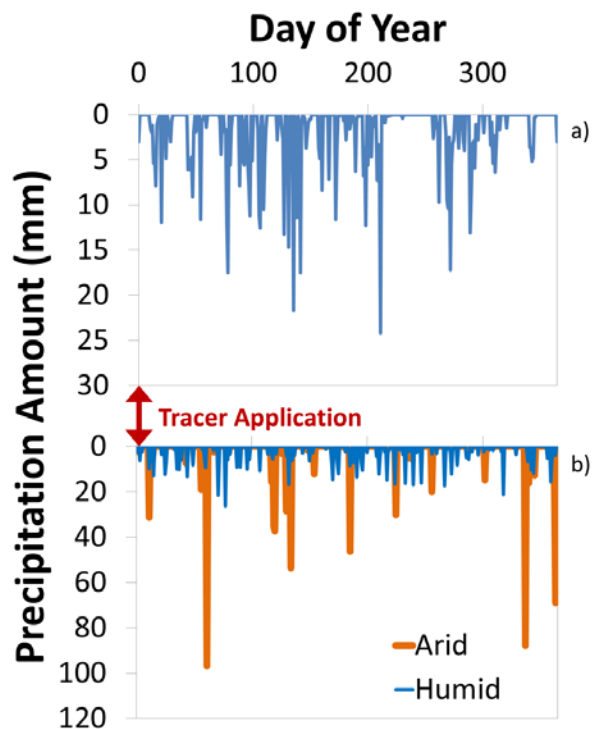
242 We tested two soil depths D_{soil} , namely depths of 0.5 m and 1.0 m, evenly distributed across the entire catchment. Similarly,
 243 we chose two saturated soil hydraulic conductivities K_S , a high one with 2.0 m day^{-1} (similar to fine sand) and a low one with
 244 0.02 m day^{-1} (similar to silt). Three states of antecedent moisture content θ_{ant} were selected to represent initial conditions – 50,
 245 70 and 90 % of effective saturation. Finally the subsequent precipitation amount P_{sub} was varied in three steps from 345 over
 246 690 up to 1380 mm a^{-1} . The original We used a recorded time series of precipitation from the north-east of Germany time series
 247 (690 mm a^{-1} , Fig. 2a) was (the original one amounted to 690 mm a^{-1}) and rescaled it to obtain time series with smaller and
 248 larger amounts (Fig. 3a). The time series was 1 year long and we repeated it 32 more times to cover the entire modeling period

Kommentiert [IHh10]: - Line 204. What is the "subsequent precipitation amount"?
 Answer: Clarified (essentially a measure of the amount of precipitation after the delivery of the tracer).

Kommentiert [IHh11]: - Line 214. I guess that mm/a means mm/y
 Answer: Yes, HESS officially prefers this abbreviation.

- Line 214. Please provide more details on the rainfall time series, e.g. regime, climate etc. As a matter of fact TTD depends also on the rainfall regime, not only the total rainfall per year (e.g. Botter et al 2010).
 Answer: We agree it is correct that the TTD also depends on the distribution of rainfall. We investigate the influence of different precipitation event frequencies. The precipitation time series we used has the following properties: Average interarrival time: 2.64 days; Average event duration: 3.17 days. The climate in the north west of Germany can be described as maritime temperate (Cfb in the Köppen classification). Maximum precipitation falls usually in June (65 mm), minimum in February (28 mm). We are going to add this information to the manuscript.

249 ~~which lasted a total of 33 years.~~ With two soil depths, two soil hydraulic conductivities, three antecedent moisture conditions
 250 and three subsequent precipitation amounts this resulted in 36 model scenarios. Based on these 36 runs we evaluated the
 251 differences in the shape of the TTDs. The abbreviated names of the 36 model runs consist of four letters, each representing
 252 one of the properties that we varied: the first one is D_{soil} (T = thick; F = flat), the second one is K_s (H = high; L = low), the
 253 third one is θ_{ant} (W = wet; I = intermediate; D = dry) and the fourth one is P_{sub} (S = small; M = medium; B = big). For example
 254 the name FHIB would indicate a run with a “F”lat (shallow) soil, a “H”igh K_s , an “I”ntermediate θ_{ant} and a “B”ig (large)
 255 amount of subsequent precipitation (see Table 1 for an overview of the names of all 36 scenarios). We are well aware that
 256 “thick” and “flat” are technically incorrect descriptions of soil depth. However, in order to have unique identifiers (i.e.
 257 individual letters) for all 10 property states we decided to use T and F for describing deep and shallow soils, respectively.



259 **Figure 3:** a) One-year time series of subsequent precipitation (looped 33 times for the entire modeling period and rescaled for smaller
 260 or larger subsequent precipitation amounts). Tracer application took place during the first hour of the model runs. b) Time series
 261

262 ~~of subsequent precipitation for a high-frequency scenario (humid) and a low-frequency scenario (arid). The total precipitation~~
263 ~~amount is the same for both scenarios.~~

264 To complement the results obtained from the systematic variation of catchment and climate characteristics we tested the
265 influence of ~~seven~~ other factors: 1) 1) soil porosity, 2) 2) bedrock hydraulic conductivity, 3) 3) exponential decay in hydraulic
266 conductivity with depth in the soil, 4) 4) frequency of precipitation events, 5) 5) soil water retention curve, 6) 6) catchment shape
267 and 7) 7) effect of extreme precipitation after full saturation – conditions during which direct surface runoff may occur. These
268 additional runs with altered soil properties, boundary and initial conditions were performed on the basis of some of the 36
269 initial runs (in the following sections we always indicate which runs form the basis of the specific scenarios, also see Table S1
270 in the supplement).

271 Notable catchment properties We did not test include the role of ~~catchment~~ topography, and kept size, ~~shape~~, slope and
272 curvature ~~constant~~. Apart from investigating the effect of an exponential decay in soil hydraulic conductivity with depth we
273 did not add heterogeneity to the subsurface hydraulic properties. Therefore we cannot make statements about how multiple
274 soil layers or different spatial patterns of hydraulic conductivity would influence TTDs.

276 2.2.1. Soil porosity

277 The influence of larger and smaller soil porosity was investigated with six additional runs based on the three scenarios THDM,
278 THIM and THWM (see Table S1 in the supplement for an overview on how the additional scenarios are related to the 36 basic
279 model scenarios). Three of the additional runs had larger ($0.54 \text{ m}^3 \text{ m}^{-3}$) and three had smaller soil porosity ($0.24 \text{ m}^3 \text{ m}^{-3}$) than
280 the base-case scenarios ($0.39 \text{ m}^3 \text{ m}^{-3}$).

281 2.2.2. Bedrock hydraulic conductivity

282 Six runs were performed on the basis of the THDB scenario (which had a bedrock hydraulic conductivity K_{Br} of $10^{-5} \text{ m day}^{-1}$)
283 ¹). In the first run K_{Br} was decreased to $10^{-7} \text{ m day}^{-1}$, in the following runs it was successively increased to 10^{-3} , 10^{-2} , 10^{-1} ,
284 10^0 , $2 \cdot 10^0 \text{ m day}^{-1}$, matching K_S of the soil layer in the final run.

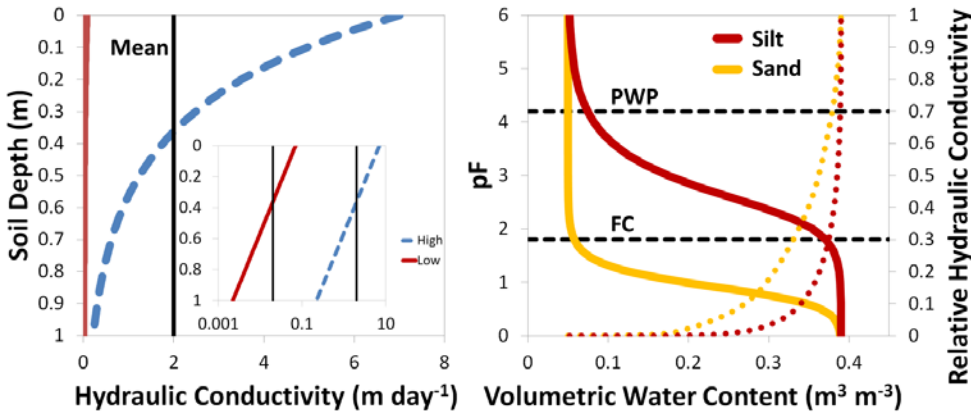
285 2.2.3. Decay in saturated hydraulic conductivity with depth

286 Because all other model scenarios had a constant hydraulic conductivity throughout the soil layer, we wanted to test whether
287 the introduction of an exponential decay in hydraulic conductivity with depth (from high conductivity at the surface to low
288 conductivity at the soil–bedrock interface; see Bishop et al., 2004; Jiang et al., 2009) would have a large influence on the TTD
289 shapes. We based the conductivity decay test on four scenarios (THDB, THWB, TLDB and TLWB) adding relationships of
290 soil depth z and saturated hydraulic conductivity K_S with a shape parameter $f = 0.29 \text{ m}$ and saturated hydraulic conductivity at

291 the surface $K_{S0} = 7 \text{ m day}^{-1}$ (for the high conductivity scenarios) or $K_{S0} = 0.07 \text{ m day}^{-1}$ (for the low conductivity scenarios),
 292 respectively (Eq. (1) and left panel on Fig. 4):

$$293 \quad K_S(z) = K_{S0} e^{-\frac{z}{L}}. \quad (1)$$

294 This preserved the mean K_S values of $2 \cdot 10^{-0}$ (high) and $2 \cdot 10^{-2} \text{ m day}^{-1}$ (low) (from the base-case scenarios), respectively.
 295



296
 297 **Figure 4:** Left panel: Exponential decay in saturated soil hydraulic conductivity with depth for the high (blue) and the low (red) K_S
 298 scenario. The x-axis in the inset has a log scale. The spatial mean K_S is indicated by the vertical black lines. Right panel: Water
 299 retention curves (solid) and relative hydraulic conductivities (dotted) for sandy and silty soils. The permanent wilting point (PWP)
 300 and the field capacity (FC) are marked as references (dashed).

301 2.2.4. Precipitation frequency

302 Five time series with high precipitation event frequency and five time series with low precipitation event frequency were
 303 created by means of using the rainfall generator used by Musolff et al. (2017) (Fig. 23b). It generates Poisson effective rainfall
 304 (Cox and Isham, 1988) which is characterized by exponentially distributed rainfall event amounts and interarrival times. The
 305 mean interarrival time was set to three days and 15 days for the high frequency scenarios (comparable to a humid precipitation
 306 distribution and intensity pattern with lower intensities and more frequent events) and low frequency scenarios (comparable
 307 to an arid precipitation distribution and intensity pattern with higher intensities and less frequent events), respectively. The
 308 total precipitation for all scenarios (both humid and arid type) was 690 mm so that it matched our medium P_{sub} scenarios.

309 2.2.5. Water retention curve

310 All the base-case model scenarios were conducted with water retention curves (WRC) resembling silty soils (Eq. 2):

$$\theta = \theta_r + \frac{\theta_s - \theta_r}{[1 + (\alpha_{vG} |\psi|)^{\beta_{vG}}]^\nu}, \quad (2)$$

with van Genuchten parameters α_{vG} (m^{-1}) and β_{vG} (dimensionless), saturated water content θ_s , residual water content θ_r (both $\text{m}^3 \text{m}^{-3}$), pressure head ψ (m) and $\nu = 1 - 1/\beta_{vG}$ (see Section 2.1 for van Genuchten parameter values). However, we also wanted to investigate how a different WRC in the soil layer (see right panel on Fig. 4) would influence the shape of TTDs. We chose to test a sand-type WRC since it can, in some aspects and to a certain extent, also indicate how a system with the threshold-like initiation of rapid preferential flow behaves. The sand-type WRC causes an increase in hydraulic conductivity already at relatively lower soil water contents compared to the silt-type WRC. Hence, for the same precipitation event lateral flow is initiated faster (at lower saturations) in sandy soils since water reaches the soil–bedrock interface more quickly where it is diverted from vertical to lateral flow. The relative hydraulic conductivity k_r was derived with Eq. 3:

$$k_r = S_{eff}^{l_p} \left[1 - \left(1 - S_{eff}^{v^{-1}} \right)^{\nu} \right]^2, \quad (3)$$

with effective saturation S_{eff} and pore-connectivity parameter l_p (both dimensionless). Other aspects of preferential flow – like bypass flow through macropores in deeper soil layers – are, however, not captured by sand-type WRCs. The van Genuchten parameters for the sand-type WRC were defined as follows: $\alpha_{vG} = 14.5 \text{ m}^{-1}$ and $\beta_{vG} = 2.68$. We based the additional eight runs on the scenarios THDB, THWB, THDS, THWS, TLDB, TLWB, TLDS and TLWS.

2.2.6. Catchment shape

In addition to the oval catchment we designed two more shapes to get an idea whether it would have a significant impact on the resulting TTDs (see black box in Fig. 1). One of the catchments had the center of gravity located farther away from the outlet (Top; 60 m) the other catchment had the center of gravity located closer to the outlet (Bottom; 40 m). This increased the average flow path length from 61 m to 70 m for Top and decreased it to 55 m for Bottom – while catchment length, area, and slope stayed the same for all cases. The four additional runs we conducted were based on the scenarios THWM and THDM.

2.2.6.2.7. Full saturation and extreme precipitation intensity

We tested these effects for two scenarios (THWB and TLWB) out of the 36 systematic model runs since both of these scenarios were already close to creating overland flow. Full saturation in this case means that the initial condition for these model runs consisted of a fully saturated domain (both in the bedrock and in the soil), i.e. S_{eff} was 100 % ($\theta_{ant} = 39 \%$). Additionally, we increased the intensity of the input precipitation event (delivering the tracer) from 0.1 mm h^{-1} (normal) over 10 mm h^{-1} (very large, +) to 100 mm h^{-1} (extreme, +++), in an attempt to create infiltration excess overland flow and record its influence on the shape of TTDs.

2.3. Influence of the sequence of precipitation events

We also tested to what extent the sequences of subsequent precipitation events with different magnitude, intensity and interarrival time influence TTD shapes. This was necessary to assure that our resulting TTD shapes were not primarily a product of the point in time – within the sequence of precipitation events – at which the tracer was applied to the catchment. To this end 15 precipitation event time series were created by means of using the rainfall generator used by Musolff et al. (2017). The mean interarrival time was set to three days (comparable to a precipitation distribution and intensity pattern found in humid environments with low intensities and more frequent events) and the total precipitation amount for all scenarios was 690 mm matching our medium P_{sub} scenarios (Fig. S2 in the supplement4). The generated precipitation time series resembled our original time series of precipitation which also had an interarrival time close to three days. All other parameters and properties of the 15 model runs were based on the THDM scenario.

2.4. Processing of the output data

The output data from HydroGeoSphere was mainly processed with Microsoft Excel. We summed surface and subsurface flows, computed total tracer outflow from the catchment, created the probability density and cumulative probability density distribution for tracer outflow, calculated the shape parameters of the forward TTDs, fitted theoretical distributions to our data and smoothed the original TTDs for better visual comparability of the shapes. HydroGeoSphere keeps track of the mass balance of inflow, outflow and storage and calculates the discrepancy (mass balance error) between the three terms (Fig. S23 in the supplement). The absolute mean mass balance error for the 36 runs was negligible ($6.8 \cdot 10^{-2} \pm 7.2 \cdot 10^{-2} \%$).

2.4.1. Creation of TTDs

The probability density distributions of transit time (the forward TTDs) were created by normalizing the mass outflux J_{out} (kg d^{-1}) for each time step by the total inflow mass M_{in} (kg) (Eq. 4).

$$TTD(t) = J_{\text{out}}^{\text{norm}}(t) = \frac{J_{\text{out}}(t)}{M_{\text{in}}}. \quad (4)$$

The cumulative TTDs (dimensionless) were created by multiplying the normalized mass outflux (d^{-1}) of each time step by the associated time step length Δt (d) before cumulating it (Eq. 5):

$$TTD_{\text{cml}}(t) = \sum_{i=0}^t (J_{\text{out}}^{\text{norm}}(t) * \Delta t). \quad (5)$$

2.4.2. Calculation of TTD metrics

For each TTD we calculated seven parameters to characterize its shape: the first quartile (Q_1), the median (Q_2), the mean (mTT), the third quartile (Q_3), the standard deviation (σ), the skewness (v) and the excess kurtosis (γ) (see Text S12 and Fig. S34 in the supplement for details on the calculation and for visual comparison of the metrics). Furthermore we determined the young water fraction F_{yw} as the fraction of water leaving the catchment after 2.3 months (Jasechko et al., 2016; Kirchner, 2016;

Wilusz et al., 2017). For more details on how F_{yw} changes with catchment and climate properties, see Text S32, Fig. S45 and Table S2 in the supplement.

2.4.3. Fitting

We fitted predefined mathematical probability density functions to the modeled data since condensing the main characteristics of an observed probability distribution into just one to three parameters of a mathematical function is appealing and eases the potential of transferability of the findings. Massoudieh et al. (2014) explored the use of freeform histograms as groundwater age distributions and concluded that mathematical distributions performed better in terms of their ability to capture the observed tracer data relative to their complexity. In order to determine which theoretical probability density function best captures the shape of our modeled TTDs, we chose two probability density functions that are commonly used to describe the transit of water through catchments (~~the Inverse Gaussian Advection Dispersion~~ and ~~the Gamma model~~), as well as the less common Log-normal Beta distribution which also has just two adjustable parameters because its shape is extremely flexible:
~~1) The Inverse Gaussian distribution Advection Dispersion distribution (AD) with dispersion parameter D (dimensionless) and mean mTT (d) that is a particular solution of the advection-dispersion equation of the form of an inverse Gaussian distribution~~
(Eq. 6):

$$InvGauAD(t) = \left(\frac{4mTt}{mTT}\right)^{-0.5} \frac{1}{t} \exp\left\{-\left[\left(1 - \frac{t}{mTT}\right)^2 * \frac{mTT}{4Dt}\right]\right\}, \quad (6)$$

~~2) The three parameter Beta distribution with shape parameters α and β (dimensionless) and upper limit c (d) (with mean $mTT=ac/(\alpha+\beta)$) (Eq. 7):~~

$$Beta(t) = \frac{t^{\alpha-1}(c-t)^{\beta-1}}{c^{\alpha+\beta-1}B(\alpha,\beta)}, \quad (7)$$

~~The fourth parameter of the Beta distribution is the lower limit a . It is not included in the above definition since in our case it is zero.~~

~~23) The Gamma distribution with shape parameter α (dimensionless) and scale parameter β (d) (with mean $mTT=\alpha\beta$) (Eq. 78):~~

$$Gamma(t) = t^{\alpha-1} \frac{e^{-t/\beta}}{\beta^\alpha \Gamma(\alpha)}, \quad (78)$$

Gamma distributions are quite flexible and can take on very different shapes when α is changed: $\alpha < 1$, highly skewed distributions with initial maximum and heavier (i.e. sub-exponential) tails; $\alpha = 1$, exponential distribution; $\alpha > 1$, less skewed, "humped" distributions with initial value of 0, a mode and lighter tails (see Fig. S9 in the supplement for examples). Gamma distributions can be stretched or compressed with a scale parameter (β) and their mean is the product of α and β . Thus when using Gamma distributions for the determination of mTTs, it is necessary to choose the correct shape parameter α to

Kommentiert [IHh12]: - Line 338. I don't like the definition, I would rather speak of "The Inverse Gaussian distribution, with parameters D , ..., that is a particular solution of the Advection Dispersion Equation". AD is misleading, as ADE can have several different solutions.
 Answer: We would like to follow your suggestion. If have reformulated the description in the following way:
 1) The inverse Gaussian distribution with dispersion parameter D (dimensionless) and mean mTT (d) that is a particular solution of the advection dispersion equation (Eq. 6):

398 avoid problems of equifinality. The same holds true for all multiple parameter distributions. Thus when using Gamma
399 distributions for the determination of mean transit times (mTTs), it is necessary to choose the correct shape parameter α to
400 avoid problems of equifinality.

401 3) Log-normal distribution with standard deviation σ and mean μ (both dimensionless) of the natural logarithm of the variable
402 (with mean $mTT = \exp(\mu + \sigma^2/2)$) (Eq. 8):

$$403 \text{Log}N(t) = \frac{1}{t\sigma\sqrt{2\pi}} \exp\left[-\frac{(\ln t - \mu)^2}{2\sigma^2}\right]. \quad (8)$$

404 We tested two more probability density functions both having three (instead of just two) adjustable parameters:

405 4) Three parameter Beta distribution with shape parameters α and β (dimensionless) and upper limit c (d) (with mean
406 $mTT = ac/(\alpha + \beta)$) (Eq. 9):

$$407 \text{Beta}(t) = \frac{t^{\alpha-1}(c-t)^{\beta-1}}{c^{\alpha+\beta-1}\Gamma(\alpha, \beta)}. \quad (9)$$

408 The fourth parameter of the Beta distribution could be the lower limit a . It is not included in the above definition since in our
409 case it is zero.

410 5) Truncated Log-normal distribution with the time of truncation λ (d) as the third parameter (Eq. 10):

$$411 \text{Trunc}(t) = \left\{ \frac{1}{(t+\lambda)\sigma\sqrt{2\pi}} \exp\left[-\frac{(\ln t - \mu)^2}{2\sigma^2}\right] \right\} / \left\{ 1 - \int_{t=0}^{\lambda} \frac{1}{t\sigma\sqrt{2\pi}} \exp\left[-\frac{(\ln t - \mu)^2}{2\sigma^2}\right] dt \right\}. \quad (10)$$

412 For visual examples of all five types of distributions please refer to Fig. S6 in the supplement.

413 The method of least squares was used to find the best fit between the modeled TTDs and the theoretical distribution functions
414 (i.e. minimizing the sum of the squared residuals with the Solver function in Excel using one value for each of the 12000 days
415 of the modeled TTDs).

416 The fitting was performed on the cumulative probability distributions since their shape is not subject to the more extreme
417 internal variability that the probability distributions can experience.

418 **2.4.4. Smoothing**

419 Smoothing was only applied to enhance the visual comparability of the TTDs. All calculations were performed on the
420 unsmoothed TTDs. For details on the smoothing method see Text S43 and Fig. S57 in the supplement.

421 **2.5. Flow path number**

422 The flow path number F is a dimensionless number proposed by Heidbüchel et al. (2013) that relates catchment inflow to
423 outflow (in the numerator) while simultaneously assessing available storage space (in the denominator) for each point in time
424 and at the catchment scale. It was introduced to define thresholds for the activation and deactivation of different flow paths

that transport water more slowly (e.g. groundwater flow), faster (interflow) or very fast (macropore flow, overland flow). For this paper we modified F slightly so that both numerator and denominator have the dimensions (m^3) (Eq. 9):

$$F(t) = \frac{P_{dr}(t) - K_{rem}}{D_{soil}(n - \theta_{ant}(t))A_{in}}, \quad (9)$$

where soil depth D_{soil} (m), catchment surface area A_{in} (m^2), porosity n ($\text{m}^3 \text{m}^{-3}$) and antecedent moisture content θ_{ant} ($\text{m}^3 \text{m}^{-3}$) are paired with the driving precipitation amount P_{dr} (m^3) which is calculated as the average subsequent precipitation amount P_{sub} (m a^{-1}) over the average event duration t_{eEv} (d) (Eq. 10):

$$P_{dr}(t) = \frac{t_{eEv} P_{sub}(t) A_{in}}{365.25}. \quad (10)$$

The subsequent precipitation amount P_{sub} (m a^{-1}) is calculated for every time step as the amount of precipitation falling within the year that follows this time step using a moving window. Note that differing from Heidbüchel et al. (2013) we used the event duration t_{eEv} instead of the interevent duration t_{ie} to compute P_{dr} since it better represents the amount of precipitation falling during an average event filling up the available storage. Furthermore, there is the subsurface discharge capacity of the soil K_{rem} (m^3) consisting of the effective saturated soil hydraulic conductivity K_S (m day^{-1}), the sum of the average interevent and event duration $t_{ie} + t_{eEv}$ (d), the porosity n ($\text{m}^3 \text{m}^{-3}$) and the cross-sectional area of the soil layer at the outlet of the catchment A_{out} (m^2) (Eq. 11):

$$K_{rem} = (t_{ie} + t_{eEv}) K_S n A_{out}. \quad (11)$$

The cross-sectional area of the soil layer at the outlet of the catchment A_{out} can be ~~considered~~ regarded to represent the connection of the catchment to either a river channel or to the alluvial valley fill where medium to rapid subsurface outflow from the catchment can occur. Note that differing from Heidbüchel et al. (2013) we used the sum of the interevent and event duration $t_{ie} + t_{eEv}$ instead of just the event duration t_{eEv} to compute K_{rem} since it better represents the amount of water that can be removed from the catchment during an average precipitation cycle.

The flow path number F varies in time mainly due to the changes in antecedent moisture content θ_{ant} since variations in the amount of driving precipitation P_{dr} are damped due to the moving window approach that is used to compute it. That means F can vary quite rapidly (towards either more positive or negative values) during the wet up of a catchment and change more slowly (towards 0) during the dry down phase. A positive flow path number F indicates that there is a surplus of water entering the catchment that cannot be removed by subsurface transport at the same rate. Hence, the storage fills up. Conversely, a negative F indicates that the drainage capacity of the catchment exceeds the water inputs and the amount of stored water decreases. Furthermore, values between 0 and 1 signal that the available soil storage space is able to accommodate the net inflow of water, while values larger than 1 mean that the catchment receives more water than it can discharge or store in the subsurface. In turn, the larger the storage capacity in the subsoil, the more F converges towards 0. There is only one notable important exception to this last rule: In highly conductive soils the increase in discharge capacity (caused by the increase in

456 the cross-sectional area of the soil layer at the outlet A_{out}) can be larger than the increase in storage capacity itself – leading to
457 F becoming even more negative with increasing storage capacity.

458 3. Results

459 Output from the model runs comprised subsurface discharge, overland discharge and tracer concentration in the discharge
460 from which we derived TTDs (for an example see Fig. S86 in the supplement). Additionally, the model provided spatially and
461 temporally resolved tracer concentrations throughout the entire domain. The differences emerging between the individual
462 TTDs can be tracked by looking at the spatio-temporal evolution of the applied tracer impulse throughout the entire catchment.
463 For a detailed example please refer to Text S45 and Fig. S79 in the supplement.

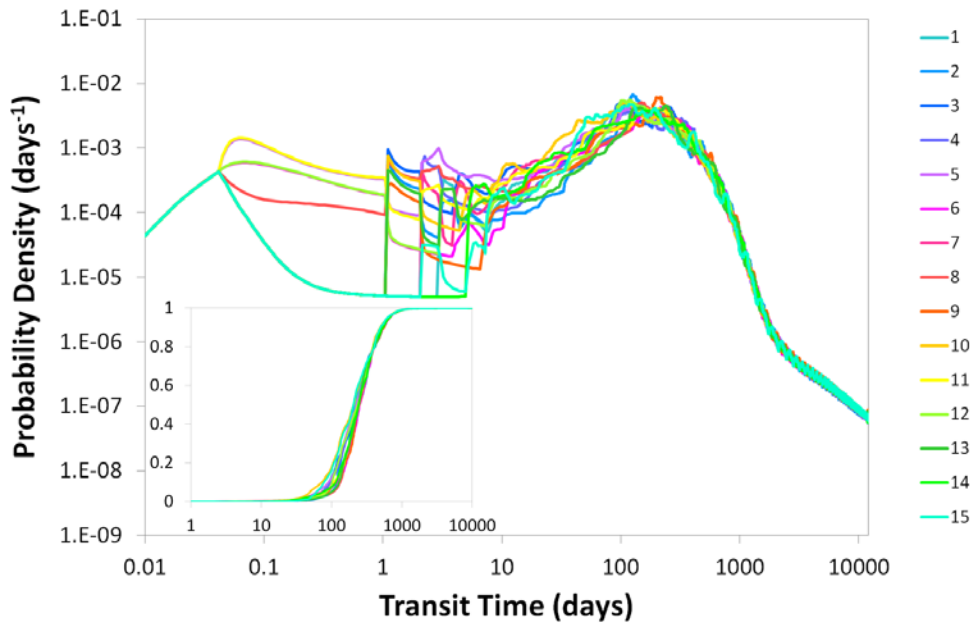
464 3.1. Influence of the sequence of precipitation events

465 Changing the sequence of precipitation events affects the shape of the TTDs to a certain degree. Especially the timing and
466 magnitude of the first precipitation event determines how strong the early response turns out. This can be observed in Fig. 5
467 where the different TTDs split up into different branches according to the arrival and magnitude of the first event after tracer
468 application. However, following this initial split – with more and more precipitation events taking place – all TTDs tend to
469 converge towards a single line. Examining the cumulative TTDs in Fig. 5 it is obvious that the variability in the TTD shape
470 introduced by different precipitation event sequences is much smaller than the variability introduced by the other catchment
471 and climate properties. While the range of Q_1 observed for the 15 scenarios with different event sequences is still 14 % of the
472 total range observed for the 36 base-case scenarios, this percentage decreases down to 2 % for Q_3 . The other distribution
473 metrics describing the shape of the TTDs also vary a lot less between the scenarios with different event sequences compared
474 to the scenarios with different catchment and climate properties (the range of all event sequences is only 1.1 % of the range of
475 all base-case scenarios for the standard deviation, 1.6 % for the skewness and 1.0 % for the excess kurtosis). A table with the
476 distribution metrics for all 15 scenarios can be found in the supplement (Table S3). Therefore we can assume that the shape of
477 TTDs is not significantly influenced by the precipitation event sequence – at least in environments with a naturally short
478 interarrival time resembling humid climate conditions and an event amount distribution that is exponential.

479

Kommentiert [IHh13]: - Line 401. This discussion is based on log-log plots, which many times are misleading. The convergence of curves at large time can be an artifact of the plots.
Answer: It is correct that log-log plot can make large differences at large times appear smaller. However, they also exaggerate small differences at short times. In this particular case we are interested more in the short time differences because we expect the largest differences at the beginning of the TTDs. At late times, differences are averaged out more and more.

Kommentiert [IHh14]: - Line 408-409. Differences seems larger to me. Again, the log-log plot does not help.
Answer: We double-checked the numbers and they are correct. The fact that the differences seem larger is probably due to the very high resolution of the log-log plot for short and very short times.

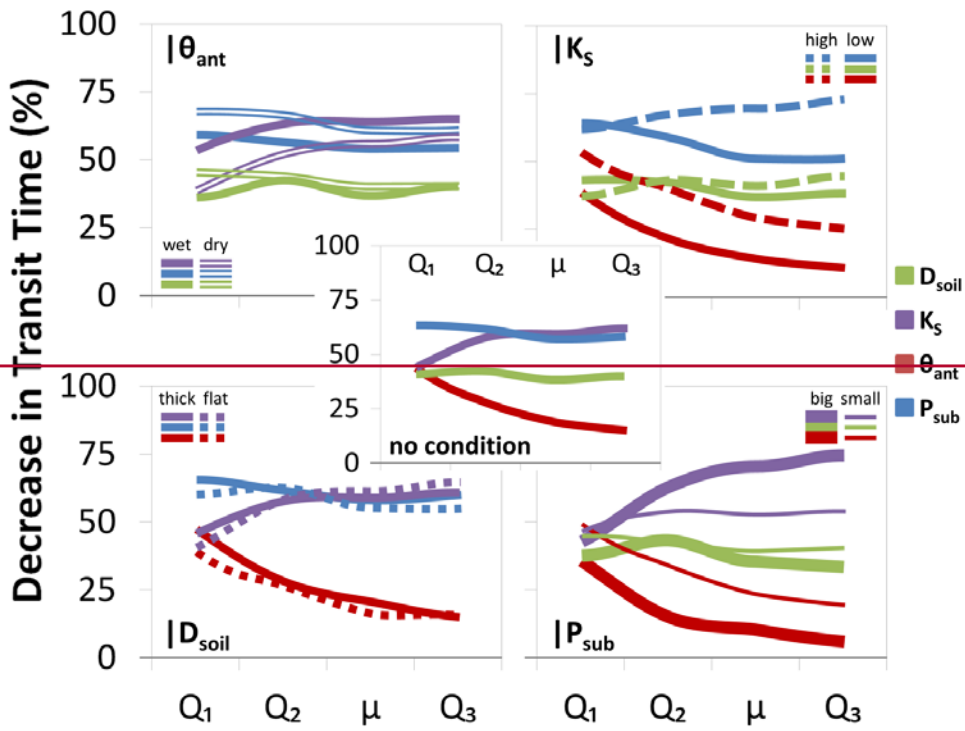


480
481 **Figure 5: 15 TTDs resulting from 15 different precipitation time series with all other catchment and climate properties being equal.**
482 **The first few events have the largest influence on the TTD shapes, while subsequent events gradually even out the differences. Inset**
483 **shows cumulative distributions.**

484 3.2. Effects on TTD metrics

485 We found that θ_{ant} affects the young parts of TTDs (the first 10 days) a lot more than the older parts (its influence is hardly
486 discernible after approximately 100 days, [see center panel in Fig. 6](#)). By contrast, K_S affects the older parts more than the
487 young parts. [This difference is due to the fact that \$\theta_{ant}\$ constitutes one of the initial conditions that also directly influences the](#)
488 [current soil hydraulic conductivity while the influence of different \$K_S\$ values gains more importance later when the soil](#)
489 [moisture conditions become more similar.](#) D_{soil} and P_{sub} influence all parts of the TTDs equally strong and hence have the
490 smallest influence on the actual shape of the distributions ([center panel in Fig. 6](#)). As can be observed in the upper left panel,
491 the influence of K_S is a lot stronger in scenarios with [wethigh](#) θ_{ant} while the influence of P_{sub} decreases with increasing θ_{ant} .
492 The upper right panel shows that both θ_{ant} and P_{sub} have a larger influence when K_S is high, but for P_{sub} this increased ~~in~~
493 influence is only seen for the longer transit times. [The influence of the initial condition \$\theta_{ant}\$ is larger when \$K_S\$ is high because](#)
494 [the relative differences in flow through a dry soil and a wet soil are larger for soils with high \$K_S\$ compared to soils with low](#)
495 [\$K_S\$.](#) The lower left panel confirms the impression that D_{soil} only has a minor influence on the shape of TTDs – all parts of the

496 TTDs are equally affected and it does not make a significant difference for the influence of the other factors whether the soils
497 are deeper or shallower. Finally in the lower right panel it is demonstrated that P_{sub} has opposite effects on the influence of θ_{ant}
498 and K_S : Larger P_{sub} causes the influence of K_S to increase for the longer transit times while the influence of θ_{ant} decreases when
499 P_{sub} becomes larger. The fact that different catchment and climate properties have varying degrees of control on transit times
500 depending on current conditions and the interplay of dominant hydrologic processes has already been observed in the field
501 (Heidbüchel et al., 2013). Table 1 lists all metrics of the 36 TTDs resulting from the base-case scenarios.
502



503

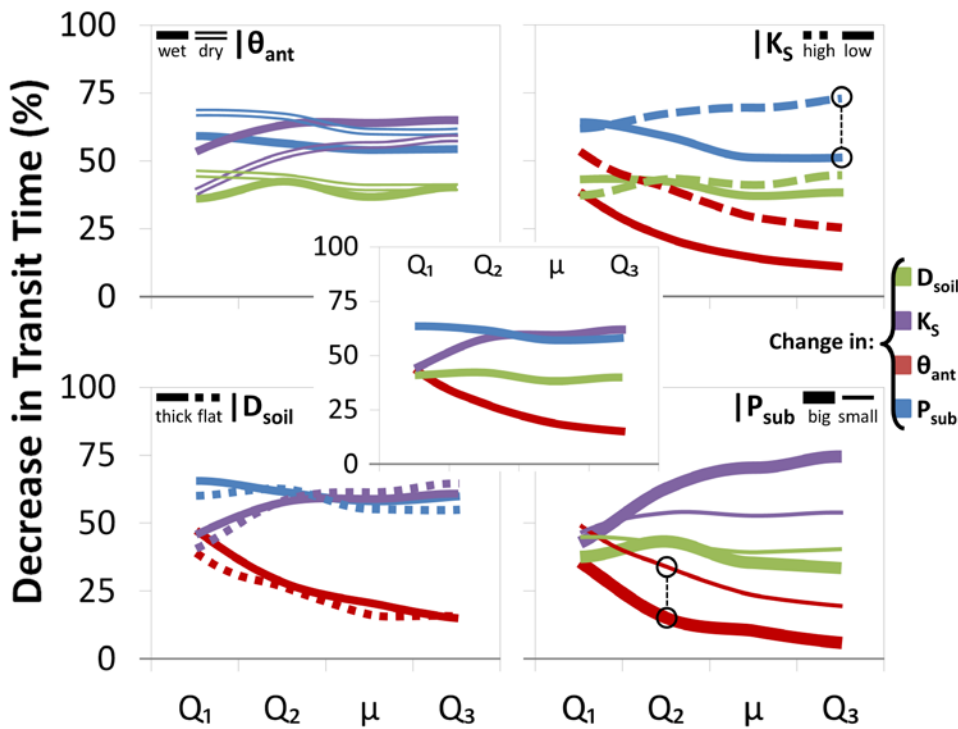


Figure 6: Influence of different properties on different parts of the TTDs. Shown is the average percent decrease in transit time for each quartile (Q_1 , Q_2 , Q_3) and the mean (μ) of the TTDs caused by a decrease in D_{soil} from 1 to 0.5 m (green), an increase in K_s from 0.02 to 2 m day^{-1} (purple), an increase in θ_{ant} from 50 % to 90 % effective saturation S_{eff} (red) and an increase of P_{sub} from 0.3 to 1.4 m a^{-1} (blue). The panel in the center in the foreground shows the average decrease in transit time for changing each of the four properties, the four panels in the background show the decrease in transit time conditional on the variation of one of the four properties (θ_{ant} , K_s , D_{soil} , and P_{sub}), respectively. Two examples are illustrated by the black circles: 1) The dashed blue line in the upper right panel shows that the increase of P_{sub} has a larger influence on the third quartile transit time (Q_3) – a decrease of ~75 % instead of just ~50 % – for a catchment with a high K_s compared to a catchment with a low K_s . 2) The thick red line in the lower right panel shows that the increase in θ_{ant} from 50 % to 90 % S_{eff} has a smaller influence on the second quartile transit time (Q_2) – a decrease of just ~15 % instead of ~35 % – for a catchment with a big P_{sub} compared to a catchment with a small P_{sub} .

Kommentiert [IHh15]: Figure 6. I think the order of the legend does not correspond with the panels. But this figure is really hard to understand. For example the center front panel shows "no condition", but still it causes a decrease in traveltime. (y axis). So the decrease is relative to what? All the different colors and linetypes make it hard to understand. Agreed. This is a very complex figure that is hard to understand. We have made another effort to make it clearer and simpler (also adding more explanation in the text and in the caption). We double-checked and all the different colors and line types are indeed correct (also the order in the legends).

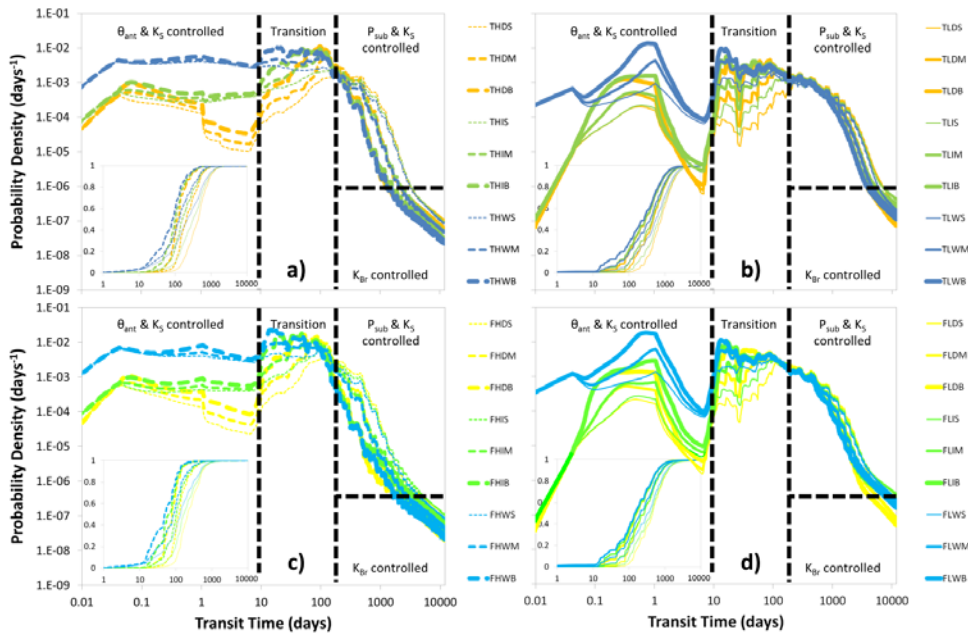
3.2.1. Antecedent moisture content

Dry θ_{ant} result in a lower probability for shorter transit times while wet High θ_{ant} trigger results faster responses and in higher initial peaks for TTDs (Fig. 7). When increasing θ_{ant} by 14 % (from S_{eff} 50 % to 90 %), on average Q_1 is shortened by 44 %, Q_2 decreases by 27 %, the mTT by 19 % and Q_3 by 15 % (Fig. 6 center, Table 1). The median F_{yw} increases by 16 %. Neither

519 the standard deviation (and hence the width) nor the skewness nor the kurtosis values of the TTDs are affected much by θ_{ant}
520 though. Higher θ_{ant} initially promotes faster lateral transport (both on the surface and in the subsurface) while impeding
521 percolation of tracer towards the bedrock, therefore more tracer is transported fast towards the outlet and less tracer is entering
522 the deeper soil layers and the bedrock. Long-term trends or interannual shifts in P_{sub} can cause temporal changes in TTDs but
523 substantial short-term variations are derived mainly from differences in θ_{ant} . Therefore variations in TTD shape and scale can
524 be high even in relatively small catchments. Generally, the influence of θ_{ant} is stronger for catchments with higher K_S and for
525 climates with smaller P_{sub} (Fig. 6).

526 3.2.2. Saturated hydraulic conductivity

527 High K_S values are associated with TTDs that have higher initial values and lighter tails. Also, a decrease in K_S causes more
528 pronounced ups and downs in the TTD with the effect of individual rainfall events being better discernible even in the later
529 parts of the TTD (right panel on Fig. 8). Increasing K_S by 2 orders of magnitude on average shortens Q_1 by 44 %, Q_2 by 58 %,
530 the mTT by 59 % and Q_3 by 62 % (Fig. 6 center, Table 1). The median F_{yw} increases by 13 %. The standard deviation increases
531 with decreasing K_S , while the skewness and kurtosis both decrease significantly – TTDs become less skewed and more
532 platykurtic (flatter). The interplay between K_S and θ_{ant} is obvious in that the influence of θ_{ant} decreases over time while the
533 influence of K_S increases. Initially θ_{ant} controls the soil hydraulic conductivity, the partitioning of the tracer into surface and
534 subsurface flow and also the spreading within the soil. Later on, as moisture conditions become more similar for scenarios
535 with identical P_{sub} and D_{soil} , K_S gains in importance while θ_{ant} becomes less relevant. The influence of K_S increases for wet θ_{ant}
536 (especially for short transit times) and for big P_{sub} (especially for long transit times) since both maximize the differences in
537 hydraulic conductivity between catchments – the drier the conditions the more similar are the unsaturated hydraulic
538 conductivities in general (Fig. 6).



540

541 Figure 7: Results of the 36 model runs. TTDs are grouped by soil depth (upper panels a and b = deep (thick); lower panels c and d
 542 = shallow (flat)) and hydraulic conductivity (left panels a and c = high; right panels b and d = low). Yellow colors indicate dry, green
 543 intermediate and blue wet antecedent moisture conditions; thick lines indicate large, mid-sized lines medium and thin lines small
 544 amounts of subsequent precipitation amounts. Insets show cumulative TTDs. Dashed black lines divide TTDs into four parts, each
 545 part controlled by different properties. Note the log-log axes.

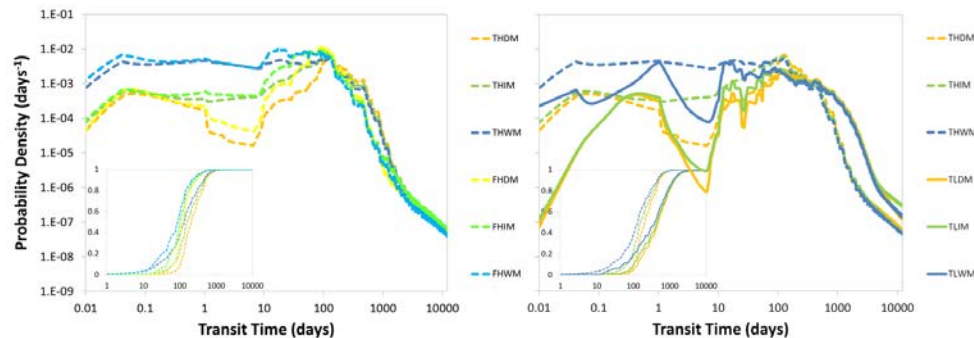
546 3.2.3. Subsequent precipitation amount

547 **BigLarge** P_{sub} compresses the TTDs (Fig. 7). Doubling P_{sub} , on average shortens Q_1 by 63 %, Q_2 decreases by 61 %, the mTT
 548 by 57 % and Q_3 by 58 % (Fig. 6 center, Table 1). The median F_{yw} increases by 22 %. The standard deviation (and hence the
 549 width) decreases by 42 %, while the skewness of the TTDs more than doubles. **BiggerLarger** P_{sub} causes more leptokurtic
 550 (peaked) TTDs. Big amounts of P_{sub} increase the total flow through the catchment (both in the soil and bedrock) and hence
 551 control how effectively tracer is flushed out of the system. TTDs will have lighter tails and shorter mTTs mainly due to the
 552 fact that a bigger P_{sub} flushes the soils faster and only allows a smaller fraction of the precipitation events to infiltrate into the
 553 bedrock. The fraction of water entering the bedrock depends strongly on the contact time of that water with the soil–bedrock
 554 interface. That means that in regions with small P_{sub} a larger fraction of precipitation has the chance to infiltrate into the
 555 bedrock before it is flushed out of the soil layer by subsequent precipitation. Therefore the tails of TTDs in more arid regions

556 tend to be heavier than the TTD tails in humid regions. The influence of P_{sub} is larger for dry θ_{amt} and high K_S (especially for
557 the longer transit times) (Fig. 6).

558 3.2.4. Soil depth

559 Decreasing D_{soil} causes a larger fraction of tracer to arrive at the outlet faster (left panel on Fig. 8). Halving D_{soil} shortens all
560 the quartiles and the mTT of the TTDs on average by approximately 40 % (Fig. 6 center, Table 1), while the median F_{yw}
561 increases by 10 %. The standard deviation (the width of the TTD) is decreased by 19 % and the skewness is increased by about
562 56 %. Shallower soils cause more leptokurtic (peaked) TTDs almost doubling the excess kurtosis. Shallower soils saturate
563 faster than deeper soils, they also redirect tracer more quickly from vertical to lateral flow, and therefore the early response in
564 shallower soils is slightly stronger. According to our findings, D_{soil} has only little influence on TTD shape. In catchments with
565 deeper soils we should, however, expect longer transport times.



567
568 Figure 8: Influence of soil depth (left) and saturated soil hydraulic conductivity (right) on the shape of TTDs. Lighter shades of one
569 color indicate shallower soils; dashed lines indicate higher hydraulic conductivity. Insets show cumulative TTDs.

570 3.3. General observations on the shape of TTDs

571 The simulation results suggest that the TTDs can be visually divided into four distinct parts (Fig. 7), where the shape of three
572 parts is clearly controlled by the catchment and climate properties and the fourth is a transition zone. The shape of the initial
573 part of the TTD (up to ~10 days) depends strongly on θ_{amt} and K_S (in accordance with Fiori et al., 2009) and less strongly on
574 D_{soil} . For example, TTDs in soils with high θ_{amt} or K_S exhibit higher initial peaks with a larger probability for short transit times.
575 Starting approximately after 10 days a transition period follows where no individual parameter dominates. During this period
576 precipitation drives the emptying of the uppermost soil layers with the presence of faster and/or larger flows (in catchments
577 with higher K_S / bigger P_{sub}) being gradually compensated by higher remaining concentrations of tracer (in catchments with
578 lower K_S / smaller P_{sub}) so that the tracer mass outflux at the catchment outlet converges towards a very similar value at around

Kommentiert [IHh16]: - Section 3.3. Some of the (interesting) conclusions here are very similar to those of Fiori et al (Stochastic analysis of transport in hillslopes: Travel time distribution and source zone dispersion, WRR 2009) which I think is important for this work. There, the different parts of the Gamma distribution pertains to different mechanisms and parameters (soil, bedrock, etc.). The main difference is that they identify the important role of KBr in the behavior of the tail, which is the exponential part of the Gamma, which in turn is related to groundwater discharge. The aquifer volume, which depends on water table, thickness and slope, has an important role here.
Answer: Thank you for pointing us to this reference. It is indeed a very interesting study that we were not aware of yet. In the revised manuscript we have included it.

579 120 days before diverging again. After the transition period, the shape of the TTDs is governed by P_{sub} (i.e. essentially the
580 climate) and K_S , with larger P_{sub} and higher K_S causing a more rapid decline of outflow and hence a compression of the TTDs.
581 Finally, the shape of the tails of the TTDs is controlled by the hydraulic conductivity of the bedrock K_{Br} (not the soil K_S) (see
582 also Fiori et al., 2009). In many cases (These tails constitute straight lines in the log-log plots (which is necessary but
583 insufficient for identifying follow-power law functions) in many (but not in all) cases. Furthermore, all modeled TTDs share
584 one common feature – for every subsequent precipitation event there is a more or less discernible spike. Generally, larger
585 subsequent events cause higher spikes (i.e., a higher proportion of outflow during those events) while the size of the spikes
586 decreases at later times. And although this multitude of local maxima in the probability density curve does invoke a sense of
587 irregularity, the general pattern of shapes of the TTDs is not influenced by the individual subsequent events (Fig. 5 and Table
588 S3 in the supplement), which is why we decided to smooth the TTDs for visual comparison so that the underlying systematic
589 changes in shapes are more clearly visible and understood (see Fig. S75 in the supplement).

590 Practical implications can be drawn from our results concerning, e.g., pollution events. Some catchments are more vulnerable
591 to pollution in the sense that they tend to store pollutants for a longer period of time and hence exhibit long legacy effects.
592 Especially catchments with TTDs with heavy tails belong in that category (i.e. catchments with deeper soils and a moderate
593 hydraulic conductivity difference between soil and bedrock). Also, certain moments in time are worse for pollution events to
594 happen – a spill occurring during dry conditions will stay in the catchment longer than a spill during wet conditions because it
595 is more likely to reach the bedrock and stay in contact with it before it is flushed out of the soils. Accordingly, locations and
596 situations that lead to a longer storage of decaying pollutants will eventually release less of the solutes downstream.

597 We also plotted the probability density replacing the actual transit time with the cumulative outflow to check whether this
598 would eradicate the differences between the different distributions (see Fig. S108 in the supplement). We made two interesting
599 observations: 1. For the scenarios with high K_S , the differences between the distributions were reduced considerably. Especially
600 for the cumulative probability distributions there were hardly any discernible differences left. The largest discrepancies could
601 still be found in the early part of the distributions where the distributions with high θ_{amt} continued to have larger outflow
602 probabilities. 2. For the scenarios with low K_S , the individual distributions did not collapse into a single cumulative probability
603 distribution. They rather split up into three distributions according to their P_{sub} values. That means that for the scenarios with
604 larger P_{sub} a larger amount of cumulative outflow was necessary to flush out the same amount of tracer compared to the
605 scenarios with smaller P_{sub} .

606 3.4. Distribution fitting

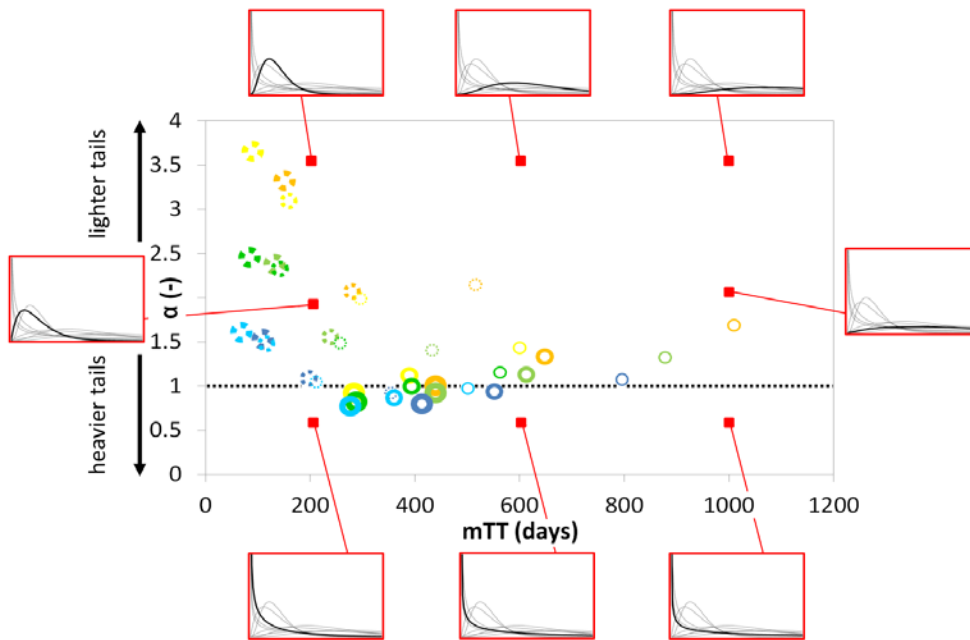
607 Shape parameters of the best-fit Inverse Gaussian (D), Gamma (α) and Log-normal Advection-Dispersion (σ) (D) distributions
608 as well as flow path numbers (F) for the 36 different scenarios are listed in Table 2. The parameters D , α and σ range from
609 0.15 to 0.98, from 0.78 to 3.66 and from 0.51 to 1.15 ~~0.15 to 0.98~~, respectively. F ranges from -0.22 to 0.63 .

610 First we compared the performances of only these three probability distributions with two parameters. Out of the 36 model
611 scenarios, the Inverse Gaussian Advection-Dispersion model (AD) yielded the best fit 549 times, the GammaBeta model 135

Kommentiert [IHh17]: - Line 490. I don't see the power law.
Answer: We are aware of the fact that straight lines in log-log plots are necessary for identifying power laws but insufficient as evidence. So we cannot be sure whether they are actually power laws just from this graphical analysis. Therefore we have changed our focus away from the power-law towards the characteristic break in the slope where the tail part begins.

612 times and the Log-normal Gamma model 128 times (however, 14 times there was no significant difference in the performance
613 of the Beta and Gamma models). In general, the Log-normal AD model works a little better for high K_S and dry θ_{ant} and small
614 P_{sub} , the Beta and Gamma models for low K_S and wet θ_{ant} and big P_{sub} , while the Inverse Gaussian is less ideal for capturing
615 the shape of the modeled TTDs (Table 3 and S34 in the supplement). Contrary to that, the Inverse Gaussian Gamma model
616 represents the mean transit time (mTT) better/less correctly than the other two distributions models (Table 3). On average, the
617 mTT of the fitted Gamma models deviates from the observed mean by 2430 % (88 days) with a maximum deviation of 423
618 days for one scenario, underpredicting in dry and overpredicting for wet θ_{ant} , while the Inverse Gaussian AD and Beta models
619 performs much better in this regard with an average deviation from the mTT of only 5 and 4 % (17 and 13 days) with a
620 maximum deviations of 102 and 38 days, respectively. The Beta model almost always slightly underpredicts the mTT while
621 the Gamma AD model especially underoverpredicts the mean when P_{sub} is small. The correct identification of the median transit
622 time works much better for the Gamma model— here the average deviation of the fitted median from the observed median is
623 only 4 % (12 days) with a maximum deviation of 59 days—matching the performance of the Beta model. The Inverse
624 Gaussian AD and Log-normal model yields average deviations from the median transit time of 6 and 5 % (15 and 13 days)
625 with a maximum deviations of 50 and 43 days, respectively.
626 Then we included the two probability distributions with three parameters (Beta, Truncated Log-normal) into the analysis and
627 investigated how they compared to the two-parameter distributions. The performance of the Beta was quite similar to the one
628 of the Gamma in terms of representing TTD shapes and the median transit times. However, it was able to capture the mTTs a
629 lot better than the Gamma, even surpassing the performance of the Inverse Gaussian on average (average deviation 4 %, 13
630 days, maximum deviation 38 days), especially in environments with low K_S values. Finally, the Truncated Log-normal
631 distribution performed best in every regard capturing TTD shapes, mTTs and median transit times better than all other
632 distributions (mTT average deviation 3 %, 10 days, maximum deviation 91 days; median transit time average deviation 4 %,
633 11 days, maximum deviation 36 days) (Table 3).
634 Figure 9 gives an overview of the shape and scale of our modeled TTDs (using the best-fit Gamma distribution parameters).
635

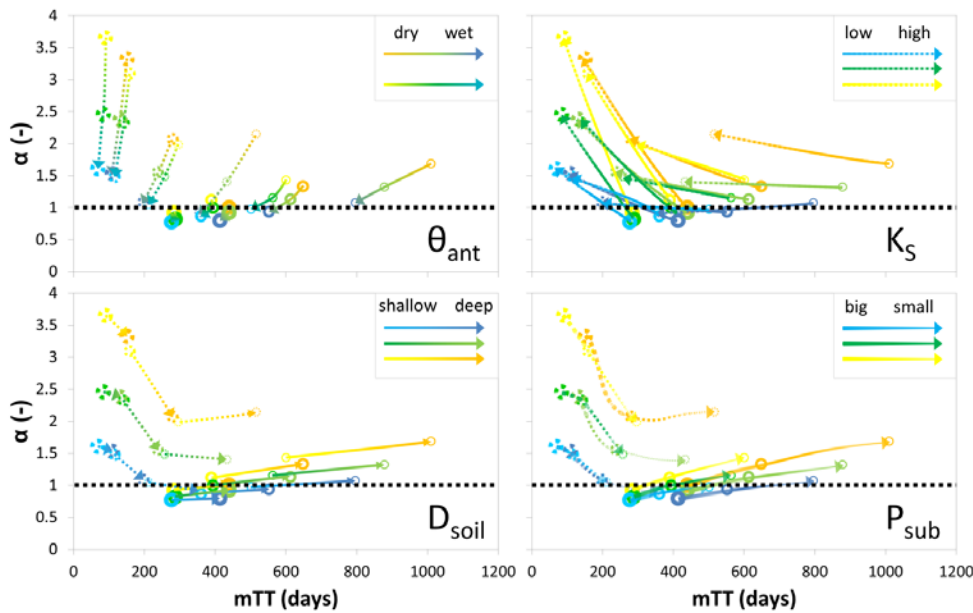
Kommentiert [IHh18]: - Line 510. How is the fitting done? What inference methods? How one can say that a distribution performs better than another? Any statistical test?
Answer: In Section 2.4.3 (Fitting) we describe the procedure. It was done by the least squares method on the cumulative distributions.



636
 637 Figure 9: Gamma shape parameters (α) and mean transit times (mTTs) for individual scenarios with different combinations of
 638 catchment and climate properties. Yellow colors indicate dry, green intermediate and blue wet θ_{amt} ; thick marker lines indicate
 639 large, mid-sized lines medium and thin lines small P_{sub} ; solid lines indicate low, dashed lines high K_S ; lighter shades of a color
 640 indicate shallow, darker shades deep D_{soil} . The red boxes contain exemplary Gamma distributions with shape and scale
 641 corresponding to the red dot location.

642
 643 **3.5. Predicting the shape of TTDs**

644 Figure 10 shows how the shape and scale of TTDs change with the individual catchment and climate properties. For increasing
 645 θ_{amt} , TTDs converge towards L-shaped distributions with shorter mTTs (in highly conductive soils the shape is more affected
 646 than the scale, in soils with low K_S the scale is more affected than the shape). When K_S is increasing, mTT is decreasing (in
 647 case P_{sub} is big then the shapes of the TTDs also changes towards having lighter tails). Quite similar patterns can be observed
 648 for increasing D_{soil} and decreasing P_{sub} , – with mTTs becoming longer and TTD shapes increasing the tail weight when K_S is
 649 high and becoming more humped when K_S is low.



651 **Figure 10: Change of Gamma shape parameters (α) and mean transit times (mTTs) for four catchment and climate properties.**
 652 **Yellow colors indicate dry, green intermediate and blue wet θ_{ant} ; thick marker lines indicate large, mid-sized lines medium and thin**
 653 **lines small P_{sub} ; solid lines indicate low, dashed lines high K_S ; lighter shades of a color indicate shallow, darker shades deep D_{soil} .**

655 Non-linear regression analysis relating the shape and scale parameters of the fitted Log-normal-AD and Gamma distributions
 656 to any single soil, precipitation or storage property (D_{soil} , K_S , θ_{ant} , P_{sub}) did not yield satisfying relations that could be used to
 657 predict TTD shapes. **The best relationships we found were between the shape and scale parameters and K_S :** 1) α is related to
 658 K_S via a positive exponential relationship ($R^2 = 0.74$) for dry θ_{ant} ; 2) β is related to K_S via a negative exponential relationship
 659 ($R^2 = 0.73$) for dry θ_{ant} ; 3) D is related to K_S via a negative exponential relationship ($R^2 = 0.74$) for dry θ_{ant} ; and 4) mTT is
 660 related to K_S via a negative exponential relationship ($R^2 = 0.60$) for wet θ_{ant} . Here, we would like to present the significant non-
 661 linear relationships we found between the shape parameters of the fitted TTDs and the flow path number F ($R^2 = 0.90$) (Eq.
 662 12 and 13), mainly because we can draw much more general conclusions on TTD shapes using a dimensionless number (Fig.
 663 9[1]):

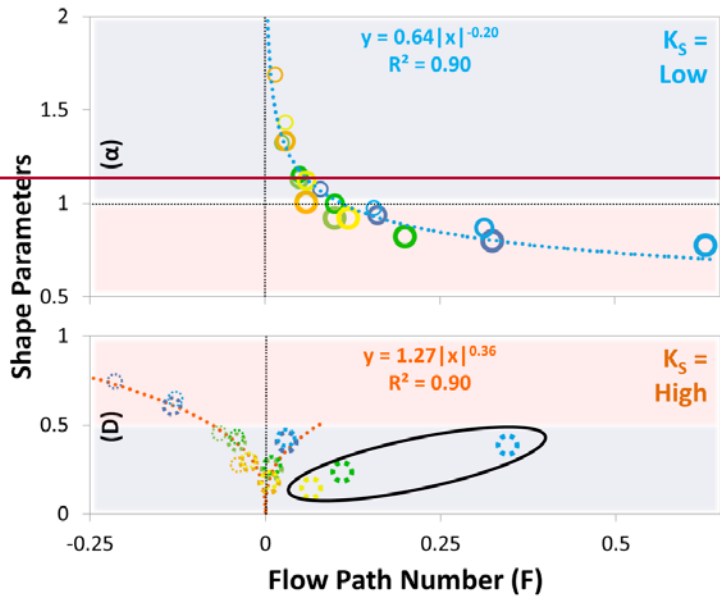
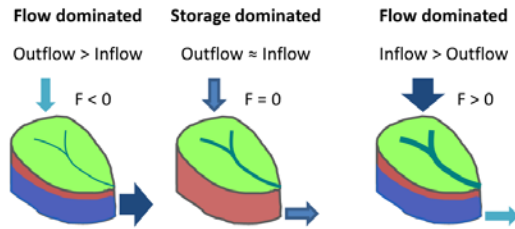
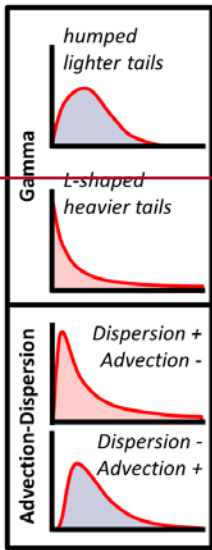
664 Shape parameter $\alpha(F) = 0.64|F|^{-0.20}$, $\text{if } K_S < 0.2 \text{ md}^{-1}$, ————
 665 (12)

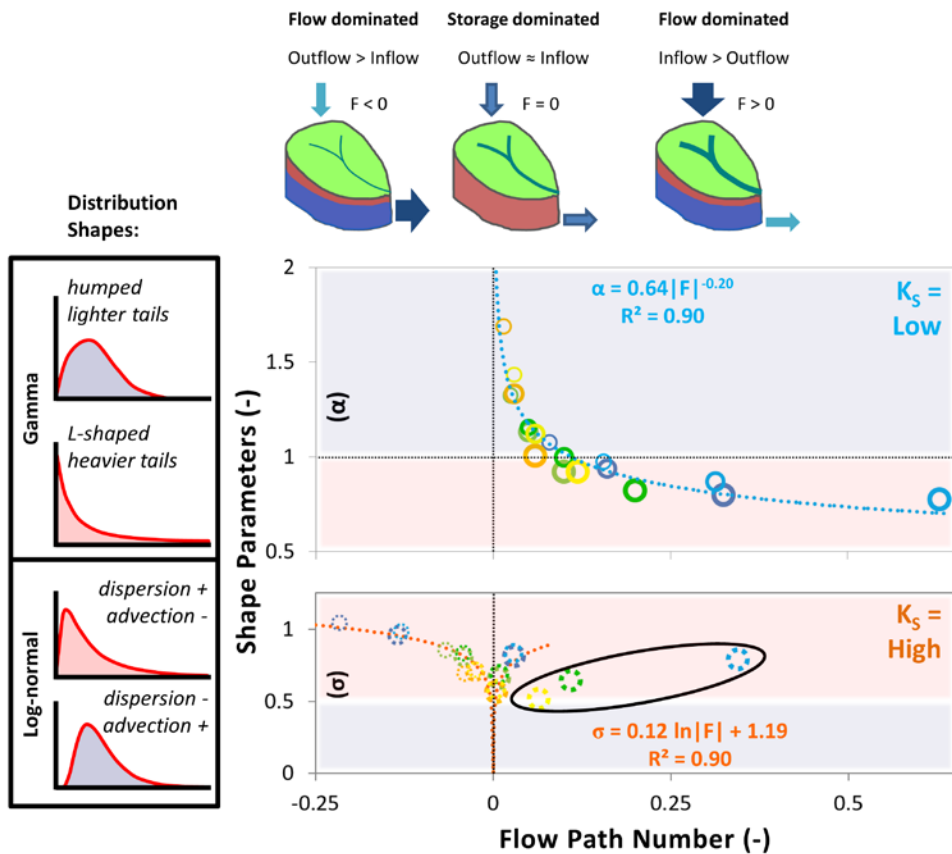
Kommentiert [IHh19]: Figure 11: why does panel D have curved lines while all the others are straight.
 If you look closely, you can see that the lines in panel A are also slightly curved. This is due to the fact that both P_{sub} and θ_{ant} have three different modes (large, medium, small and wet, intermediate, dry) while D_{soil} and K_S have both only two modes.

666 Shape parameter $D\sigma(F) = 0.127 \ln|F| + 1.194|F|^{0.36}$, if $K_s \geq 0.2 \text{ md}^{-1}$. ———
 667 (13)

668 Generally, for similar catchments with low K_s , Gamma distributions are more likely to fit the TTDs. The relatively higher
 669 proportion of surface flow within and surface outflow from these catchments seems to favor flow and transport dynamics that
 670 are best represented by the shapes of Gamma distributions because they are able to capture both rapid response (high initial
 671 values) as well as the relatively slow outflow from the soils and the bedrock (long tails). In contrast, similar catchments with
 672 high K_s and only small proportions of surface flow are more likely to behave according to ~~Log-normal Advection-Dispersion~~
 673 distributions with less rapid response from surface flow (low initial values) and faster outflow from the more conductive soils
 674 (~~higher and narrower modes at intermediate transit times; shorter tails~~). A notable exception are scenarios where catchments
 675 with highly conductive soils still experience larger proportions of surface outflow (> 25 %; $F > 0.05$) due to large amounts of
 676 P_{sub} – these dynamics cannot be predicted by the same relationship since they produce ~~AD~~-distributions with larger
 677 contributions of advective transport ~~and lighter tails~~ and hence smaller values of $D\sigma$ (indicated by the black circle in Fig. 911).
 678

Distribution Shapes:



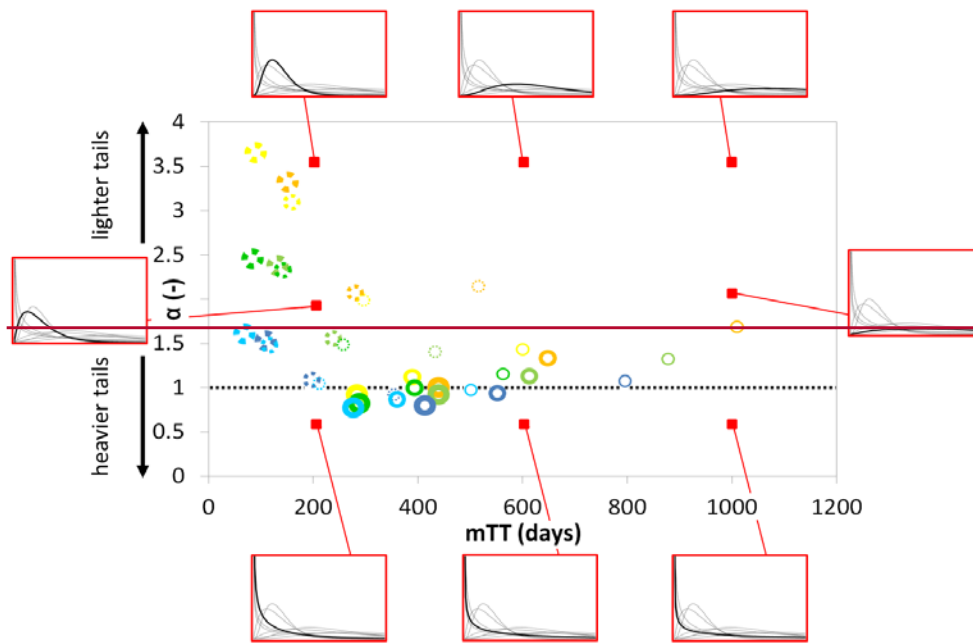


680
 681 **Figure 911:** Relationship between the dimensionless flow path number F and the shape parameters α (upper panel, scenarios with
 682 low K_S) and σ (lower panel, scenarios with high K_S) of the Gamma and the LogAdvection-normalDispersion distribution,
 683 respectively. Yellow colors indicate dry, green intermediate and blue wet θ_{ant} antecedent moisture conditions; thick marker lines
 684 indicate large, mid-sized lines medium and thin lines small P_{sub} amounts of subsequent precipitation; solid lines indicate low, dashed
 685 lines high K_{sat} saturated hydraulic conductivities; lighter shades of a color indicate shallow, darker shades deep D_{soil} soils. The dotted
 686 trend lines are the best-fit regressions for the relationship between the flow path number and the shape parameters α (light blue)
 687 and σ (orange). The points in the black circle are excluded from the regression analysis since they are associated with scenarios of
 688 excessive surface outflow.

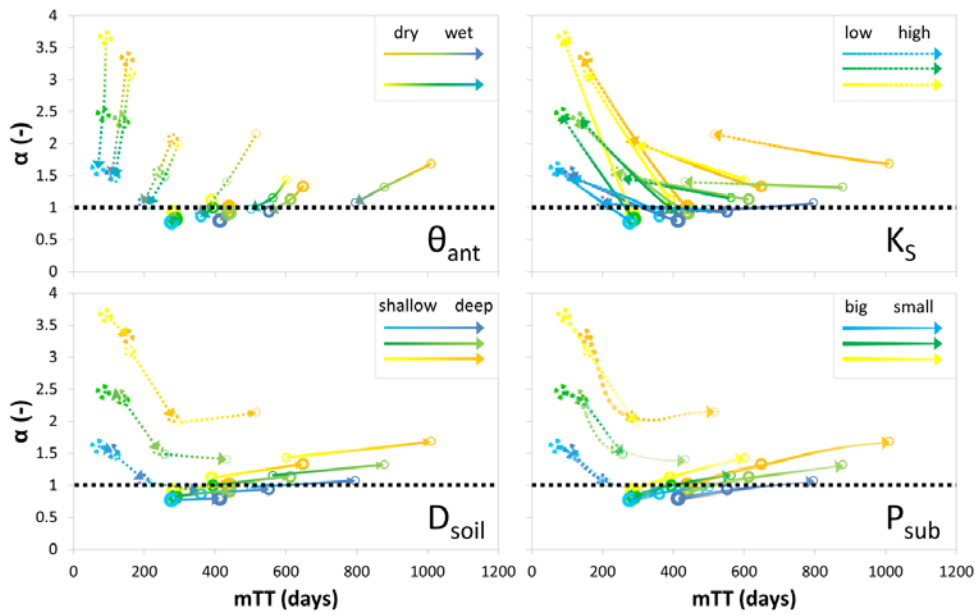
689 Figure 10 gives an overview of the shape and scale of our modeled TTDs. Figure 11 shows how the shape and scale of TTDs
 690 change with the individual catchment and climate properties. For increasing θ_{ant} , TTDs converge towards L-shaped

Kommentiert [1Hh20]: Figure 9 and 10: Fig 9 I don't understand why the alpha-plot has no dashed symbols and the D-plot has no solid symbols. This also doesn't seem to match with fig. 10 that has both dashed and solid symbols? This correct observation is due to the fact that we recommend using gamma distributions for catchments with low hydraulic conductivity (solid) and Log-normal distributions for catchments with high hydraulic conductivity (dashed). In figure 10 we show relationships for all (low and high K_S) scenarios.

691 distributions with short mTTs (in highly conductive soils the shape is more affected than the scale, in soils with low K_S the
 692 scale is more affected than the shape). When K_S is decreasing mTT is decreasing (in case P_{sub} is big then the shapes of the
 693 TTDs also changes towards having lighter tails). Quite similar patterns can be observed for increasing D_{soil} and decreasing P_{sub}
 694 — with mTTs becoming longer and TTD shapes increasing the tail weight when K_S is high and becoming more humped when
 695 K_S is low.



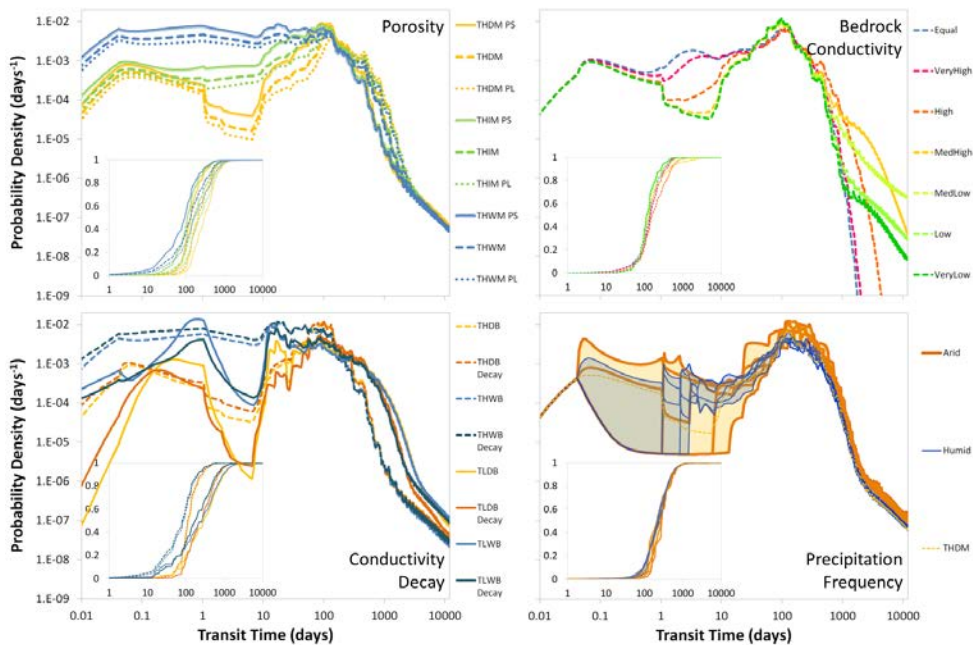
697
 698 **Figure 10: Gamma shape parameters (α) and mean transit times (mTTs) for individual scenarios with different combinations of**
 699 **catchment and climate properties. Yellow colors indicate dry, green intermediate and blue wet antecedent moisture conditions; thick**
 700 **marker lines indicate large, mid-sized lines medium and thin lines small amounts of subsequent precipitation; solid lines indicate**
 701 **low, dashed lines high saturated hydraulic conductivities; lighter shades of a color indicate shallow, darker shades deep soils. The**
 702 **red boxes contain exemplary Gamma distributions with shape and scale corresponding to the red dot location.**



704
705 **Figure 11: Change of Gamma shape parameters (α) and mean transit times (mTTs) for four catchment and climate properties.**
706 **Yellow colors indicate dry, green intermediate and blue wet antecedent moisture conditions; thick marker lines indicate large, mid-**
707 **sized lines medium and thin lines small amounts of subsequent precipitation; solid lines indicate low, dashed lines high saturated**
708 **hydraulic conductivities; lighter shades of a color indicate shallow, darker shades deep soils.**

709 **3.6. Effects of other factors on the shape of TTDs**

Kommentiert [IHH21]: Figure 11: why does panel D have curved lines while all the others are straight. If you look closely, you can see that the lines in panel A are also slightly curved. This is due to the fact that both P_{sub} and θ_{ant} have three different modes (large, medium, small and wet, intermediate, dry) while D_{soil} and K_S have both only two modes.



711
 712 **Figure 12: Overview of how certain catchment and climate characteristics influence the shape of TTDs. 1. Porosity – solid lines**
 713 **indicate small, dotted lines large porosity. 2. Hydraulic conductivity of the bedrock – characterized in comparison to the K_s of the**
 714 **soil layer. 3. Decay in saturated soil hydraulic conductivity with depth – darker shades of one color represent scenarios with decay,**
 715 **lighter shades scenarios without decay. 4. Precipitation frequency – orange TTDs are low-frequency (“arid type”) scenarios, blue**
 716 **TTDs are high-frequency (“humid type”) scenarios. The shaded areas between the lines illustrate the higher shape variability for**
 717 **the low-frequency TTDs. Insets show cumulative TTDs.**

718 3.6.1. Porosity

719 The influence that soil porosity exerts on the shape of TTDs is quite similar to the influence of D_{soil} . Larger soil porosity causes
 720 a dampening of the initial response and increasing transit times in all parts of the TTD (just like deeper soils, see Fig. 12 and
 721 Table S5 in the supplement4). Increasing porosity also causes larger standard deviations, smaller skewness and smaller kurtosis
 722 (i.e. less peaked TTDs).

723 3.6.2. Hydraulic conductivity of the bedrock

724 Variations in the saturated hydraulic conductivity of the bedrock K_{Br} affect the shape of TTDs both in the initial part of the
 725 distributions but even more so in the tail (Fig. 12 and Table S6 in the supplement5). If K_{Br} is increased so that it equals the K_s

of the soil layer, we basically create one large continuum of homogeneous bedrock (or soil). Hence, the resulting TTD does not contain any abrupt breaks in slope and basically resembles outflow from a larger homogeneous reservoir. For lower K_{Br} breaks in the slope of the TTD tails start to appear indicating that the soil layers have already been emptied while the bedrock still contains water from the input precipitation event. For scenarios where K_{Br} is at least 3 orders of magnitude smaller than the soil K_S , the tails initially resemble power law distributions with constants (a) around 0.2 and exponents (k) around 1.6 for longer periods of time (Eq. 14):

$$TTD(t) = at^{-k}. \quad (14)$$

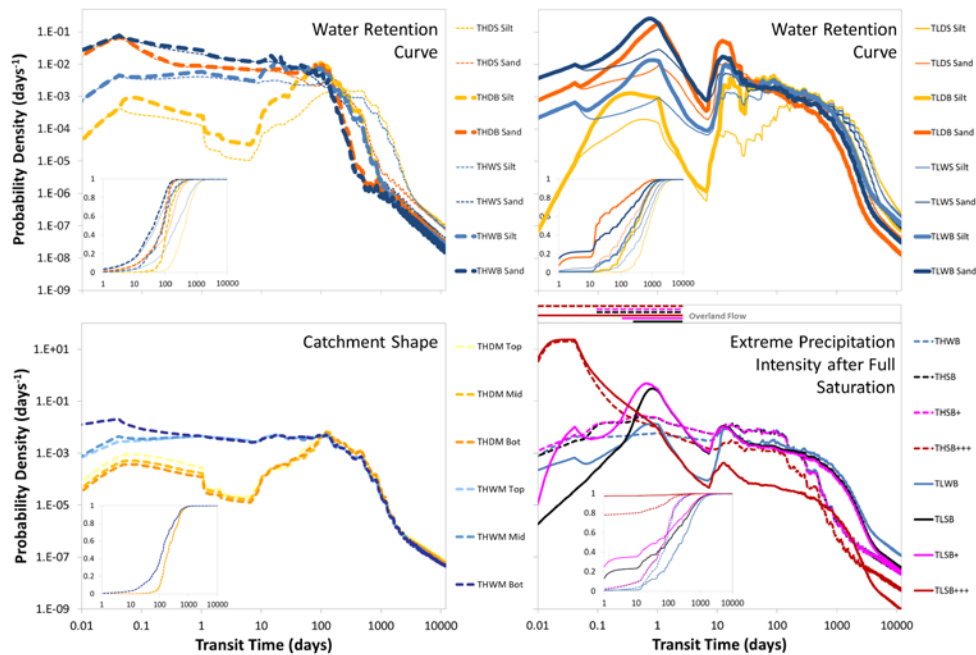
An exponent k smaller than 2 indicates that a mean value of the power law distribution cannot be defined since it is basically infinite, however, in our simulation results, the power law tails eventually break down when the bedrock domain is almost empty. Somewhat counterintuitively, the scenario with the lowest K_{Br} exhibits the shortest quartile and mean transit times. This is clearly an effect of a smaller fraction of water infiltrating into the bedrock and more water being transported laterally in the relatively conductive soil layer. We observe the longest quartile transit times in the scenario where K_{Br} is one order of magnitude lower than K_S and the longest mean transit time when it is 2 orders of magnitude lower. This is due to the fact that for these cases the higher K_{Br} causing faster transport within the bedrock is counterbalanced by the larger fraction of event water that enters into the bedrock where it is transported more slowly than in the soil. Therefore what seems paradoxical in the first place – longer mTTs when K_{Br} is higher – can be explained by differences in the runoff partitioning between soil and bedrock. This also explains the observation that the standard deviation of the TTDs initially increases with increasing K_{Br} while both skewness and excess kurtosis decrease.

3.6.3. Decay in saturated hydraulic conductivity with depth

For catchments that already have highly conductive soils, adding a decay in K_S (with higher K_S close to the surface and lower K_S close to the soil–bedrock interface) does not change the shape of TTDs to a great extent – all fitted shape parameters remain rather similar and transit times across the entire TTD are moderately shortened (Fig. 12 and Table S7 in the supplement6). We observe a larger impact if soil K_S is low. In these cases adding a decay reduces the standard deviation and increases the skewness and the kurtosis of the resulting TTDs (i.e., they become narrower, more skewed and more peaked). Additionally, the difference in transit times increases towards the late part of the TTD with mTT and Q_3 being considerably shorter when there is a decay in K_S . This difference between the smaller effects of a K_S decay in an already highly conductive soil compared to the larger effects for a low conductivity soil can be explained by the fact that the additional soil zones of higher conductivity are more effectively used for scenarios of generally low conductivity – in soils that are already quite conductive, a larger fraction of the incoming event water will still infiltrate to deeper soil layers before moving laterally whereas in low conductivity soils the faster lateral transport possible due to the K_S decay will be triggered much sooner and for a larger fraction of the incoming event water.

757 **3.6.4. Precipitation frequency**

758 The shape of TTDs is not influenced significantly by precipitation frequency since the mean values of all distribution metrics
 759 for the low-frequency (arid type) and the high-frequency (humid type) scenarios are quite similar to each other (Fig. 12 and
 760 Table S87). However, transit times in the high-frequency (humid) environment are shorter ($Q_1 = -17\%$, $Q_2 = -11\%$, $mTT =$
 761 -9% , $Q_3 = -3\%$). Additionally, the higher the precipitation frequency the **smaller** is the variation between individual
 762 TTDs. This is mainly due to two facts: When the precipitation frequency is high 1) the interarrival times are shorter which will
 763 more often mobilize event water and avoid longer periods of relative inactivity when the water “just sits” in the soil, 2) the
 764 amounts of precipitation events are on average smaller so that there is a smaller chance of a very big event “flushing” the entire
 765 system creating very short transit times for a preceding event followed by a long period of no or only small precipitation events.
 766 These transit time dynamics with regard to different patterns of precipitation have already been observed in the field
 767 (Heidbüchel et al., 2013).

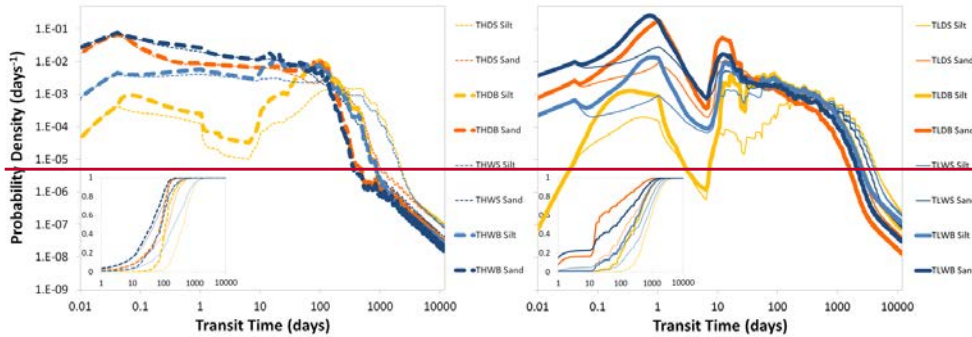


769 **Figure 13: Overview of how certain catchment and climate characteristics influence the shape of TTDs (continued). 1. Changes in**
 770 **TTDs due to differences in water retention curves (WRCs) – Left panel: scenarios with high K_s , right panel: scenarios with low**
 771

772 K_S . Light blue and yellow lines indicate silt-type soil WRCs, dark blue and orange lines indicate sand-type soil WRCs. Upper left
 773 panel: scenarios with high K_S , upper right panel: scenarios with low K_S . Insets show the cumulative TTDs. 2. Catchment shape –
 774 lighter shades of a color indicate top-heavy, darker shades bottom-heavy catchments. 3. Full saturation and extreme precipitation –
 775 black lines indicate fully saturated initial conditions, pink lines fully saturated initial conditions and very large event precipitation
 776 (+), red lines fully saturated initial conditions and extreme event precipitation (+++). The horizontal lines in the box above the
 777 diagram indicate periods where actual overland flow was recorded during the respective runs. The inset shows the cumulative TTDs.

3.6.5. Water retention curve

780 The TTDs from the scenarios with sand-type WRCs have higher initial peaks and lighter tails compared to the ones with silt-
 781 type WRCs (Fig. 13). Their transit times are consistently shorter over the entire distributions and the influence of other
 782 parameters (like K_S and θ_{ant}) on their shape is reduced. Sand-type TTDs are more skewed and more peaked than silt-type TTDs
 783 (Table S9 in the supplement⁸). Therefore they more closely resemble TTDs that we would expect in environments where
 784 preferential flow is present. Generally, the differences in TTDs between the different WRCs are more pronounced in the
 785 scenarios with low K_S because the wetting of the upper soil layers and hence the increase in the hydraulic conductivity takes
 786 relatively more time such that the differences between the two WRC scenarios are amplified. In the scenarios with silt-type
 787 WRCs the saturation process causes a slower increase in hydraulic conductivity since soil water potential decreases more
 788 gently with increasing soil water content.



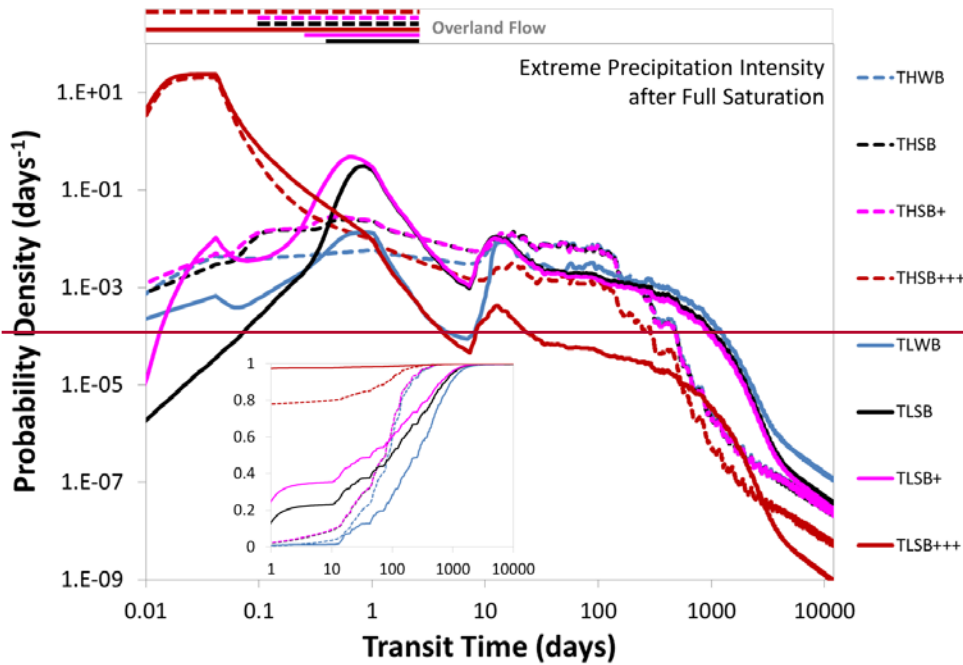
791 **3.6.6. Figure 13: Changes in TTDs due to differences in water retention curves (WRCs).**
 792 **Left panel: scenarios with high K_S , right panel: scenarios with low K_S . Light blue and**

793 ~~yellow lines indicate silt type soil WRCs, dark blue and orange lines indicate sand type~~
794 ~~soil WRCs. Insets show the cumulative TTDs.~~ Catchment shape

795 We observe unexpectedly little variation between the TTDs of the differently shaped catchments (Fig. 13). While Q_1 , Q_2 and
796 the mTT are all more or less similar, Q_3 increases slightly for catchments with a lower center of gravity and on average
797 shorter flow paths (Table S10 in the supplement). The influence of the catchment shape is fractionally larger for dry θ_{ant} .
798 Still, apparently the differences in catchment shape need to be a lot more pronounced than we explored in order to
799 significantly affect the TTD shape.

801 3.6.6.3.6.7. Full saturation and extreme precipitation

802 Starting runs with fully saturated soils increased the fractions of overland flow for both the high and the low K_S scenario
803 (THSB and TLSB). For THSB the fraction of outflow during the first 10 days that was overland outflow (SOF_{10}) increased
804 from 1 to 9 %. For TLSB the increase was even higher from 76 to 91 %. The increase had clear effects on the resulting transit
805 times. Especially the short transit times decreased while the longer transit times were less affected. That means the changes
806 we observed in the shape of the TTDs followed the pattern of increasing θ_{ant} (i.e. a higher percentage of transit time decrease
807 in the young fraction of the TTD, smaller impact at later times and in the shape metrics). Increasing the precipitation amount
808 and intensity of the input event by a factor of 100 (+; from 0.1 to 10 mm h⁻¹) affected only the low K_S scenario (TLSB+) further
809 decreasing the short transit times while the high K_S scenario was unaffected (THSB+). We had to increase the precipitation
810 intensity of the input event by a factor of 1000 (to 100 mm h⁻¹) to eventually create substantial amounts of initial overland
811 flow for both scenarios. Once this was triggered, the shape of the TTDs changed considerably. For these scenario (THSB+++
812 and TLSB+++), all quartiles of the TTDs decreased to less than one day and the whole distribution became extremely
813 leptokurtic (Fig. 143 and Table S11 in the supplement⁹).



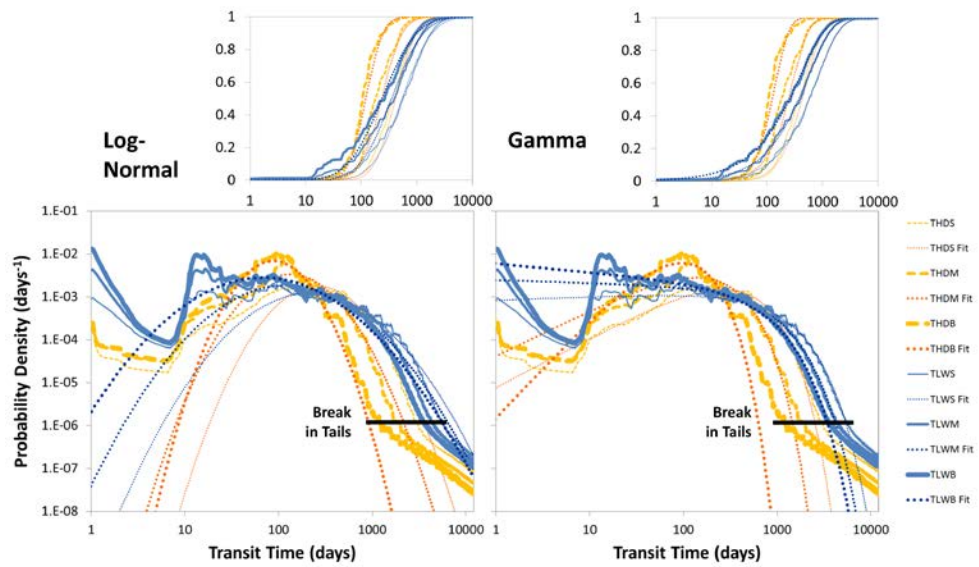
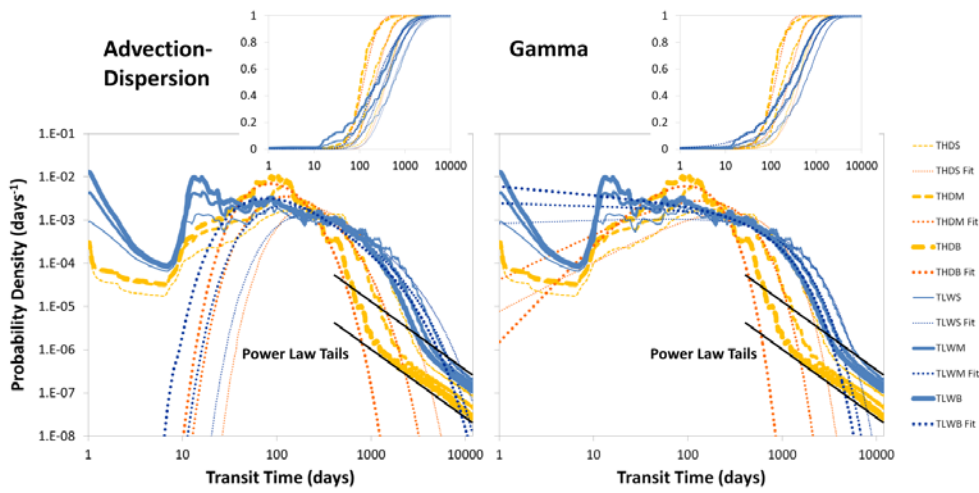
815
 816 Figure 14: Full saturation and extreme precipitation — black lines indicate fully saturated initial conditions, pink
 817 lines fully saturated initial conditions and very large event precipitation (+), red lines fully saturated initial
 818 conditions and extreme event precipitation (+++). The horizontal lines in the box above the diagram indicate
 819 periods where actual overland flow was recorded during the respective runs. The inset shows the cumulative
 820 TTDs.

821 **4. Discussion**

822 **4.1. Use of theoretical distributions**

823 None of the theoretical distribution functions we tested captures the shape of the observed TTDs adequately over the entire
 824 age range. On the one hand, this is due to the missing power law tails, on the other hand—and this is more relevant from a
 825 mass balance perspective—it results from a misrepresentation of the initial response. Looking at Fig. 7, 8 and 12 to 14, it

826 becomes clear that all TTDs are humped distributions, with none of them having an initial maximum (with a monotonically
827 decreasing limb afterwards) and none of them having a value of 0 after 1.5 minutes (the first time step reported). Since all AD
828 distributions start with a value of 0 and all Beta and Gamma distributions are either monotonically decreasing or start with a
829 value of 0 they are not perfect representations of the modelled TTDs for porous media. A set of theoretical probability
830 distributions—with initial values larger than 0, a rising limb to a maximum probability density and a falling limb with lighter
831 or heavier tails—would be the best option to represent variable TTDs. Potential candidates for these theoretical distributions
832 are truncated Gamma or lognormal distributions. The fact that TTDs in highly conductive soils and in under dry antecedent
833 conditions are better represented by the Log-normal AD distributions model can be explained by the circumstance that the
834 (rather empty) catchment storage has to be filled at least a little bit before faster flow paths are activated and substantial flow
835 out of the system can occur. This means that the early response is much better captured by a distribution that starts with an
836 initial value of close to 0. Furthermore, Log-normal distributions also work better in highly conductive soils than the high K_S
837 produces TTD modes tails that are higher and narrower lighter than the ones of Gamma distributions and more closely related
838 to the AD model. Contrary to that, low K_S values and wet antecedent conditions favor Gamma distributions because initial
839 outflow values are generally higher when the soil is closer to saturation while the TTD modes tails are lower and wider heavier
840 in soils that are less conductive (Fig. 14).



844 **Figure 154:** Modeled TTDs for low K_s , high θ_{ant} (blue) and high K_s , low θ_{ant} (yellow). Best-fit theoretical distributions (dotted lines)
845 for the individual scenarios for the **Log-normal Advection-Dispersion** model (left panels) and the Gamma model (right panels).
846 **Breaks in the Power-law** tails of the modeled TTDs are marked by the solid black lines. Small panels show cumulative TTDs.

847 None of the theoretical distribution functions we tested captures the shape of all of the observed TTDs adequately over the
848 entire age range. On the one hand, this is due to the misfit after the quite sudden break in slope at the tail end of the distributions,
849 on the other hand – and this is more relevant from a mass balance perspective – it results from a misrepresentation of the initial
850 response. Looking at Fig. 7, 8, 12 and 13, it becomes clear that all TTDs are humped distributions, with none of them exhibiting
851 an initial maximum (with a monotonically decreasing limb afterwards) and none of them possessing a value of 0 after 1.5
852 minutes (the first time step reported). Since all Inverse Gaussian distributions start with a value of 0 and all Gamma, Log-
853 normal and Beta distributions are either monotonically decreasing or start with a value of 0 they cannot be perfect
854 representations of the modelled TTDs for porous media. Instead, a set of probability distributions – with initial values larger
855 than 0, a rising limb to a maximum probability density and a falling limb with lighter or heavier tails – would theoretically be
856 the best option to represent variable TTDs. We can confirm this expectation since the Truncated Log-normal distributions we
857 tested do indeed capture the modelled TTD shapes best in most of our scenarios. Still they too are not None of the theoretical
858 distributions was able to reproduce the break in the TTD tails we observed in the model output after which the tails at initially
859 seem to follow a power law. This, however, does not constitute a substantial problem with regard to the correct mass balance
860 since these heavier power-law tails only comprise a very small fraction of the mass that was added to the system as a tracer.
861 Still, if the tailing of the TTDs is relevant to a problem (e.g. when dealing with legacy contamination) one can add the observed
862 breaks in the power-law tails to the distributions (for a description see Text S65 and Fig. S69 in the supplement). As for the
863 application of three-parameter distributions: although (Although the Beta model performed better than the two-parameter
864 models overall (by a slim margin)–, we do not recommend using it due to its additional fitting parameter (the upper limit c)
865 which increases equifinality problems (that we set out to eliminate). The same logic applies to the Truncated Log-normal
866 distribution. It performs best in almost all regards (see Table 3) but is more difficult to parameterize (e.g. we found no good
867 relationships between the parameters σ , λ and F) and no straight-forward mathematical expressions exist that define its
868 moments. Therefore we recommend utilizing the two-parameter Log-normal distribution model for high K_s and the Gamma
869 model distribution for low K_s scenarios. When doing that, we have to be careful though and consider – but only taking the
870 distribution median as a more (and not the mean) as a reliable transit time estimate than the mean (see Table 3).
871 Further theoretical developments should include the use of TTDs for non-conservative solute transport. This could be achieved
872 by considering the TTD shape a basic function to which different reaction terms can be added (like “cutting the tail” of solutes
873 that decay after a certain time in the catchment or shifting, damping and extending the TTD for solutes that experience
874 retardation). An example is provided for an exponential decay reaction in Text S7 and Fig. S11 in the supplement.
875

Kommentiert [IHh22]: - Line 668. I don't agree with this analysis, the presumed power-law tail covers less than one logscale. Also, identification of power law tails is not simple (see e.g. Pedretti and Bianchi, Reproducing tailing in breakthrough curves: Are statistical models equally representative and predictive? AWR 2018), the emergence of a (short) straight line in a log-log plot may not be enough. At any rate, I would not say that the inadequacy of the distributions in fitting the TTD is because of the tail, that by the way involves a tiny fraction of the mass, which is magnified by the log-log representation. I think that the issue of powerlaw tails is too much emphasized here.
Answer: We agree with your comment. We have changed our description of the TTD tail behavior (now we just describe the fact that the tails begin with a sudden break in the slope of the TTD and continue from there on as straight lines on a log-log plot). It's also clear that the tails are not relevant in terms of the total mass balance and will hardly be noticed for most solutes – with the exception of highly toxic pollutants. We have made sure to stress this in the revised manuscript.

Kommentiert [IHh23]: Line 685: not fully sure what you mean to say with “but only taking”. I suggest to replace it with “and use”
Good suggestion. We have modified this section anyways due to the new results we received from the fitting of the lognormal distributions.

4.2. Connection between the shape of TTDs and the flow path number F

We can pretty accurately predict the general shape of a TTD within the parameter range of our model scenarios using F alone (Fig. 119). Instead of using TTDs with constant shapes for determining variable transit times with transfer function-convolution models, one can use these relationships to pre-define the TTD shapes – reducing the problem of equifinality that stems from the simultaneous determination of shape and scale parameters (Fig. 15). Linked to that, some interesting conclusions can be drawn from the identified relationships between F and the shape parameters α and $D\sigma$:

1. A flow path number between -1 and $+1$ characterizes catchments where the available storage is currently larger than the change in storage caused by the incoming and outgoing flows – over the characteristic timescale of the combined average interevent and event duration $t_{ic}+t_{ev}$ (~5 days).

2. If the system receives more water than it can remove during $t_{ic}+t_{ev}$ (it is inflow-dominated), F is positive and the shape of TTDs is generally better represented by Gamma distributions.

3. With increasing F , α decreases to values below 1. This decrease in the shape parameter α is mainly caused by the initial peaks of the TTDs becoming higher while the tails remain rather similar. Our simulation results suggest that the tails of the TTDs become lighter with increasing positive F values. Therefore α should increase with increasing positive F values. The circumstance that we find a better relationship between increasing positive F and decreasing α values is due to the fact that the change in the initial response (higher initial values and peaks) outweighs the tails becoming lighter in the total mass balance. Therefore we can conclude that the early response dominates TTD shapes (at least from a mass balance perspective).

4. If the system has the capacity to remove more water in the subsurface than it receives during $t_{ic}+t_{ev}$, it is (outflow-dominated), F becomes negative and the shape of the TTDs is generally better represented by Log-normalAD distributions.

5. When F becomes more negative, $D\sigma$ increases from values around/below 0.5 to values above 1.0.5 (although the tails of the modeled TTDs become lighter), indicating higher peaks.

6. F converges towards 0 for systems with increasing available storage (because the denominator keeps increasing) or if inflows and outflow capacity are evenly balanced. For these cases both Gamma and Log-normalAD distributions become more and more dominated by smaller initial and early values as well as the later arrival of the peak concentration, which is illustrated by α becoming larger and by σ becoming smaller. This should not be interpreted as growing dominance of advective over σ and less by dispersive transport because the TTD tails still become heavier in these situations (while their initial peaks decrease).

The theoretical framework around the flow path number F can also be used to assess the impact that other catchment and climate properties have on TTD shapes. For example catchment size would only have an impact on TTD shape if the cross-sectional area of the outflow boundary A_{out} changed disproportionately. If, e.g., the catchment area A_{in} increased but the cross-sectional area A_{out} remained the same, then the subsurface outflow capacity K_{rem} would decrease and hence F would change. Our simulation results suggest that the tails of the Gamma TTDs become lighter with increasing F values. Therefore α should increase with increasing F values. The circumstance that we find a better relationship between increasing F and decreasing α

Kommentiert [IHh24]: - Section 4.2. This part is not entirely convincing, I can't see the validity of the prediction based on F . By the way the latter does not include other relevant ingredients, like e.g. KBr.
Answer: We understand your concerns. This section is not meant to represent to full and complete truth about TTD shapes. It is rather an attempt to find some structure in the way TTD shapes change with certain parameters, an attempt to explore overarching principles. Many of the potential shape-controlling parameters are still excluded from this analysis (like KBr). We have tried to put more emphasis on this interpretation of our results in the revised manuscript.

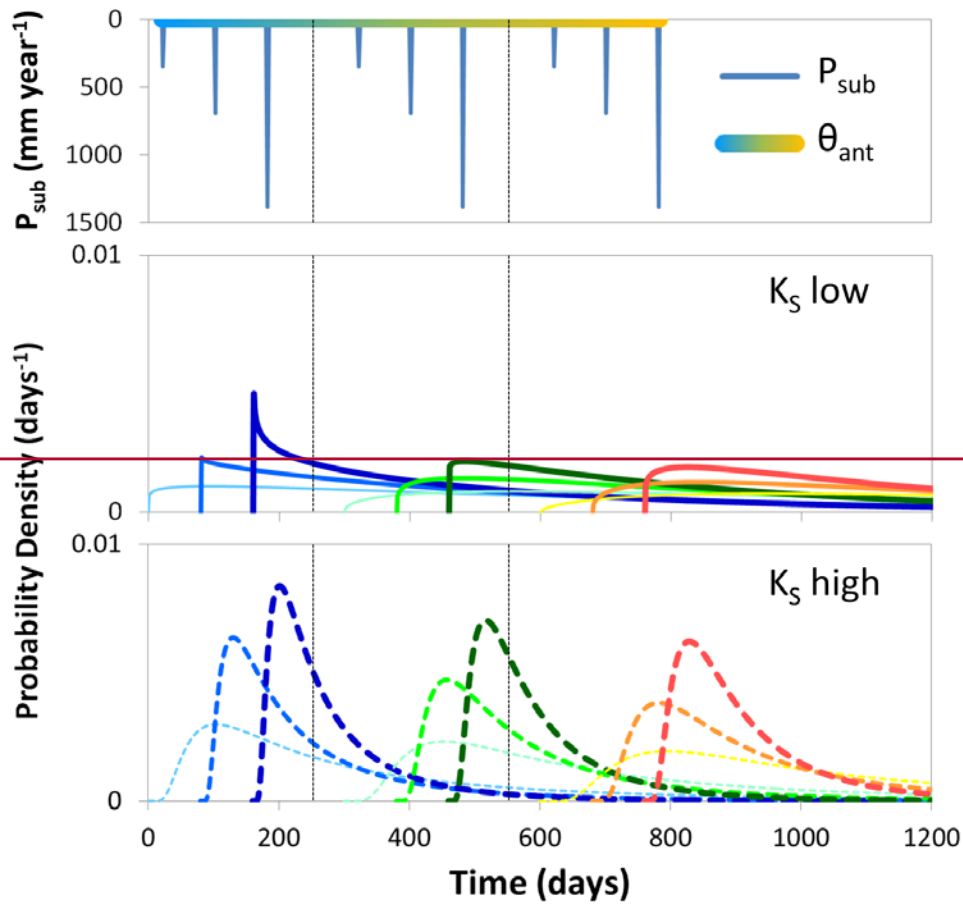
Kommentiert [IHh25]: Line 701. Available storage > storage change. Here I miss the timescale. Do you refer to yearly storage change?
The timescale is the combined average interevent and event duration (~5 days). A much shorter time scale – compared to the yearly storage change – that makes F more variable/responsive in time. We have added this information to the manuscript.

Kommentiert [IHh26]: Line 701 more water than it can remove (yearly or daily or hourly?) I think you need some kind of characteristic timescale here to define these definition (probably closely related to flowpath number F ?) similar in figure 9.
Yes, we have added the characteristic time scale (combined average interevent and event duration) to the description.

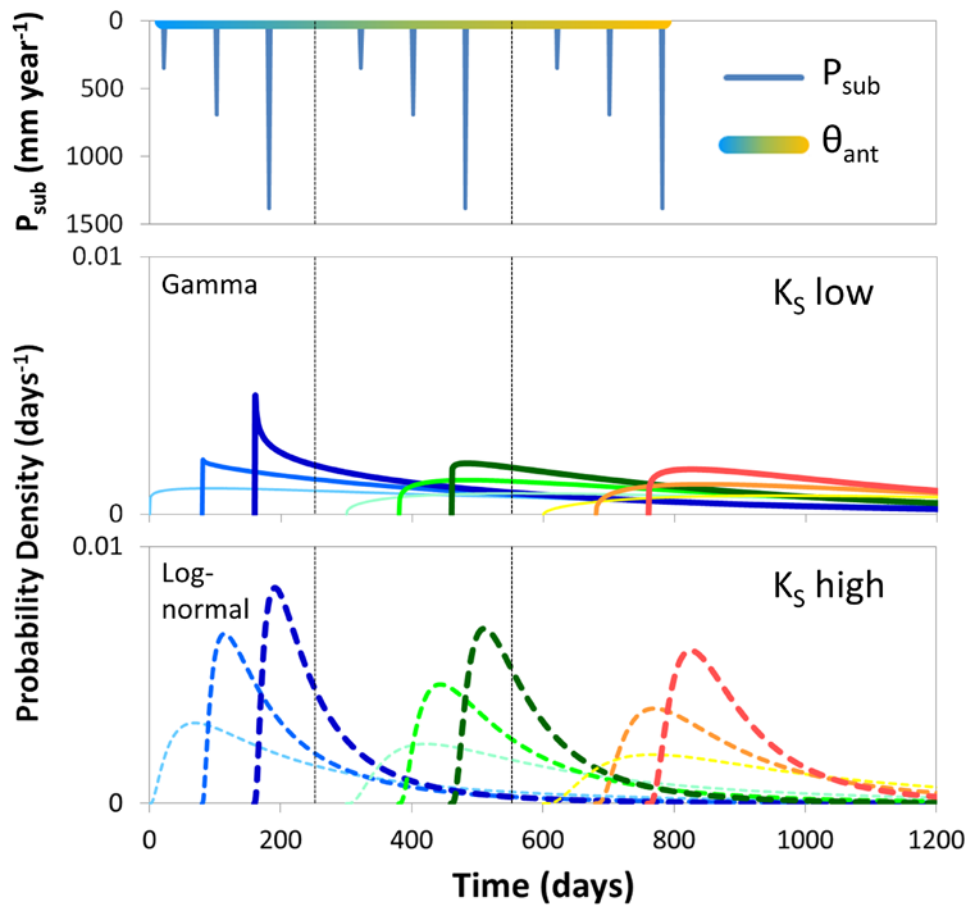
909 values is due to the fact that the change in the initial response (higher initial values and peaks) outweighs the tails becoming
910 lighter in the total mass balance. The same logic applies to the AD distributions where D becomes larger with more negative
911 F values.

912 Instead of using TTDs with constant shapes for determining variable transit times with transfer function convolution models,
913 one can use these relationships to pre-define the TTD shapes—reducing the problem of equifinality that stems from the
914 simultaneous determination of shape and scale parameters (Fig. 16).

915



916



917
 918 Figure 165: Predicted TTD shapes based on their relationship to the flow path number F , resulting from different antecedent
 919 moisture conditions θ_{ant} (from blue – wet on the left to yellow – dry on the right, blue – wet) and subsequent precipitation amounts
 920 P_{sub} . TTDs for low K_S are Gamma distributions (middle panel), for high K_S they are Log-normal distributions (lower panel).
 921 Individual TTDs start with time shifts so that they do not overlap (individual start times correspond to the P_{sub} markers in the upper
 922 panel).

923 This research can also contribute to the field of catchment evolution. One could argue that positive flow path numbers are not
 924 sustainable over longer periods of time because that would mean that the subsurface outflow capacity of the (zero-order)
 925 catchment is permanently insufficient and the catchment is not capable of efficiently discharging all of the incoming

926 precipitation via the subsurface. Consequently, the catchment storage would be filled up completely and overland flow would
927 be occurring on a regular basis. Since widespread overland flow is rarely observed in most catchments it could be argued that
928 most catchments have already evolved towards negative flow path numbers (e.g. by increasing K_S or D_{soil}). That, in turn, could
929 also mean that L-shaped (or initially slightly humped) TTDs with heavier tails and Gamma shape parameters α around 0.5 are
930 the natural endpoint of catchment evolution.

932 4.3. Replacing transit time with cumulative outflow

933 For certain scenarios we still see differences in the probability distributions if we replace transit time with cumulative outflow
934 (see Fig. S10 in the supplement). This observation can be explained by the fact that for the high K_S scenarios (where differences
935 are reduced) we only generate external flow variability while for the low K_S scenarios (where differences remain) we also
936 cause internal flow variability (Kim et al. 2016). That means that in the high K_S scenarios an increase in P_{sub} increases the flow
937 in all of the available flow paths proportionally (without changing the flow path partitioning or activating previously unused
938 flow paths) while for the low K_S scenarios an increase in P_{sub} causes pronounced shifts in the flow path partitioning where the
939 additional amount of precipitation can bypass the subsurface by predominantly utilizing overland flow paths (leading to the
940 observation that a larger amount of P_{sub} is necessary to flush out an equal amount of tracer). This can serve as direct proof that
941 replacing transit time with cumulative outflow does not erase all differences between TTDs, however it also shows that it may
942 be adequate for many applications where large shifts in flow path partitioning are not expected.

943 4.4. Limitations and Outlook

944 ~~O~~Again, we would like to point out that our results can be considered valid for systems that do not experience a large fraction
945 of preferential flow in the soil and bedrock since we only model flow taking place in the porous matrix of the subsurface
946 domain. This is the likely reason that we also encounter α values that are larger than 1 – although such high α values were not
947 found in previous studies (Hrachowitz et al., 2009; Godsey et al., 2010; Berghuijs and Kirchner, 2017; Birkel et al., 2016).
948 Therefore, in terms of expanding the modeling effort, it would be very beneficial to include both evapotranspiration and
949 macropore flow into the simulations. An inclusion of these processes will shift the flow path number F towards more negative
950 values. On the one hand, evapotranspiration will provide an additional way to remove water from the subsurface (representing
951 another sink term similar to K_{rem}) and macropore flow will enhance the subsurface outflow capacity of the catchment. ~~This~~
952 ~~could~~ result~~ing~~ in a shift towards TTDs with higher initial peaks. On the other hand, evapotranspiration also has the potential
953 of reducing θ_{ant} below moisture levels obtainable with free drainage alone. This more extreme dryness could lead to even more
954 humped TTDs with initial values closer to 0. The inclusion of additional heterogeneity in soil properties (layering, small-scale
955 variations) would also be a worthwhile exercise that is, however, out of the scope of our study. ~~Therefore, since some of the~~
956 ~~potential shape-controlling parameters are still excluded from the analysis (like, e.g., K_{Br} or the precipitation event amount~~
957 ~~P_{Ev}), this study is not meant to represent to full and complete truth about TTD shapes. It is rather an attempt to find some~~

Kommentiert [IHh27]: - Line 750. Again, the method cannot erase "all" differences, but perhaps is adequate for many applications.
Answer: Agreed. We have added this remark to the revised manuscript.

958 structure in the way TTD shapes change with certain parameters and boundary conditions, an attempt to illuminate essential
959 dynamics and to explore overarching principles in catchment hydrology.

960 It is quite unlikely that we can predict the shape of real-world TTDs with the relationship between F and α that we found in
961 our virtual experiments because we did not consider some (probably) very important processes — like evapotranspiration and
962 macropore flow. The TTDs we derived are based on surface flow coupled with subsurface flow in a porous matrix. Therefore
963 certain transport and mixing processes related to preferential flow are not included in this analysis. However, the relationships
964 we find can illuminate essential dynamics in catchment hydrology and help forming the basis for further investigations that
965 include additional hydrologic processes. It will be very interesting to see how, e.g., the introduction of evapotranspiration will
966 modify the relationship between F and α . Moreover, these experiments can be repeated with other potentially more appropriate
967 theoretical probability distributions in the future.

968 An interesting question that remains is whether backward TTDs can be linked to catchment and climate properties in a similar
969 fashion to the one we used, since backward TTDs are comprised of many individual water inputs that entered the catchment
970 over a very long period of time with potentially greatly varying initial conditions. That leads to the question of whether it is
971 more important to know the conditions at the time of entry to the catchment or the conditions at the time of exit from the
972 catchment (or both) in order to make predictions about TTD shapes and mTTs. Remondi et al. (2018) were among the first to
973 tackle this problem by water flux tracking with a distributed model. They found that mainly soil saturation and groundwater
974 storage affected backward TTDs.

975 The theoretical framework around the flow-path number F could also be used to assess the impact that other catchment and
976 climate properties have on TTD shapes. For example catchment size would only have an impact on TTD shape if the cross-
977 sectional area of the outflow boundary A_{out} changed disproportionately. If, e.g., the catchment area A_w increased but the cross-
978 sectional area A_{out} remained the same, then the subsurface outflow capacity K_{rem} would decrease and hence F would change.

979 4.3. Replacing transit time with cumulative outflow

980 For certain scenarios we still see differences in the probability distributions if we replace transit time with cumulative outflow
981 (see Fig. S8 in the supplement). This observation can be explained by the fact that for the high K_S scenarios (where differences
982 are reduced) we only generate external flow variability while for the low K_S scenarios (where differences remain) we also
983 cause internal flow variability (Kim et al., 2016). That means that in the high K_S scenarios an increase in P_{sub} increases the flow
984 in all of the available flow paths proportionally (without changing the flow path partitioning or activating previously unused
985 flow paths) while for the low K_S scenarios an increase in P_{sub} causes pronounced shifts in the flow path partitioning where the
986 additional amount of precipitation can bypass the subsurface flow paths by predominantly utilizing overland flow paths
987 (leading to the observation that a larger amount of P_{sub} is necessary to flush out an equal amount of tracer). This can serve as
988 direct proof that replacing transit time with cumulative outflow does not erase all differences between TTDs.

5. Conclusion

In our simulations for a virtual low-order catchment we observed that the shape of TTDs changes systematically with the four investigated catchment and climate properties (D_{soil} , K_S , θ_{amt} and P_{sub}) so that it is possible to predict the change using the dimensionless flow path number F . The results can be summarized in three main conclusions (see also Fig. 119):

1) The shape of TTDs converges towards L-shaped distributions with high initial values if a catchment's capacity to store inflow decreases or if the actual inflow to a catchment does not equal its subsurface outflow capacity.

2) Heavier tails are produced when the system is in a more "relaxed" state when all potential flow paths (deep and shallow, slower and faster) are equally used for transport. This is generally the case if P_{sub} is relatively small. Lighter tails appear when the system is in a more "stressed" state where the shallow and faster flow paths are disproportionately used for transport. This can be associated with larger P_{sub} values. In addition, we observe a distinct break in the TTD tails if there is a sufficiently large difference in hydraulic conductivity between the bedrock K_{Br} and the soil K_S .

3) For catchments with low K_S values, Gamma functions are able to capture the time-variance of TTDs in an appropriate way, especially for low K_S and wet θ_{amt} scenarios, while Log-normal distributions work well for high K_S and dry θ_{amt} scenarios. Gamma distributions are generally better representations of the TTDs (due to the heavier tails associated with lower K_S); for catchments with high K_S values, AD distributions work better (due to the lighter tails). 3) Heavier tails are observed when the system is in a more "relaxed" state where all potential flow paths (deep and shallow, slower and faster) are equally used for transport. This is generally the case if P_{sub} is relatively small. Lighter tails appear when the system is in a more "stressed" state where the shallow and faster flow paths are disproportionately used for transport. This can be associated with larger P_{sub} values. Moreover, power-law tails emerge if there is a sufficiently large difference in hydraulic conductivity between the bedrock K_{Br} and the soil K_S .

According to our findings, D_{soil} has only little influence on TTD shape and is linearly related to the mTT. That means that in catchments with deeper soils we should expect longer transport times but the same relation of solute advection to solute dispersion as in catchments with shallower soils. High K_S values are associated with TTDs that have higher initial values and lighter tails while K_S and mTT are related via a negative power law relationship. The influence of K_S increases for wet θ_{amt} (especially for short transit times) and for large P_{sub} (especially for long transit times) since both maximize the differences in hydraulic conductivity between catchments—the drier the conditions the more similar are the unsaturated hydraulic conductivities generally. In locations with higher precipitation amounts TTDs will have lighter tails and shorter mTTs (there is a power-law relationship between P_{sub} and mTT) mainly due to the fact that a larger P_{sub} flushes the soils faster and only allows a smaller fraction of the precipitation events to infiltrate into the bedrock. The influence of P_{sub} is larger for dry θ_{amt} and high K_S (especially for the longer transit times). Long-term trends or interannual changes in P_{sub} can cause temporal variations in TTDs but substantial short-term temporal variations in TTDs are derived mainly from differences in θ_{amt} . While under dry θ_{amt} there is a lower probability for shorter transit times, wet θ_{amt} triggers faster responses and hence higher initial peaks. Also, there is a negative linear relationship between mTT and θ_{amt} . The influence of θ_{amt} is stronger for catchments with higher K_S .

Kommentiert [1Hh28]: - Conclusion section. It is too long, one cannot see immediately the main results of the work. It's a pity because there is a lot of interesting material, that however needs to be better distilled and conveyed.

Answer: There is definitely room for improvement in the conclusion section. We agree with your criticism and we have done our best to condense, restructure and clarify the conclusions in the revised manuscript. To this end we moved a lot of text from the conclusion to the results and discussion sections.

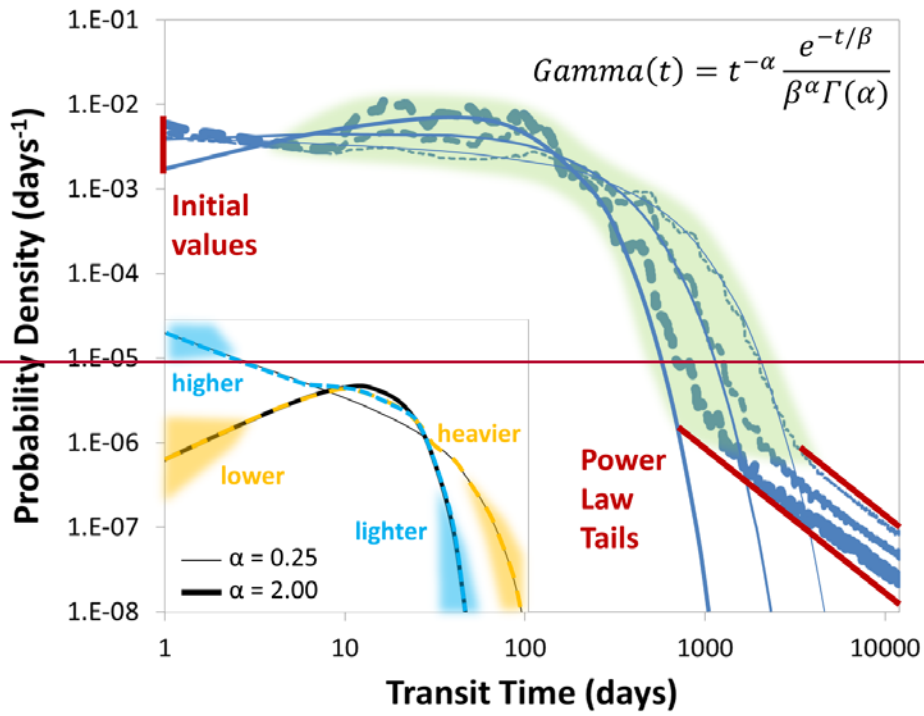
Kommentiert [1Hh29]: - Line 754-755. "...it is possible to predict the change using the dimensionless flow path number F ". At the third line of the Conclusion section this seems the major conclusion of the work. Is it so? It does not seem like after reading the text.

Answer: This can indeed be considered the main conclusion of our work. We have made sure that this outcome is conveyed better in the revised conclusion section.

Kommentiert [1Hh30]: Line 760 "where" or "when"? When sounds indeed better. Thanks.

1022 and for climates with smaller P_{sub} . Due to the changes in θ_{ant} , variations in TTD shape and scale can be high even in relatively
1023 small catchments. The influence of precipitation frequency on the shape of TTDs is detectable but relatively minor, however
1024 changes in the sequence of subsequent precipitation events can be relevant in regions with a low precipitation frequency. The
1025 fraction of water entering the bedrock depends strongly on the contact time of that water with the soil-bedrock interface. That
1026 means that in regions with small P_{sub} , a larger fraction of precipitation has the chance to infiltrate into the bedrock before it is
1027 flushed out of the soil layer by subsequent precipitation. Therefore the tails of TTDs in more arid regions tend to be heavier
1028 than the TTD tails in humid regions.

1029 Gamma functions were able to capture the time variance of TTDs in an appropriate way, especially for low K_s scenarios and
1030 wet antecedent soil moisture conditions, while AD distributions worked well for high K_s scenarios and dry antecedent
1031 conditions. However, neither the Gamma nor the Log-normal of the theoretical distributions is able to correctly
1032 represent/described the early part of the simulated distributions with non-zero initial values combined with a mode shortly after
1033 (i.e. the humped form) that weis observed in most cases. Moreover, we noticed/observed the general pattern that TTDs with
1034 high initial values tend to have lighter tails than TTDs with low initial values. Gamma distributions, unfortunately, exhibit the
1035 opposite behavior (with high initial values being associated with heavier tails than low initial values; see Fig. 167). Based on
1036 the results from our modelling efforts, we therefore encourage the exploration/search for a set of better fitting theoretical
1037 distributions. These distributions should be able to a) represent high initial values paired with lighter tails as well as low initial
1038 values paired with heavier tails and b) take on a “humped” form with non-zero initial values. We found that truncated
1039 distributions fulfil these requirements a lot better but have more degrees of freedom and are harder to parameterize. Concerning
1040 the TTD metrics, in most cases the median transit time was much better predicted by the theoretical distributions than the
1041 mean.



1043

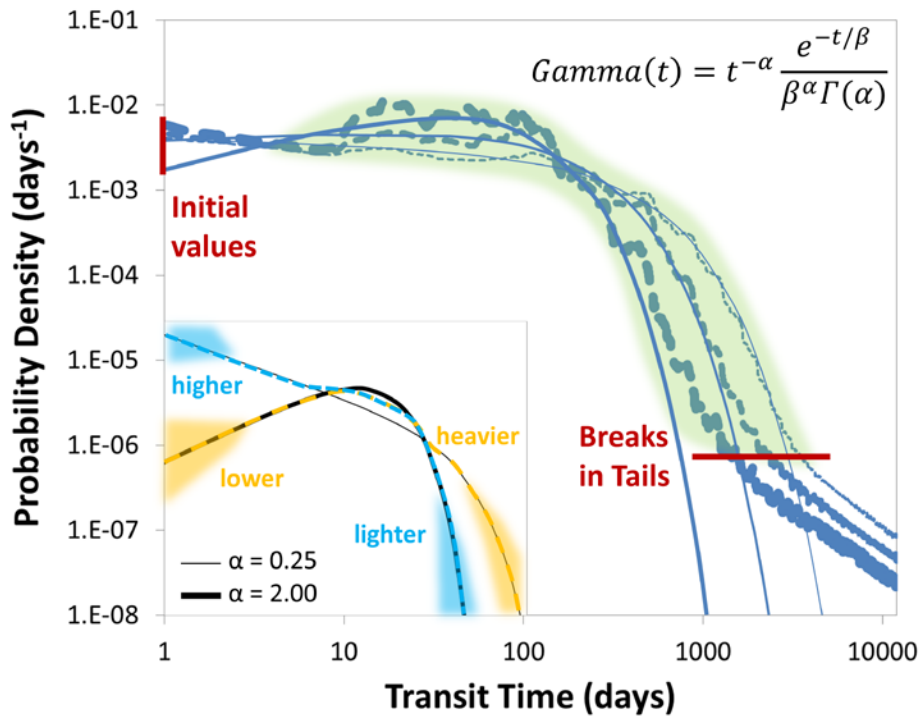


Figure 176: Gamma distributions (solid lines) capture the middle part of the modeled TTDs (dashed lines; thickness corresponds to P_{sub} amount) quite well but do not correctly represent their initial parts, and breaks in the power-law tails and heavier tails. Inset: Gamma distributions (thick and thin black solid lines) combine either high initial values with heavier tails or zero initial values with lighter tails while modeled TTDs often are best described by high initial values and lighter tails (blue dashed line) or low (albeit non-zero) initial values with heavier tails (yellow dashed line).

5.1. Outlook

It is quite unlikely that we can predict the shape of real-world TTDs with the relationship between F and α that we found in our virtual experiments because we did not consider some (probably) very important processes — like evapotranspiration and macropore flow. The TTDs we derived are based on surface flow coupled with subsurface flow in a porous matrix. Therefore certain transport and mixing processes related to preferential flow are not included in this analysis. However, the relationships we find can illuminate essential dynamics in catchment hydrology and help forming the basis for further investigations that include additional hydrologic processes. It will be very interesting to see how, e.g., the introduction of evapotranspiration will

1057 modify the relationship between F and α . Moreover, these experiments can be repeated with other potentially more appropriate
1058 theoretical probability distributions in the future.

1059 An interesting question that remains is whether backward TTDs can be linked to catchment and climate properties in a similar
1060 fashion to the one we used here, since backward TTDs are comprised of many individual water inputs that entered the
1061 catchment over a very long period of time with potentially greatly varying initial conditions. That leads to the question of
1062 whether it is more important to know the conditions at the time of entry to the catchment or the conditions at the time of exit
1063 from the catchment (or both) in order to make predictions about TTD shapes and mTTs. Remondi et al. (2018) were the first
1064 to tackle this problem by water flux tracking with a distributed model. They found that mainly soil saturation and groundwater
1065 storage affected backward TTDs.

1066 Practical implications can be drawn from these results concerning, e.g., pollution events. Some catchments are more vulnerable
1067 to pollution in the sense that they tend to store pollutants for a longer period of time and hence exhibit long legacy effects.
1068 Especially catchments with TTDs with heavy tails belong in that category (i.e. catchments with deeper soils and a moderate
1069 hydraulic conductivity difference between soil and bedrock). Also, certain points in time are worse for pollution events to
1070 happen — a spill occurring during dry conditions will stay in the catchment longer because it is more likely to reach the bedrock
1071 and stay in contact with it before it is flushed out of the soils than a spill during wet conditions. Accordingly, locations and
1072 situations that lead to a longer storage of decaying pollutants will eventually release less of the solutes to the downstream
1073 rivers. Further theoretical developments could include the use of TTDs for non-conservative solute transport. This could be
1074 achieved by considering the TTD shape a basic function to which different reaction terms can be added (like “cutting the tail”
1075 of solutes that decay after a certain time in the catchment or shifting, damping and extending the TTD for solutes that
1076 experience retardation). An example is provided for an exponential decay reaction in Text S6 and Fig. S10 in the supplement.
1077 Finally, this research can also contribute to the field of catchment evolution. One could argue that positive flow path numbers
1078 are not sustainable over longer periods of time because that would mean that the subsurface outflow capacity of the (zero-
1079 order) catchment is permanently insufficient and the catchment is not capable of efficiently discharging all of the incoming
1080 precipitation in the subsurface. Consequently, the catchment storage would be filled up completely and overland flow would
1081 be occurring on a regular basis. Since widespread overland flow is rarely observed in most catchments it could be argued that
1082 most catchments have already evolved towards negative flow path numbers (e.g. by increasing K_S or D_{soil}). That, in turn, could
1083 also mean that L-shaped (or initially slightly humped) TTDs with heavier tails and Gamma shape parameters α around 0.5 are
1084 the natural endpoint of catchment evolution.

1085 Ideally, this work will help to generate new or to expand existing hypotheses on hydrologic and hydrochemical catchment
1086 response that can be tested in future field experiments.

1087 **Data availability**

1088 All data used in this study is presented either in the main manuscript or in the supplement.

1089 **Author contribution**

1090 Conceptualization, I.H., P.T., and T.F.; Formal Analysis, I.H.; Funding Acquisition, J.F.; Investigation, I.H., A.M., J.Y., and
1091 J.F.; Software, J.Y.; Writing – Original Draft, I.H.; Writing – Review & Editing, I.H., A.M., J.F., J.Y., P.T., and T.F.

1092 **Competing interests**

1093 The authors declare that they have no conflict of interest.

1094 **Acknowledgments**

1095 This research was supported by the Helmholtz Research Programme “Terrestrial Environment”, topic 3: “Sustainable Water
1096 Resources Management”, with the integrated project: “Water and Matter Flux Dynamics in Catchments”. We would like to
1097 thank Carlotta Scudeler for her guidance on hydrologic modeling and her contribution to a previous version of this manuscript.
1098 Thanks also to René Therrien for his help with the HGS modeling. Finally, we would like to acknowledge Stefanie Lutz for
1099 an excellent discussion of the manuscript.

1100 **References**

- 1101 [Ali, M., Fiori, A., and Russo, D.: A comparison of travel-time based catchment transport models, with application to numerical](#)
1102 [experiments. *J. Hydrol.*, 511, 605-618, <https://doi.org/10.1016/j.jhydrol.2014.02.010>, 2014.](#)
- 1103 Ameli, A. A., Amvrosiadi, N., Grabs, T., Laudon, H., Creed, I. F., McDonnell, J. J., and Bishop, K.: Hillslope permeability
1104 architecture controls on subsurface transit time distribution and flow paths, *J. Hydrol.*, 543, 17-30,
1105 <https://doi.org/10.1016/j.jhydrol.2016.04.071>, 2016.
- 1106 [Becker, M. W. and Shapiro, A. M.: Interpreting tracer breakthrough tailing from different forced-gradient tracer experiment](#)
1107 [configurations in fractured bedrock. *Water Resour. Res.*, 39\(1\), <https://doi.org/10.1029/2001WR001190>, 2003.](#)
- 1108 Begemann, F. and Libby, W. F.: Continental water balance, ground water inventory and storage times, surface ocean mixing
1109 rates and world-wide water circulation patterns from cosmic-ray and bomb tritium, *Geochim. Cosmochim. Ac.*, 12(4), 277-
1110 296, [https://doi.org/10.1016/0016-7037\(57\)90040-6](https://doi.org/10.1016/0016-7037(57)90040-6), 1957.
- 1111 Benettin, P., Kirchner, J. W., Rinaldo, A., and Botter, G.: Modeling chloride transport using travel time distributions at
1112 Plynlimon, Wales, *Water Resour. Res.*, 51(5), 3259-3276, <https://doi.org/10.1002/2014WR016600>, 2015.
- 1113 Benettin, P., Soulsby, C., Birkel, C., Tetzlaff, D., Botter, G., and Rinaldo, A.: Using SAS functions and high-resolution isotope
1114 data to unravel travel time distributions in headwater catchments, *Water Resour. Res.*, 53(3), 1864-1878,
1115 <https://doi.org/10.1002/2016WR020117>, 2017.

1116 Berghuijs, W. R. and Kirchner, J. W.: The relationship between contrasting ages of groundwater and streamflow, *Geophys.*
1117 *Res. Lett.*, 44(17), 8925-8935, <https://doi.org/10.1002/2017GL074962>, 2017.

1118 Birkel, C., Geris, J., Molina, M. J., Mendez, C., Arce, R., Dick, J., et al.: Hydroclimatic controls on non-stationary stream
1119 water ages in humid tropical catchments, *J. Hydrol.*, 542, 231-240, <https://doi.org/10.1016/j.jhydrol.2016.09.006>, 2016.

1120 Birkel, C., Soulsby, C., Tetzlaff, D., Dunn, S., and Spezia, L.: High-frequency storm event isotope sampling reveals time-
1121 variant transit time distributions and influence of diurnal cycles, *Hydrol. Process.*, 26(2), 308-316,
1122 <https://doi.org/10.1002/hyp.8210>, 2012.

1123 Bishop, K., Seibert, J., Köhler, S., and Laudon, H.: Resolving the double paradox of rapidly mobilized old water with highly
1124 variable responses in runoff chemistry, *Hydrol. Process.*, 18(1), 185-189, <https://doi.org/10.1002/hyp.5209>, 2004.

1125 Botter, G., Bertuzzo, E., and Rinaldo, A.: Transport in the hydrologic response: Travel time distributions, soil moisture
1126 dynamics, and the old water paradox, *Water Resour. Res.*, 46(3), <https://doi.org/10.1029/2009WR008371>, 2010.

1127 [Botter, G., Bertuzzo, E., and Rinaldo, A.: Catchment residence and travel time distributions: The master equation, *Geophys.*
1128 *Res. Lett.*, 38\(11\), <https://doi.org/10.1029/2011GL047666>, 2011.](https://doi.org/10.1029/2011GL047666)

1129 Cardenas, M. B. and Jiang, X. W.: Groundwater flow, transport, and residence times through topography-driven basins with
1130 exponentially decreasing permeability and porosity, *Water Resour. Res.*, 46(11), <https://doi.org/10.1029/2010WR009370>,
1131 2010.

1132 Chapman, S. W., Parker, B. L., Sale, T. C., and Doner, L. A.: Testing high resolution numerical models for analysis of
1133 contaminant storage and release from low permeability zones, *J. Contam. Hydrol.*, 136, 106-116,
1134 <https://doi.org/10.1016/j.jconhyd.2012.04.006>, 2012.

1135 [Cox, D. R. and Isham, V.: A simple spatial-temporal model of rainfall, *P. Roy. Soc. Lond. A, Mat.*, 415\(1849\), 317-328, 1988.
1136 <https://doi.org/10.1098/rspa.1988.0111>.](https://doi.org/10.1098/rspa.1988.0111)

1137 Danesh-Yazdi, M., Klaus, J., Condon, L. E., and Maxwell, R. M.: Bridging the gap between numerical solutions of travel time
1138 distributions and analytical storage selection functions, *Hydrol. Process.*, 32(8), 1063-1076,
<https://doi.org/10.1002/hyp.11481>, 2018.

1139 Dinçer, T., Payne, B. R., Florkowski, T., Martinec, J., and Tongiorgi, E.: Snowmelt runoff from measurements of tritium and
1140 oxygen-18, *Water Resour. Res.*, 6(1), 110-124, <https://doi.org/10.1029/WR006i001p00110>, 1970.

1141 Eriksson, E.: The Possible Use of Tritium for Estimating Groundwater Storage, *Tellus*, 10(4), 472-478,
1142 <https://doi.org/10.3402/tellusa.v10i4.9265>, 1958.

1143 [Fiori, A. and Becker, M. W.: Power law breakthrough curve tailing in a fracture: The role of advection, *J. Hydrol.*, 525, 706-
1144 710, <https://doi.org/10.1016/j.jhydrol.2015.04.029>, 2015.](https://doi.org/10.1016/j.jhydrol.2015.04.029)

1145 Fiori, A. and Russo, D.: Travel time distribution in a hillslope: Insight from numerical simulations, *Water Resour. Res.*, 44(12),
1146 <https://doi.org/10.1029/2008WR007135>, 2008.

1147 [Fiori, A., Russo, D., and Di Lazzaro, M.: Stochastic analysis of transport in hillslopes: Travel time distribution and source
1148 zone dispersion, *Water Resour. Res.*, 45\(8\), <https://doi.org/10.1029/2008WR007668>, 2009.](https://doi.org/10.1029/2008WR007668)

1149

1150 [Gelhar, L. W., Welty, C., and Rehfeldt, K. R.: A critical review of data on field-scale dispersion in aquifers. *Water Resour.*](#)
1151 [Res., 28\(7\), 1955-1974, <https://doi.org/10.1029/92WR00607>, 1992.](#)

1152 Gilfedder, B. S., Cartwright, I., Hofmann, H., & Frei, S.: Explicit Modeling of Radon-222 in HydroGeoSphere During Steady
1153 State and Dynamic Transient Storage, *Groundwater*, 57(1), 36-47, <https://doi.org/10.1111/gwat.12847>, 2019.

1154 Godsey, S. E., Aas, W., Clair, T. A., De Wit, H. A., Fernandez, I. J., Kahl, J. S., et al.: Generality of fractal 1/f scaling in
1155 catchment tracer time series, and its implications for catchment travel time distributions, *Hydrol. Process.*, 24(12), 1660-1671,
1156 <https://doi.org/10.1002/hyp.7677>, 2010.

1157 [Haggerty, R., McKenna, S. A., and Meigs, L. C.: On the late-time behavior of tracer test breakthrough curves. *Water Resour.*](#)
1158 [Res., 36\(12\), 3467-3479, <https://doi.org/10.1029/2000WR900214>, 2000.](#)

1159 Haitjema, H. M.: On the residence time distribution in idealized groundwatersheds, *J. Hydrol.*, 172(1-4), 127-146,
1160 [https://doi.org/10.1016/0022-1694\(95\)02732-5](https://doi.org/10.1016/0022-1694(95)02732-5), 1995.

1161 Harman, C. J., Rao, P. S. C., Basu, N. B., McGrath, G. S., Kumar, P., and Sivapalan, M.: Climate, soil, and vegetation controls
1162 on the temporal variability of vadose zone transport, *Water Resour. Res.*, 47(10), <https://doi.org/10.1029/2010WR010194>,
1163 2011.

1164 [Harman, C. J. and Kim, M.: An efficient tracer test for time-variable transit time distributions in periodic hydrodynamic](#)
1165 [systems, *Geophys. Res. Lett.*, 41\(5\), 1567-1575, <https://doi.org/10.1002/2013GL058980>, 2014.](#)

1166 Harman, C. J.: Time-variable transit time distributions and transport: Theory and application to storage-dependent transport of
1167 chloride in a watershed, *Water Resour. Res.*, 51(1), 1-30, <https://doi.org/10.1002/2014WR015707>, 2015.

1168 Heidbüchel, I., Troch, P. A., and Lyon, S. W.: Separating physical and meteorological controls of variable transit times in
1169 zero-order catchments, *Water Resour. Res.*, 49(11), 7644-7657, <https://doi.org/10.1002/2012WR013149>, 2013.

1170 Heidbüchel, I., Troch, P. A., Lyon, S. W., and Weiler, M.: The master transit time distribution of variable flow systems, *Water*
1171 *Resour. Res.*, 48(6), <https://doi.org/10.1029/2011WR011293>, 2012.

1172 Hrachowitz, M., Benettin, P., Van Breukelen, B. M., Fovet, O., Howden, N. J., Ruiz, L., et al.: Transit times—the link between
1173 hydrology and water quality at the catchment scale, *Wiley Interdisciplinary Reviews: Water*, 3(5), 629-657,
1174 <https://doi.org/10.1002/wat2.1155>, 2016.

1175 Hrachowitz, M., Savenije, H., Bogaard, T. A., Soulsby, C., and Tetzlaff, D.: What can flux tracking teach us about water age
1176 distribution patterns and their temporal dynamics? *Hydrol. Earth Syst. Sc.*, 17(2), 533–564, [https://doi.org/10.5194/hess-17-](https://doi.org/10.5194/hess-17-533-2013)
1177 [533-2013](#), 2013.

1178 Hrachowitz, M., Soulsby, C., Tetzlaff, D., Dawson, J. J. C., Dunn, S. M., and Malcolm, I. A.: Using long-term data sets to
1179 understand transit times in contrasting headwater catchments, *J. Hydrol.*, 367(3), 237-248,
1180 <https://doi.org/10.1016/j.jhydrol.2009.01.001>, 2009.

1181 Hrachowitz, M., Soulsby, C., Tetzlaff, D., and Malcolm, I. A.: Sensitivity of mean transit time estimates to model conditioning
1182 and data availability, *Hydrol. Process.*, 25(6), 980-990, <https://doi.org/10.1002/hyp.7922>, 2011.

1183 Hrachowitz, M., Soulsby, C., Tetzlaff, D., Malcolm, I. A., and Schoups, G.: Gamma distribution models for transit time
1184 estimation in catchments: Physical interpretation of parameters and implications for time-variant transit time assessment,
1185 Water Resour. Res., 46(10), <https://doi.org/10.1029/2010WR009148>, 2010.

1186 Jasechko, S., Kirchner, J. W., Welker, J. M., and McDonnell, J. J.: Substantial proportion of global streamflow less than three
1187 months old, Nat. Geosci., 9(2), 126-129, <https://doi.org/10.1038/NGEO2636>, 2016.

1188 Jiang, X. W., Wan, L., Wang, X. S., Ge, S., and Liu, J.: Effect of exponential decay in hydraulic conductivity with depth on
1189 regional groundwater flow, Geophys. Res. Lett., 36(24), <https://doi.org/10.1029/2009GL041251>, 2009.

1190 Kim, M., Pangle, L., Cardoso, C., Lora, M., Volkmann, T., Wang, Y., et al.: Transit time distributions and StorAge Selection
1191 functions in a sloping soil lysimeter with time-varying flow paths: Direct observation of internal and external transport
1192 variability, Water Resour. Res., 52(9), 7105–7129, <https://doi.org/10.1002/2016WR018620>, 2016.

1193 Kirchner, J. W.: Aggregation in environmental systems—Part 1: Seasonal tracer cycles quantify young water fractions, but not
1194 mean transit times, in spatially heterogeneous catchments, Hydrol. Earth Syst. Sc., 20(1), 279–297,
1195 <https://doi.org/10.5194/hess-20-279-2016>, 2016.

1196 Kirchner, J. W., Feng, X., and Neal, C.: Fractal stream chemistry and its implications for contaminant transport in catchments,
1197 Nature, 403(6769), 524-527, <https://doi.org/10.1038/35000537>, 2000.

1198 Kirchner, J. W., Feng, X., and Neal, C.: Catchment-scale advection and dispersion as a mechanism for fractal scaling in stream
1199 tracer concentrations, J. Hydrol., 254(1), 82-101, [https://doi.org/10.1016/S0022-1694\(01\)00487-5](https://doi.org/10.1016/S0022-1694(01)00487-5), 2001.

1200 Kollet, S. J. and Maxwell, R. M.: Demonstrating fractal scaling of baseflow residence time distributions using a fully-coupled
1201 groundwater and land surface model, Geophys. Res. Lett., 35(7), <https://doi.org/10.1029/2008GL033215>, 2008.

1202 Kollet, S., Sulis, M., Maxwell, R. M., Paniconi, C., Putti, M., Bertoldi, G., et al.: The integrated hydrologic model
1203 intercomparison project, IH-MIP2: A second set of benchmark results to diagnose integrated hydrology and feedbacks, Water
1204 Resour. Res., 53(1), 867-890, <https://doi.org/10.1002/2016WR019191>, 2017.

1205 Liggett, J. E., Partington, D., Frei, S., Werner, A. D., Simmons, C. T., and Fleckenstein, J. H.: An exploration of coupled
1206 surface–subsurface solute transport in a fully integrated catchment model, J. Hydrol., 529, 969-979,
1207 <http://doi.org/10.1016/j.jhydrol.2015.09.006>, 2015.

1208 Lutz, S. R., Velde, Y. V. D., Elsayed, O. F., Imfeld, G., Lefrancq, M., Payraudeau, S., and Breukelen, B. M. V.: Pesticide fate
1209 on catchment scale: conceptual modelling of stream CSIA data, Hydrol. Earth Syst. Sc., 21(10), 5243-5261,
1210 <https://doi.org/10.5194/hess-21-5243-2017>, 2017.

1211 Małoszewski, P., Rauert, W., Stichler, W., and Herrmann, A.: Application of flow models in an alpine catchment area using
1212 tritium and deuterium data, J. Hydrol., 66(1-4), 319-330, [https://doi.org/10.1016/0022-1694\(83\)90193-2](https://doi.org/10.1016/0022-1694(83)90193-2), 1983.

1213 Małoszewski, P. and Zuber, A.: Determining the turnover time of groundwater systems with the aid of environmental tracers:
1214 1. Models and their applicability, J. Hydrol., 57(3-4), 207-231, [https://doi.org/10.1016/0022-1694\(82\)90147-0](https://doi.org/10.1016/0022-1694(82)90147-0), 1982.

1215 Massoudieh, A., Visser, A., Sharifi, S., and Broers, H. P.: A Bayesian modeling approach for estimation of a shape-free
1216 groundwater age distribution using multiple tracers, *Appl. Geochem.*, 50, 252-264,
1217 <https://doi.org/10.1016/j.apgeochem.2013.10.004>, 2014.

1218 Maxwell, R. M., Putti, M., Meyerhoff, S., Delfs, J. O., Ferguson, I. M., Ivanov, V., et al.: Surface-subsurface model
1219 intercomparison: A first set of benchmark results to diagnose integrated hydrology and feedbacks, *Water Resour. Res.*, 50(2),
1220 1531-1549, <https://doi.org/10.1002/2013WR013725>, 2014.

1221 McDonnell, J. J., McGuire, K., Aggarwal, P., Beven, K. J., Biondi, D., Destouni, G., et al.: How old is streamwater? Open
1222 questions in catchment transit time conceptualization, modelling and analysis, *Hydrol. Process.*, 24(12), 1745-1754,
1223 <https://doi.org/10.1002/hyp.7796>, 2010.

1224 McGuire, K. J. and McDonnell, J. J.: A review and evaluation of catchment transit time modeling, *J. Hydrol.*, 330(3), 543-
1225 563, <https://doi.org/10.1016/j.jhydrol.2006.04.020>, 2006.

1226 McGuire, K. J., McDonnell, J. J., Weiler, M., Kendall, C., McGlynn, B. L., Welker, J. M., and Seibert, J.: The role of
1227 topography on catchment-scale water residence time, *Water Resour. Res.*, 41(5), <https://doi.org/10.1029/2004WR003657>,
1228 2005.

1229 McMillan, H., Tetzlaff, D., Clark, M., and Soulsby, C.: Do time-variable tracers aid the evaluation of hydrological model
1230 structure? A multimodel approach, *Water Resour. Res.*, 48(5), <https://doi.org/10.1029/2011WR011688>, 2012.

1231 Musolff, A., Fleckenstein, J. H., Rao, P. S. C., and Jawitz, J. W.: Emergent archetype patterns of coupled hydrologic and
1232 biogeochemical responses in catchments, *Geophys. Res. Lett.*, 44(9), 4143-4151, <https://doi.org/10.1002/2017GL072630>,
1233 2017.

1234 [Nauman, E. B.: Residence time distribution theory for unsteady stirred tank reactors, *Chem. Eng. Sci.*, 24\(9\), 1461-1470,](https://doi.org/10.1016/0009-2509(69)85074-8)
1235 [https://doi.org/10.1016/0009-2509\(69\)85074-8](https://doi.org/10.1016/0009-2509(69)85074-8), 1969.

1236 Niemi, A. J.: Residence time distributions of variable flow processes, *Int. J. Appl. Radiat. Is.*, 28(10-11), 855-860,
1237 [https://doi.org/10.1016/0020-708X\(77\)90026-6](https://doi.org/10.1016/0020-708X(77)90026-6), 1977.

1238 Nir, A.: On the interpretation of tritium 'age' measurements of groundwater, *J. Geophys. Res.*, 69(12), 2589-2595,
1239 <https://doi.org/10.1029/JZ069i012p02589>, 1964.

1240 Nyström, U.: Transit time distributions of water in two small forested catchments, *Ecol. Bull.*, 37, 97-100, 1985.

1241 Pangle, L. A., Kim, M., Cardoso, C., Lora, M., Meira Neto, A. A., Volkmann, et al.: The mechanistic basis for storage-
1242 dependent age distributions of water discharged from an experimental hillslope, *Water Resour. Res.*, 53(4), 2733-2754,
1243 <https://doi.org/10.1002/2016WR019901>, 2017.

1244 [Pedretti, D. and Bianchi, M.: Reproducing tailing in breakthrough curves: Are statistical models equally representative and](https://doi.org/10.1016/j.advwatres.2018.01.023)
1245 [predictive?, *Adv. Water Resour.*, 113, 236-248, https://doi.org/10.1016/j.advwatres.2018.01.023, 2018.](https://doi.org/10.1016/j.advwatres.2018.01.023)

1246 Pedretti, D., Fernández-García, D., Bolster, D., and Sanchez-Vila, X.: On the formation of breakthrough curves tailing during
1247 convergent flow tracer tests in three-dimensional heterogeneous aquifers, *Water Resour. Res.*, 49(7), 4157-4173,
1248 <https://doi.org/10.1002/wrcr.20330>, 2013.

1249 Peralta-Tapia, A., Soulsby, C., Tetzlaff, D., Sponseller, R., Bishop, K., and Laudon, H.: Hydroclimatic influences on non-
1250 stationary transit time distributions in a boreal headwater catchment, *J. Hydrol.*, 543, 7-16,
1251 <https://doi.org/10.1016/j.jhydrol.2016.01.079>, 2016.

1252 Remondi, F., Kirchner, J. W., Burlando, P., and Faticchi, S.: Water Flux Tracking With a Distributed Hydrological Model to
1253 Quantify Controls on the Spatio-temporal Variability of Transit Time Distributions, *Water Resour. Res.*, 54(4), 3081-3099,
1254 <https://doi.org/10.1002/2017WR021689>, 2018.

1255 Rinaldo, A., Beven, K. J., Bertuzzo, E., Nicotina, L., Davies, J., Fiori, A., et al.: Catchment travel time distributions and water
1256 flow in soils, *Water Resour. Res.*, 47(7), <https://doi.org/10.1029/2011WR010478>, 2011.

1257 Roa-García, M. C. and Weiler, M.: Integrated response and transit time distributions of watersheds by combining hydrograph
1258 separation and long-term transit time modeling, *Hydrol. Earth Syst. Sc.*, 14(8), 1537-1549, [https://doi.org/10.5194/hess-14-](https://doi.org/10.5194/hess-14-1537-2010)
1259 [1537-2010](https://doi.org/10.5194/hess-14-1537-2010), 2010.

1260 Rodhe, A., Nyberg, L., and Bishop, K.: Transit times for water in a small till catchment from a step shift in the oxygen 18
1261 content of the water input, *Water Resour. Res.*, 32(12), 3497-3511, <https://doi.org/10.1029/95WR01806>, 1996.

1262 [Schulze-Makuch, D.: Longitudinal dispersivity data and implications for scaling behavior. *Groundwater*, 43\(3\), 443-456,
1263 <https://doi.org/10.1111/j.1745-6584.2005.0051.x>, 2005.](https://doi.org/10.1111/j.1745-6584.2005.0051.x)

1264 Seeger, S. and Weiler, M.: Reevaluation of transit time distributions, mean transit times and their relation to catchment
1265 topography, *Hydrol. Earth Syst. Sc.*, 18(12), 4751-4771, <https://doi.org/10.5194/hess-18-4751-2014>, 2014.

1266 Soulsby, C., Birkel, C., Geris, J., and Tetzlaff, D.: Spatial aggregation of time-variant stream water ages in urbanizing
1267 catchments, *Hydrol. Process.*, 29(13), 3038-3050, <https://doi.org/10.1002/hyp.10500>, 2015.

1268 Sprenger, M., Seeger, S., Blume, T., and Weiler, M.: Travel times in the vadose zone: Variability in space and time, *Water*
1269 *Resour. Res.*, 52(8), 5727-5754, <https://doi.org/10.1002/2015WR018077>, 2016.

1270 Stockinger, M. P., Bogaen, H. R., Lücke, A., Diekkruuger, B., Weiler, M., and Vereecken, H.: Seasonal soil moisture patterns:
1271 Controlling transit time distributions in a forested headwater catchment, *Water Resour. Res.*, 50(6), 5270-5289,
1272 <https://doi.org/10.1002/2013WR014815>, 2014.

1273 Sudicky, E. A., Illman, W. A., Goltz, I. K., Adams, J. J., and McLaren, R. G.: Heterogeneity in hydraulic conductivity and its
1274 role on the macroscale transport of a solute plume: From measurements to a practical application of stochastic flow and
1275 transport theory, *Water Resour. Res.*, 46(1), <https://doi.org/10.1029/2008WR007558>, 2010.

1276 Tetzlaff, D., Birkel, C., Dick, J., Geris, J., and Soulsby, C.: Storage dynamics in hydrogeological units control hillslope
1277 connectivity, runoff generation, and the evolution of catchment transit time distributions, *Water Resour. Res.*, 50(2), 969-985,
1278 <https://doi.org/10.1002/2013WR014147>, 2014.

1279 Therrien, R., McLaren, R. G., Sudicky, E. A., and Panday, S. M.: *HydroGeoSphere: a three-dimensional numerical model*
1280 *describing fully-integrated subsurface and surface flow and solute transport*, Groundwater Simulations Group, University of
1281 Waterloo, Waterloo, ON, 2010.

1282 Timbe, E., Windhorst, D., Celleri, R., Timbe, L., Crespo, P., Frede, H. G., et al.: Sampling frequency trade-offs in the
1283 assessment of mean transit times of tropical montane catchment waters under semi-steady-state conditions, *Hydrol. Earth Syst.*
1284 *Sc.*, 19(3), 1153-1168, <https://doi.org/10.5194/hess-19-1153-2015>, 2015.

1285 van der Velde, Y., de Rooij, G. H., Rozemeijer, J. C., van Geer, F. C., and Broers, H. P.: Nitrate response of a lowland
1286 catchment: On the relation between stream concentration and travel time distribution dynamics, *Water Resour. Res.*, 46(11),
1287 <https://doi.org/10.1029/2010WR009105>, 2010.

1288 van der Velde, Y., Torfs, P. J. J. F., van der Zee, S. E. A. T. M., and Uijlenhoet, R.: Quantifying catchment-scale mixing and
1289 its effect on time-varying travel time distributions, *Water Resour. Res.*, 48(6), <https://doi.org/10.1029/2011WR011310>, 2012.

1290 van der Velde, Y., Heidbüchel, I., Lyon, S. W., Nyberg, L., Rodhe, A., Bishop, K., and Troch, P. A.: Consequences of mixing
1291 assumptions for time-variable travel time distributions, *Hydrol. Process.*, 29(16), 3460–3474,
1292 <https://doi.org/10.1002/hyp.10372>, 2015.

1293 Weiler, M., McGlynn, B. L., McGuire, K. J., and McDonnell, J. J.: How does rainfall become runoff? A combined tracer and
1294 runoff transfer function approach, *Water Resour. Res.*, 39(11), <https://doi.org/10.1029/2003WR002331>, 2003.

1295 Wilusz, D. C., Harman, C. J., and Ball, W. P.: Sensitivity of catchment transit times to rainfall variability under present and
1296 future climates, *Water Resour. Res.*, 53(12), 10231-10256, <https://doi.org/10.1002/2017WR020894>, 2017.

1297 Yang, J., Heidbüchel, I., Musolff, A., Reinstorf, F., and Fleckenstein, J. H.: Exploring the dynamics of transit times and
1298 subsurface mixing in a small agricultural catchment, *Water Resour. Res.*, 54, <https://doi.org/10.1002/2017WR021896>, 2018.

1299 [Zhang, Y., Benson, D. A., and Baeumer, B.: Predicting the tails of breakthrough curves in regional-scale alluvial systems.](https://doi.org/10.1111/j.1745-6584.2007.00320.x)
1300 [Groundwater](https://doi.org/10.1111/j.1745-6584.2007.00320.x), 45(4), 473-484, <https://doi.org/10.1111/j.1745-6584.2007.00320.x>, 2007.

1301 **Tables**

1302 **Table 1: Metrics of the TTDs derived from the modeling of 36 scenarios with different combinations of catchment and climate**
1303 **properties. All times are given in days.**

DEEP (THICK)																					
D _{best}	K _s	θ _{best}	P _{sub}	HIGH INT						WET			DRY			LOW INT			WET		
				SMALL	MED	BIG	SMALL	MED	BIG	SMALL	MED	BIG	SMALL	MED	BIG	SMALL	MED	BIG	SMALL	MED	BIG
Name	THDS	THDM	THDB	THIS	THIM	THIB	THWS	THWM	THWB	TLDS	TLDM	TLDB	TLIS	TLIM	TLIB	TLWS	TLWM	TLWB			
1st Quartile	244	137	89	159	105	66	101	67	45	458	214	126	312	191	111	232	135	94			
Median	441	207	115	315	159	101	218	132	85	785	475	291	640	456	289	565	394	269			
Mean	515	280	151	433	238	132	354	197	110	1009	648	439	878	613	439	796	552	413			
3rd Quartile	656	366	167	569	299	143	501	258	136	1308	862	576	1191	832	576	1116	778	561			
Stand Dev	455	298	189	454	285	190	443	275	173	880	646	505	881	700	587	816	635	530			
Skewness	7	15	28	7	14	28	7	15	29	3	4	5	4	5	7	3	4	6			
Exc Kurtosis	125	407	1233	117	404	1214	123	437	1426	20	41	70	27	56	94	22	46	80			

SHALLOW (FLAT)																					
D _{best}	K _s	θ _{best}	P _{sub}	HIGH INT						WET			DRY			LOW INT			WET		
				SMALL	MED	BIG	SMALL	MED	BIG	SMALL	MED	BIG	SMALL	MED	BIG	SMALL	MED	BIG	SMALL	MED	BIG
Name	FHDS	FHDM	FHDB	FHIS	FHIM	FHIB	FHWS	FHWM	FHWB	FLDS	FLDM	FLDB	FLIS	FLIM	FLIB	FLWS	FLWM	FLWB			
1st Quartile	139	91	49	107	70	44	72	46	22	211	127	80	173	109	77	135	94	62			
Median	212	120	79	165	104	63	136	88	49	458	269	163	413	266	158	342	204	146			
Mean	296	159	90	257	142	84	211	116	68	600	389	284	563	394	288	501	360	277			
3rd Quartile	389	174	106	312	147	97	272	136	90	796	504	389	750	504	385	656	474	378			
Stand Dev	357	231	154	372	258	208	338	219	157	619	461	377	713	588	505	660	557	492			
Skewness	14	25	41	14	23	31	14	26	41	5	7	9	7	9	11	6	9	10			
Exc Kurtosis	332	903	2245	297	742	1274	345	998	2199	59	109	169	70	119	174	73	121	170			

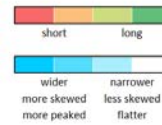


Table 2: Shape parameters of the best-fit Inverse Gaussian (D), Gamma (α) and Log-Advection-normal-Dispersion (Dg) distributions and associated flow path numbers (F) for the 36 different scenarios.

DEEP (THICK)																					
D _{best}	K _s	θ _{best}	P _{sub}	HIGH INT						WET			DRY			LOW INT			WET		
				SMALL	MED	BIG	SMALL	MED	BIG	SMALL	MED	BIG	SMALL	MED	BIG	SMALL	MED	BIG	SMALL	MED	BIG
Name	THDS	THDM	THDB	THIS	THIM	THIB	THWS	THWM	THWB	TLDS	TLDM	TLDB	TLIS	TLIM	TLIB	TLWS	TLWM	TLWB			
α	2.15	2.07	3.33	1.41	1.55	2.38	0.92	1.09	1.53	1.69	1.33	1.01	1.32	1.13	0.92	1.08	0.94	0.80			
D	0.28	0.29	0.18	0.46	0.40	0.25	0.75	0.60	0.41	0.37	0.49	0.69	0.51	0.62	0.79	0.62	0.74	0.90			
F	-0.04	-0.02	0.01	-0.07	-0.04	0.01	-0.22	-0.13	0.03	0.01	0.03	0.06	0.02	0.05	0.10	0.08	0.16	0.32			

SHALLOW (FLAT)																					
D _{best}	K _s	θ _{best}	P _{sub}	HIGH INT						WET			DRY			LOW INT			WET		
				SMALL	MED	BIG	SMALL	MED	BIG	SMALL	MED	BIG	SMALL	MED	BIG	SMALL	MED	BIG	SMALL	MED	BIG
Name	FHDS	FHDM	FHDB	FHIS	FHIM	FHIB	FHWS	FHWM	FHWB	FLDS	FLDM	FLDB	FLIS	FLIM	FLIB	FLWS	FLWM	FLWB			
α	1.99	3.09	3.66	1.49	2.33	2.46	1.05	1.48	1.61	1.43	1.12	0.92	1.16	1.00	0.82	0.97	0.87	0.78			
D	0.30	0.19	0.15	0.43	0.27	0.24	0.65	0.43	0.39	0.45	0.61	0.77	0.63	0.74	0.92	0.74	0.85	0.98			
F	-0.02	0.01	0.07	-0.04	0.01	0.11	-0.13	0.03	0.35	0.03	0.06	0.12	0.05	0.10	0.20	0.16	0.31	0.63			

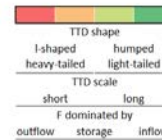


Table 3: Average and maximum deviations of mean and median transit times between the best-fit theoretical probability distributions and the modeled TTDs (given as the ratio of average deviation of the fitted distributions to the average modeled mean and median transit times as well as the average deviation in days). Sum of the squared residuals indicates the goodness of fit between the shape of theoretical probability distributions and modeled TTDs.

Metric	Mean			Median			Shape	
	Average		Max	Average		Max	Average	Max
	Unit	%	d	%	d	d	d ²	d ²
InvGau	4.7	17.5	102.2	5.7	14.9	50.3	0.88	2.63
Gamma	23.9	88.3	423.0	4.5	11.6	59.2	0.71	2.51
LogN	6.3	23.1	115.0	4.9	12.9	42.5	0.70	1.95
Beta	3.6	13.3	38.4	4.5	11.7	59.2	0.71	2.51
Trunc	2.6	9.6	90.5	4.0	10.5	36.0	0.40	1.65

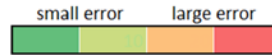


Table 3: Deviations of mean (green) and median (blue) transit times between the best-fit theoretical probability distributions and the modeled TTDs. Sum of the squared residuals (yellow) indicating goodness of fit between theoretical probability distribution and modeled TTDs.

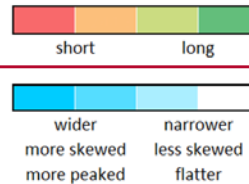
D _{sat} K _s B _{int} P _{sub} Name	DEEP (THICK)																	
	DRY			HIGH INT			WET			DRY			LOW			WET		
	SMALL	MED	BIG	SMALL	MED	BIG	SMALL	MED	BIG	SMALL	MED	BIG	SMALL	MED	BIG	SMALL	MED	BIG
AD Δ Mean	6	-4	-9	12	-2	-6	21	4	-1	31	25	22	102	44	32	60	35	18
Beta Δ Mean	-14	-14	-14	-13	-14	-12	-6	-10	-8	-19	-13	-8	38	-2	-6	6	-5	-15
Gamma Δ Mean	-282	-152	-109	-132	-94	-81	26	-25	-42	-423	-172	-10	-186	-74	30	-52	31	84
AD Δ Median	-32	7	6	-6	11	1	1	-6	-8	-22	-19	-13	17	-44	-21	-28	-50	-37
Beta Δ Median	-15	17	8	13	21	2	17	2	-4	18	10	8	59	-13	1	6	-26	-20
Gamma Δ Median	-15	17	8	12	20	2	17	2	-4	18	10	8	59	-13	1	6	-26	-20
AD Fit	0.44	0.32	0.33	0.68	0.22	0.19	1.20	0.31	0.30	0.51	0.92	1.10	1.78	1.80	1.65	2.63	2.40	2.10
Beta Fit	0.38	0.79	0.64	0.41	0.69	0.37	0.24	0.34	0.20	1.28	0.52	0.40	2.11	1.36	0.90	0.36	0.32	0.26
Gamma Fit	0.38	0.79	0.64	0.38	0.66	0.35	0.25	0.31	0.17	1.28	0.52	0.40	2.11	1.36	0.90	0.36	0.32	0.26

D _{sat} Name	SHALLOW (FLAT)																	
	FHDS			FHIS			FHWs			FLDS			FLIS			FLW		
	SMALL	MED	BIG	SMALL	MED	BIG	SMALL	MED	BIG	SMALL	MED	BIG	SMALL	MED	BIG	SMALL	MED	BIG
AD Δ Mean	-7	-11	4	-7	-12	-7	1	4	-1	13	10	9	34	16	10	29	15	8
Beta Δ Mean	-18	-17	-6	-21	-18	-10	-14	-11	-5	-20	-16	-12	-12	-18	-17	-12	-16	-18
Gamma Δ Mean	-156	-113	-67	-98	-89	-54	-23	-45	-29	-195	-56	11	-87	-17	40	1	35	57
AD Δ Median	10	3	-4	10	-2	-2	-5	-10	-2	-33	-18	6	-41	-27	0	-32	3	1
Beta Δ Median	21	6	-2	20	1	0	4	-6	1	-7	1	20	-12	-6	14	-7	20	13
Gamma Δ Median	21	6	-2	20	2	0	4	-6	1	-7	1	20	-12	-6	14	-7	20	13
AD Fit	0.38	0.41	0.14	0.36	0.30	0.20	0.36	0.25	0.29	0.68	0.53	0.44	2.13	1.40	0.98	1.71	1.21	0.92
Beta Fit	0.85	0.77	0.13	0.92	0.53	0.38	0.47	0.35	0.13	0.73	0.73	0.44	2.51	1.61	0.98	1.02	0.81	0.64
Gamma Fit	0.85	0.77	0.14	0.92	0.54	0.38	0.47	0.35	0.13	0.73	0.73	0.44	2.51	1.61	0.98	1.02	0.81	0.64



Table 4: Parameters of the TTDs derived from the simulations with different soil porosities: small = 0.24 m³·m⁻³, normal = 0.39 m³·m⁻³, large = 0.54 m³·m⁻³.

Name	THDM			THIM			THWM		
	Small	Normal	Large	Small	Normal	Large	Small	Normal	Large
1st Quartile	97	137	178	76	105	135	46	67	91
Median	135	207	301	110	159	226	94	132	168
Mean	177	280	385	152	238	326	127	197	269
3rd Quartile	202	366	502	169	299	459	143	258	384
Stand Dev	248	298	349	239	285	336	239	275	323
Skewness	23	15	10	23	14	9	23	15	9
Exc Kurtosis	777	407	223	791	404	211	825	437	220



1821 **Table 5: Parameters of the TTDs derived from the simulations with different saturated bedrock hydraulic conductivity K_{br} . Very**
 1822 **low = 10^{-7} , low = 10^{-6} , medium low = 10^{-5} , medium high = 10^{-4} , high = 10^{-3} , very high = 1, equal = 2 m day $^{-1}$. The “low” scenario**
 1823 **corresponds to THDB.**

Name	VLow	Low	MLow	MHigh	High	VHigh	Equal
1st Quartile	89	89	90	93	105	102	96
Median	113	115	122	132	160	144	138
Mean	145	151	196	258	239	182	166
3rd Quartile	163	167	180	211	308	222	206
Stand Dev	138	189	497	520	211	129	116
Skewness	26	28	14	7	2	2	2
Exc Kurtosis	1472	1233	252	79	11	4	5

1824 **Table 6: Parameters of the TTDs for the simulations with a decay in saturated soil hydraulic conductivity K_s . Mean values of**
 1825 **scenarios with and without decay are presented in the two columns on the right (μ).**
 1826

Name	THDB		THWB		TLDB		TLWB		$\mu_{NoDecay}$	μ_{Decay}
	No	Yes	No	Yes	No	Yes	No	Yes		
1st Quartile	89	84	45	37	126	128	91	81	88	82
Median	115	111	85	81	291	261	263	173	189	156
Mean	151	144	110	103	439	342	400	288	275	219
3rd Quartile	167	158	136	132	576	462	546	411	356	291
Stand Dev	189	182	173	173	505	354	519	401	347	278
Skewness	28	30	29	31	5	8	6	10	17	20
Exc Kurtosis	1233	1373	1426	1492	70	158	86	201	704	806

1827 **Table 7: Parameters of the TTDs derived from the model simulations with different precipitation frequencies (arid: low-frequency,**
 1828 **15 days interarrival time; humid: high-frequency, 3 days interarrival time). For comparison, the THDM scenario has a precipitation**
 1829 **frequency (derived from a natural precipitation time series) which is quite similar to the humid case. Means (μ) and standard deviations (σ)**
 1830 **of the arid and humid scenarios.**
 1831

Name	Arid					THDM	Humid					μ_{Arid}	μ_{Humid}	σ_{Arid}	σ_{Humid}
1st Quartile	134	162	173	180	193	137	138	143	136	144	136	168	139	20	3
Median	222	231	273	282	274	207	220	208	245	241	227	256	228	25	14
Mean	290	305	308	324	325	280	277	280	286	291	280	310	283	13	5
3rd Quartile	377	352	370	369	368	366	357	339	358	367	360	367	356	8	9
Stand Dev	293	281	288	285	286	298	299	294	298	302	302	287	299	4	3
Skewness	14	14	15	14	15	15	16	16	15	15	15	15	15	0	0
Exc Kurtosis	382	417	417	407	426	407	433	434	423	416	422	410	426	15	7

1832 **Table 8: Parameters of the TTDs derived from the modeling with silt-type and sand-type soil water retention curves (WRCs). The**
 1833 **mean values for the silt μ_{silt} and sand μ_{sand} scenarios are given on the right side.**
 1834

Name	THDS		THDB		THWS		THWB		TLDS		TLDB		TLWS		TLWB		μ_{silt}	μ_{sand}
	Silt	Sand																
1st Quartile	244	45	89	38	101	19	45	16	458	54	126	13	232	105	91	13	173	38
Median	441	142	115	81	218	50	85	42	785	160	291	16	565	393	263	76	345	120
Mean	515	175	151	87	354	98	110	58	1009	341	439	115	796	575	400	225	472	209
3rd Quartile	656	223	167	114	501	118	136	82	1308	491	576	100	1116	837	546	307	626	284
Stand Dev	455	325	189	171	443	245	173	142	880	455	505	250	816	665	519	378	497	329
Skewness	7	18	28	37	7	23	29	44	3	5	5	9	3	3	6	6	11	18
Exc Kurtosis	125	453	1233	1811	123	791	1426	2586	20	62	70	237	22	25	86	98	388	758

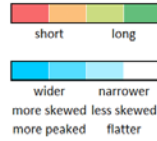
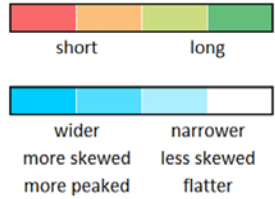


Table 9: Parameters of the TTDs derived from the modeling with wet (W) or fully saturated (S) antecedent conditions and very large ($> 10 \text{ mm h}^{-1}$) or extreme ($>>> 100 \text{ mm h}^{-1}$) event precipitation.

Name	HIGH				LOW			
	THWB	THSB	THSB ⁺	THSB ⁺⁺⁺	TLWB	TLSB	TLSB ⁺	TLSB ⁺⁺⁺
% SOF ₁₀	0.5	8.9	9.3	64.2	75.7	91.3	92.1	99.3
1st Quartile	45	26	26	0	91	12	1	0
Median	85	77	77	0	263	96	44	0
Mean	110	96	96	22	400	258	206	7
3rd Quartile	136	124	124	0	546	380	271	0
Stand Dev	173	169	169	93	519	413	378	79
Skewness	29	31	31	45	6	5	6	28
Exc Kurtosis	1426	1526	1528	4099	86	81	91	1930



1 **Supplement**

2

3 **Contents of this file**

- 4 Text S1 to S76
- 5 Figures S1 to S110
- 6 Tables S1 to S113

7 **Introduction**

8 The supplement consists of 76 text files, 101 figures and 113 tables. The individual sections contain [a comparison of TTDs](#)
9 [resulting from a looped and a continuous precipitation time series \(Text S1, Fig. S1\)](#), an overview of the different modeling
10 scenarios (Table S1), the precipitation time series created for testing the influence of the sequence of events (Fig. S24) and the
11 table containing all distributions metrics for those 15 scenarios (Table S3), the tracer mass in storage, the cumulative tracer
12 mass of the outflux and the cumulative mass balance errors for the 36 scenarios (Fig. S32), methods for the computation of
13 TTD metrics (Text S24, Fig. S43), methods for and results from the determination of young water fractions (Text S32, Fig.
14 S54, Table S2), [a comparison of different theoretical probability density functions \(Fig. S6\)](#), TTD smoothing (Text S43, Fig.
15 S75), the derivation of TTDs from tracer breakthrough curves (Fig. S86), the analysis of spatial tracer distribution over the
16 catchment and in its profile (Text S54, Fig. S97), outflow probability distributions plotted against cumulative outflow (Fig.
17 S108), [measures of how well the different theoretical probability distributions fit the modeled TTDs \(Table S4\)](#), [metrics of the](#)
18 [TTDs derived from scenarios with other catchment and climate properties \(Tables S5 to S11\)](#), a method to add power law tails
19 to ~~AD- θ~~ Gamma probability distributions (Text S65, Fig. S69) as well as an example of using TTDs for reactive solute
20 transport applications (Text S76, Fig. S110).

21 **Text S1.**

22 We looped a one-year-long time series of precipitation from the north-east of Germany and used it as a boundary condition
23 throughout the 33-year-long model period in all of the scenarios. In order to check whether the looping would cause any
24 unwanted artifacts in the resulting TTDs we additionally created a 32-year-long synthetic continuous precipitation time series
25 with similar attributes: average yearly precipitation amount of 690 mm a⁻¹, average event interarrival time of 2.64 days and
26 Poisson distributed precipitation event amounts. This continuous (non-looped) time series was attached to the one-year-long
27 recorded time series to create a second 33-year-long time series. The comparison of the two resulting TTDs shows that the
28 looping does not introduce any artifactual irregularities into the TTD shape (Fig. S1).

29 **Text S21.**

30 1) The first quartile (Q₁) was determined via the cumulative TTD. It is the transit time when 25 % of the applied tracer mass
31 has left the system.

32 2) The median (Q₂) was derived similarly (when 50 % of the applied tracer mass has left the system).

33 3) The mean transit time (mTT) was calculated according to Eq. S1:

34
$$mTT = \sum(J_{out}^{norm} * \Delta t * t). \quad (S1)$$

35 4) The third quartile (Q₃) was again determined with the help of the cumulative TTD (when 75 % of the applied tracer mass
36 has left the system).

37 5) The standard deviation (σ) is a measure describing the dispersion of a distribution, with a small standard deviation pointing
38 towards the data point cloud being clustered closely around the mean. It was calculated according to Eq. S2:

39
$$\sigma = \sqrt{\sum(J_{out}^{norm} * \Delta t * t^2) - mTT^2}. \quad (S2)$$

40 6) The skewness (ν) is a measure that informs about how much a distribution leans to one side of its mean. A negative skew
41 means that the distribution leans towards the right (the highest concentration follows after the mean), a positive skew indicates
42 that the distribution leans towards the left (the highest concentration is reached before the mean). It was calculated according
43 to Eq. S3:

44
$$\nu = \frac{\sum(J_{out}^{norm} * \Delta t * t^3) - (3 * mTT * \sigma^2) - mTT^3}{\sigma^3}. \quad (S3)$$

45 7) The excess kurtosis (γ) was calculated according to Eq. S4:

46
$$\gamma = \frac{\sum(J_{out}^{norm} * \Delta t * (t - mTT)^4)}{\sigma^4} - 3. \quad (S4)$$

47 A positive excess kurtosis means that a distribution produces more extreme outliers than the Gaussian normal distribution, so
48 this measure is related predominantly to the tail of the distribution – and only to a lesser extent to its peak. For positive values

49 of the excess kurtosis, the tail of the distribution approaches zero more slowly than a normal distribution while the peak is
50 higher (leptokurtic). For negative values of the excess kurtosis, the tail approaches zero faster than a normal distribution while
51 the peak is lower (platykurtic). There is no unanimous consent on the mathematical definition of what constitutes a “heavy”
52 or “light” tail. According to some sources heavy tails are those tails that have more weight than an exponential tail – a definition
53 which corresponds to heavy-tailed distributions being defined as possessing an increasing hazard (rate) function (Kellison and
54 London, 2011). This definition would place Gamma distributions with shape parameters $\alpha < 1$ clearly in the category of heavy-
55 tailed distributions and Gamma distributions with shape parameters $\alpha > 1$ in the category of light-tailed distributions. Other
56 sources, however, attribute heavy tails only to distributions with infinite moment generating functions (Rolski et al, 2009).
57 Therefore we are not using the (absolute) terms heavy-tailed or light-tailed to describe the TTDs but rather just refer to
58 “heavier” and “lighter” tails [in the manuscript](#).

59 **Text S32.**

60 We calculated young water fractions for the best-fit Gamma distributions to see how they are influenced by catchment and
61 event properties. The young water fraction (F_{yw}) constitutes the fraction of water in discharge with an age below 2.3 months
62 (Jasechko et al., 2016; Kirchner, 2016).

63 Modeled F_{yw} from the best-fit Gamma distributions ranged from 4 % to 100 % (Table S2). We also determined F_{yw} directly
64 from the modeled TTDs. They ranged from 0 % to 61 %. The F_{yw} derived from the best-fit Gamma distributions and directly
65 from the modeled TTDs differed considerably, especially for the scenarios with larger F_{yw} . The F_{yw} derived directly from the
66 modeled TTDs were almost always smaller than the ones derived from the best-fit Gamma distributions. [This overestimation](#)
67 [resulted from the fact that most of the best-fit Gamma distributions were found to have shape parameters \$\alpha\$ larger than 1, which](#)
68 [led to TTDs with initial values of 0 and a ‘humped’ shape causing less outflow at short transit times.](#)

69 In general, F_{yw} increases with increasing P_{sub} , θ_{ant} , K_S and with decreasing D_{soil} (Fig. S53). The highest F_{yw} was observed for
70 scenarios with shallow D_{soil} , wet θ_{ant} and large P_{sub} . [The Young water fractions increase with increasing \$\theta_{ant}\$ is found](#) because
71 [on the one hand](#), catchment soil storage is already filled and hydraulic conductivity of the soil is already high (close to
72 saturation) so that the incoming event water can immediately flow laterally towards the outlet while only a smaller fraction
73 stays in the soil storage or enters the low-conductivity bedrock. In catchments with higher K_S , F_{yw} also increases since the
74 conductivity contrast between the bedrock and the soil increases and more of the incoming event water flows laterally towards
75 the outlet with a higher velocity. Shallow soils increase F_{yw} too due to the fact that less soil storage is available where event
76 water can be stored before lateral flow is initiated. Finally, larger P_{sub} increases F_{yw} as well, which can be associated with the
77 “flushing effect” where more flow in the more fully saturated soil layer equals a larger flux through the soil layer and hence a
78 larger fraction of young water in the discharge.

79 **Text S43.**

80 The modeled TTDs were smoothed just for the purpose of better visual comparison – all the calculations and the fitting were
81 performed on the unsmoothed data (see Fig. S74 for an example of a smoothed TTD). We smoothed the TTDs by using moving
82 window averaging with increasing window size towards longer transit times according to Eq. S5 and S6:

$$83 N_{left}(t) = \begin{cases} N, & \text{if } (\ln t)^3 \leq 0 \\ \lfloor N(t) - 0.5(\ln t)^3 \rfloor, & \text{if } (\ln t)^3 > 0 \end{cases} \quad (S5)$$

$$84 N_{right}(t) = \begin{cases} N, & \text{if } (\ln t)^3 \leq 0 \\ \lfloor N(t) + (\ln t)^3 \rfloor, & \text{if } (\ln t)^3 > 0 \end{cases} \quad (S6)$$

85 with N_{left} being the model time step number at the left corner of the window, N_{right} the model time step number at the right
86 corner of the window and N the model time step number at a given transit time t . We increased the window size with increasing
87 transit time since we plotted the TTDs on a double-log scale so that the older parts of the TTDs were compressed and also
88 because the variation in the initial shape of the TTD is higher and influenced [moreless](#) by the series of subsequent precipitation
89 events.

90 **Text S54.**

91 Comparing the evolution of tracer concentrations throughout the model domain can explain the differences of the resulting
92 TTDs for the various model scenarios. Figure S96 demonstrates this by showing tracer concentrations at the soil surface and
93 in a depth profile close to the center of the catchment for two very different scenarios (FHWB with the shortest median and
94 mean transit time and TLDS with the longest median and mean transit time). The fast arrival of the tracer in the FHWB scenario
95 is possible since the tracer quickly infiltrates the entire soil column and is transported laterally towards the outlet. In the TLDS
96 scenario it takes much longer for the entire soil column to act as a pathway for lateral flow which is partly due to the fact that
97 θ_{sat} is low (more pore space can be filled up until saturated hydraulic conductivity is reached and more pore space is available
98 to be filled up before water will be diverted downslope at the bedrock–soil interface). Both TTDs peak after the entire soil
99 column is filled with tracer and starts acting as a lateral flow path and some tracer has entered the bedrock. This happens almost
100 instantly in the FHWB scenario and only after approximately 100 days in the TLDS scenario. The amount of tracer infiltrating
101 into the bedrock is higher for the TLDS scenario. This is due to the fact that the contact time between tracer in the soil and the
102 bedrock surface is longer. In the FHWB scenario the tracer is flushed out of the soil a lot faster (higher K_s and more P_{sub}),
103 therefore less tracer can infiltrate into the bedrock. The soil in the FHWB scenario is virtually free of tracer much sooner than
104 the soil in the TLDS scenario, therefore the [break in the power-law](#)-tail of the TTD (deriving from the [switch from](#)
105 [predominantly soil to predominantly](#) bedrock tracer outflux) [happensstarts](#) earlier than for the TLDS scenario (around 1000
106 days vs. around 5000 days). The [power-law](#)-tails [isare](#) heavier for TLDS since more tracer had the chance to infiltrate into the
107 bedrock at later times.

108 **Text S65.**

109 Adding power law tails to Gamma or AD distributions can be done via a simple approach that replaces the tail of the respective
110 distribution with a power law tail as soon as the probability density of the model distribution falls below that one of a power
111 law with a constant a of 0.2 and an exponent k of 1.6 (Eq. S7 and Fig. S68):

$$112 f(t) = \begin{cases} t^{\alpha-1} \frac{e^{-\frac{t}{\beta}}}{\beta^{\alpha}\Gamma(\alpha)}, & \text{if } t^{\alpha-1} \frac{e^{-\frac{t}{\beta}}}{\beta^{\alpha}\Gamma(\alpha)} \geq at^{-k} \vee t \leq \alpha\beta \\ at^{-k}, & \text{if } t^{\alpha-1} \frac{e^{-\frac{t}{\beta}}}{\beta^{\alpha}\Gamma(\alpha)} < at^{-k} \wedge t > \alpha\beta \end{cases} \quad (S7)$$

113 In order to preserve the mass balance, the combined distribution has to be re-normalized (accounting for the added mass from
114 the power law tail, Eq. S8 and S9):

$$115 w = \int_{t=0}^{\infty} f(t). \quad (S8)$$

$$116 TTD(t) = \frac{f(t)}{w}. \quad (S9)$$

117 From a mass balance perspective, however, generally it is not necessary to add these power law tails since they only account
118 for a very small fraction of the total injected mass. Yet they can alter the mTT significantly (while the median remains largely
119 unaffected).

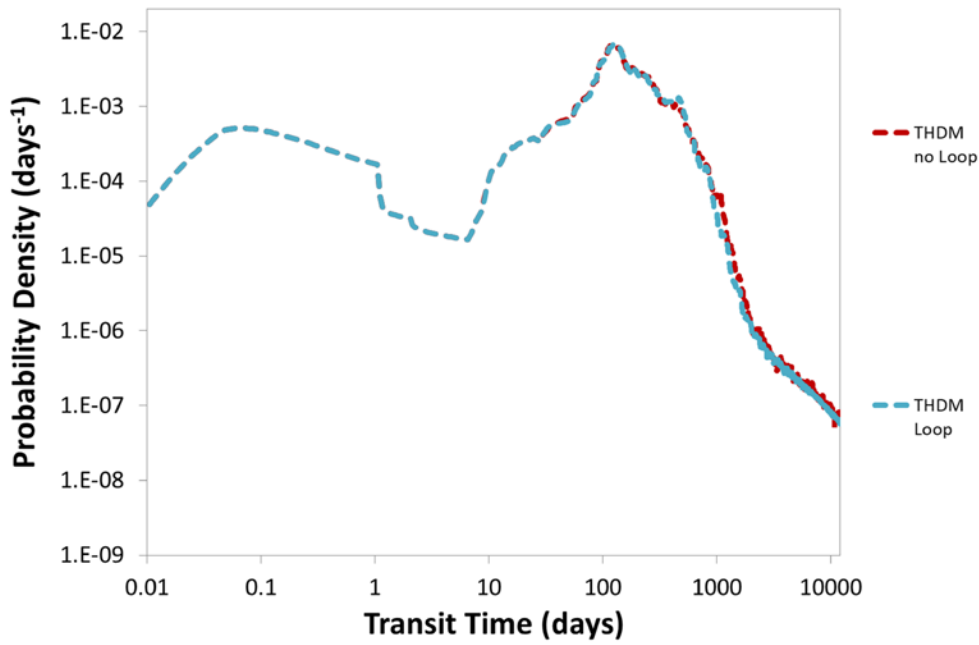
120 **Text S67.**

121 Modification of TTDs to incorporate reactive solute transport into the concept can be achieved, e.g., by multiplication of the
122 TTD with a decay function. In this example an exponential decay function is used (Eq. S10):

$$123 TTD_{react}(t) = TTD(t) * e^{-t/t_{1/2}}, \quad (S10)$$

124 where TTD(t) is the probability density at transit time t and $t_{1/2}$ is the half-life of the solute. Note that the cumulative TTD_{react}
125 does not add up to a value of 1 anymore. It rather reflects the fraction of solute that will eventually be discharged out of the
126 catchment (Fig. S911).

127 Other functions that can modify TTDs to make them suitable predictors of reactive solute transport include specific retardation
128 or removal functions for certain transit time ranges associated with flow paths through different catchment compartments (e.g.,
129 groundwater flow, soil matrix flow, macropore flow).



131
132 Figure S1: Comparison of TTDs derived from a continuous (no Loop) and from a looped one-year-long precipitation time series.
133 Looping does not cause artifacts and there is no significant difference between the two TTD shapes.
134

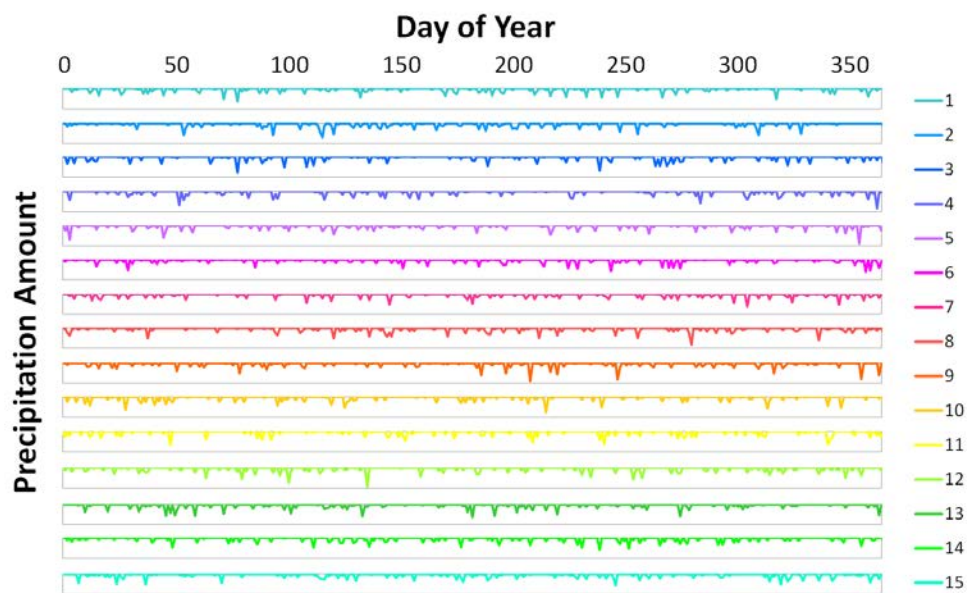
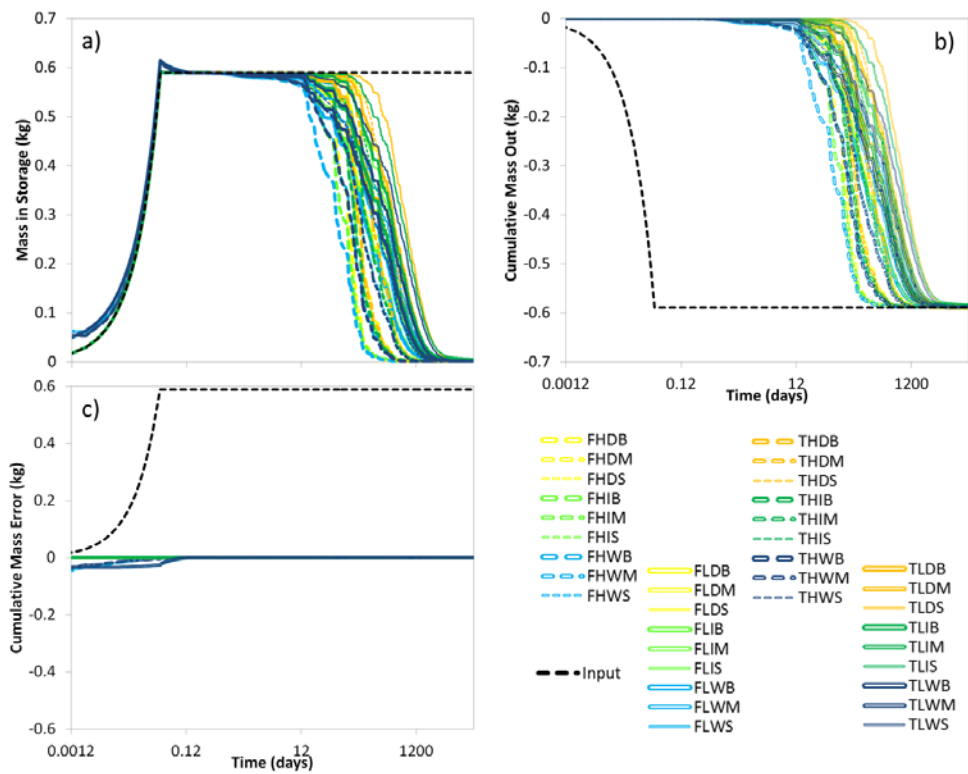


Figure S42: 15 different precipitation time series with similar exponential distributions of precipitation event amounts and interarrival times. The y-axes all range from 0 to 40 mm. The time series were created to test the influence of event sequence on the shape of TTDs.

135
136
137
138
139



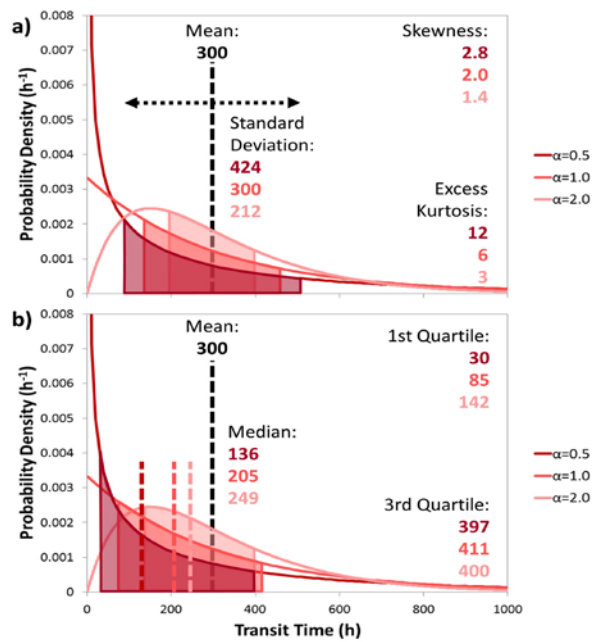
140

141

142

Figure S23: a) Total tracer mass in storage, b) cumulative tracer mass outflux, c) cumulative mass balance error for all 36 scenarios. Note that most scenarios plot on top of each other in panel c).

143



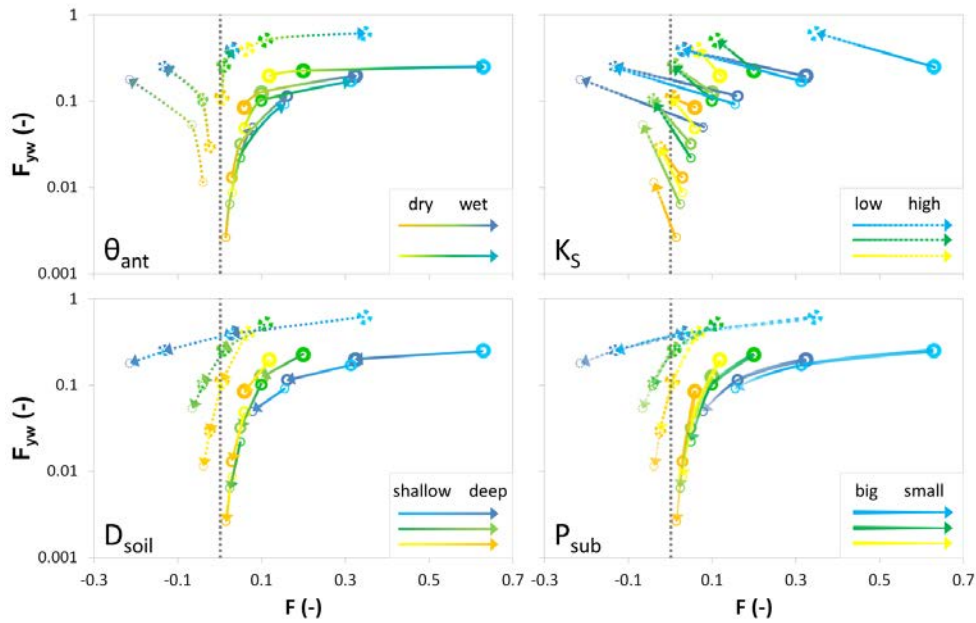
144

145 **Figure S34:** Distribution metrics of three different Gamma distributions with varying shape parameter α and equal mean (300 h).

146 a) Black dashed line: mean (300 h), dotted black line and filled areas under the curves: standard deviation. b) Black dashed line:

147 mean (300 h), colored dashed lines: medians, filled areas under the curves range from the first to the third quartile (Q_1 – Q_3).

148



149
 150 Figure S45: Change of young water fractions (F_{yw}) with the flow path number (F) for four different catchment and climate
 151 properties. Yellow colors indicate dry, green intermediate and blue wet antecedent moisture conditions θ_{ant} . Thick marker lines
 152 indicate big, large, mid-sized lines medium and thin lines small amounts of subsequent precipitation P_{sub} . Solid lines indicate low,
 153 dashed lines high saturated hydraulic conductivities K_S , lighter shades of a color indicate shallow, darker shades deep soils D_{soil} .

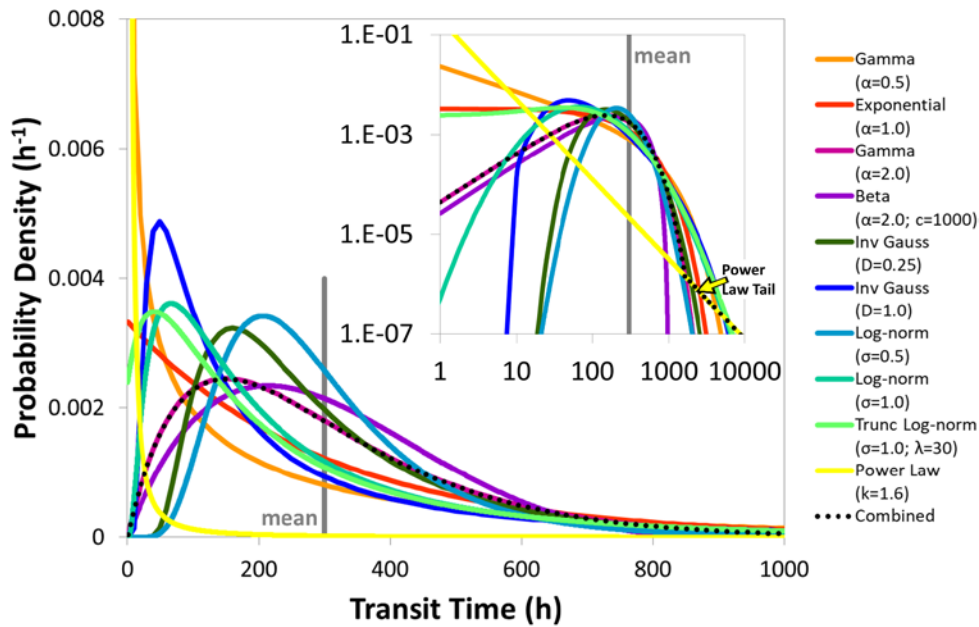
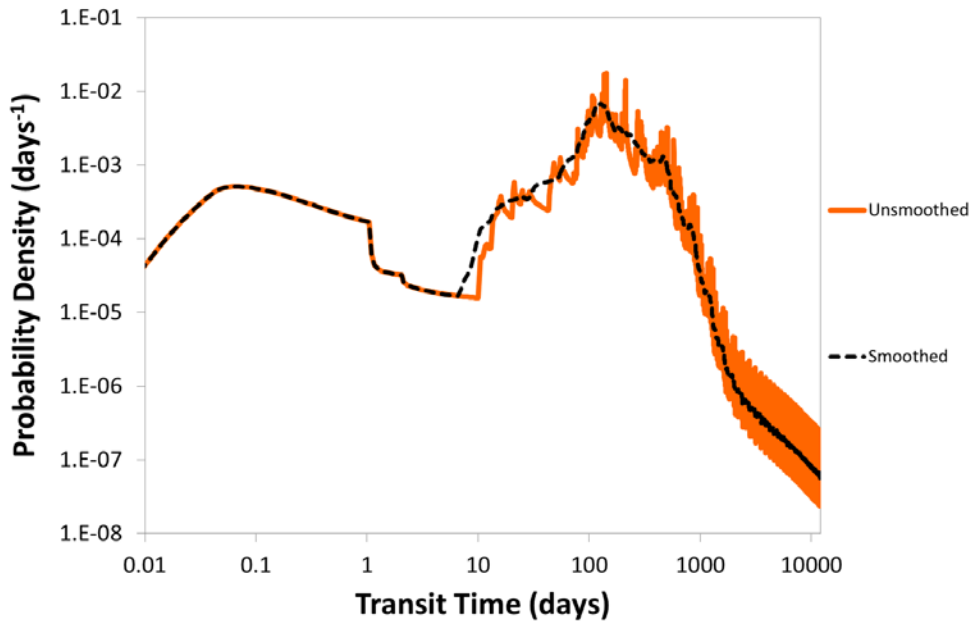
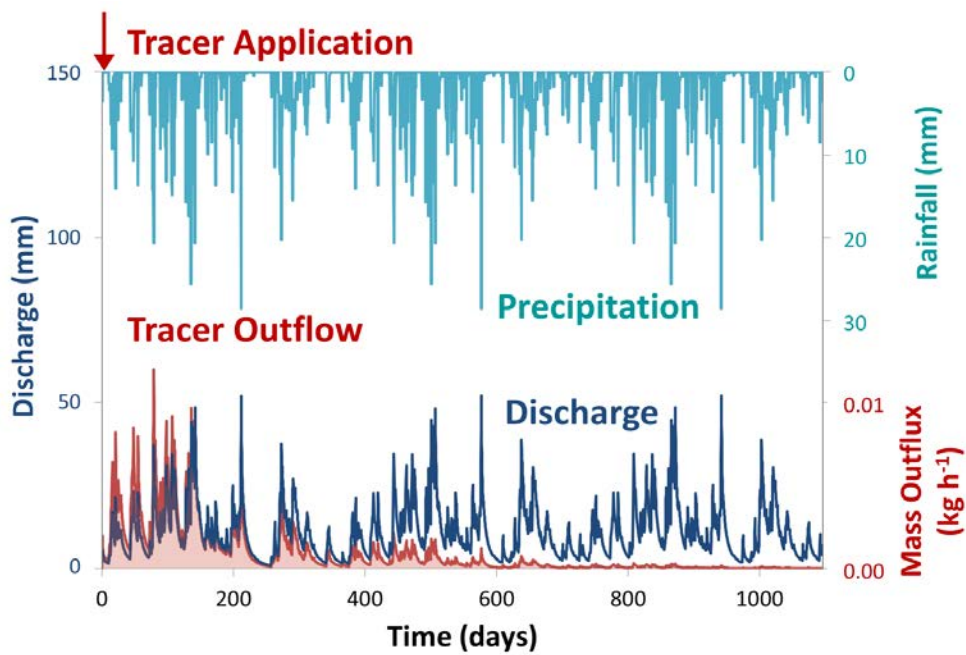


Figure S6: A set of ten different common theoretical probability distributions (all but the power law having a mean value of 300 h, grey line). The black dotted line is a distribution that is a combination of a Gamma distribution with the tail of a power law distribution. The inset has a log-log scale.



160
 161 Figure S57: Unsmoothed (orange) and smoothed (black) version of the same TTD.
 162



163

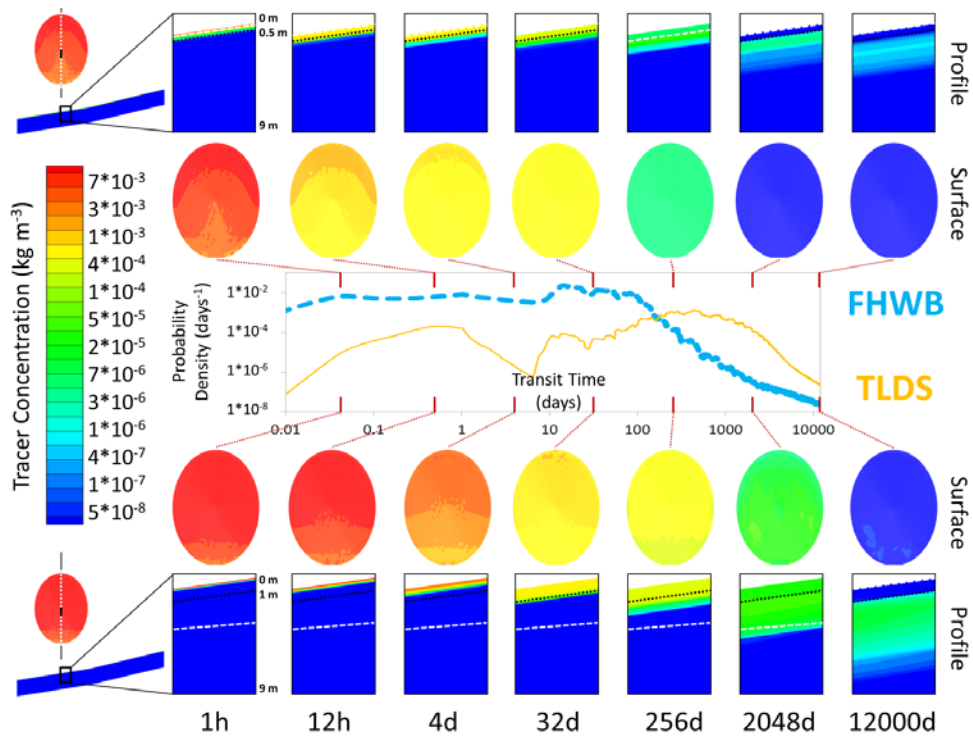
164

165

166

167

Figure S68: Precipitation input (cyan), total outflow (blue) and tracer concentration in the outflow (red) for the first three years of the model run for scenario THDM. The tracer breakthrough curve (when normalized) constitutes the TTD of the injected tracer impulse.



168

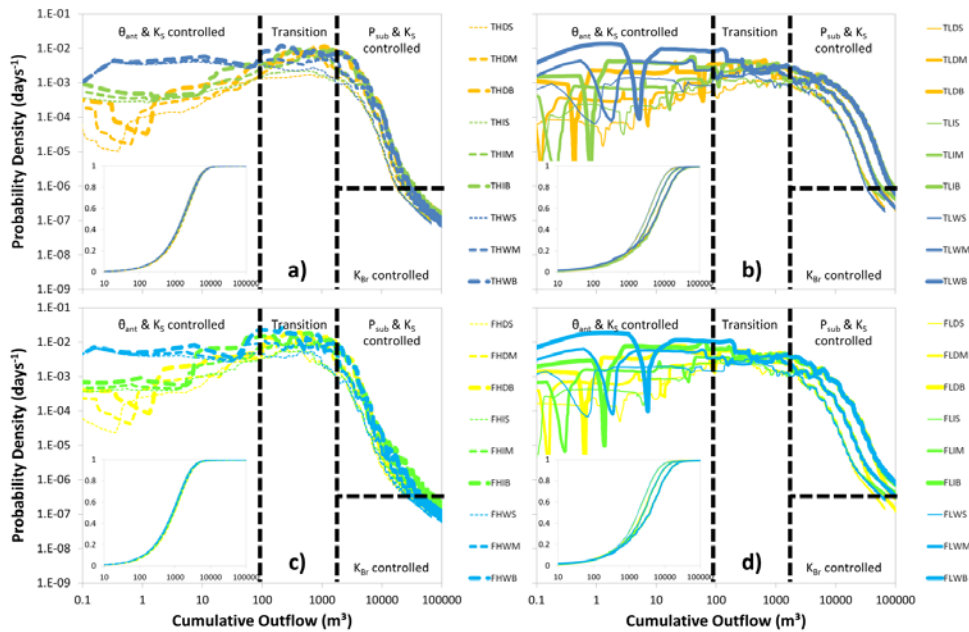
169

170

171

Figure S79: Time series of tracer concentration distribution in the subsurface soil across the entire catchment, in a depth profile in the center of the catchment for two scenarios (top: FHWB; bottom: TLDS) with very different resulting TTDs shapes. The dotted black line in the profiles represents the soil-bedrock interface; the white dashed line is the water table.

172



173

174

175

176

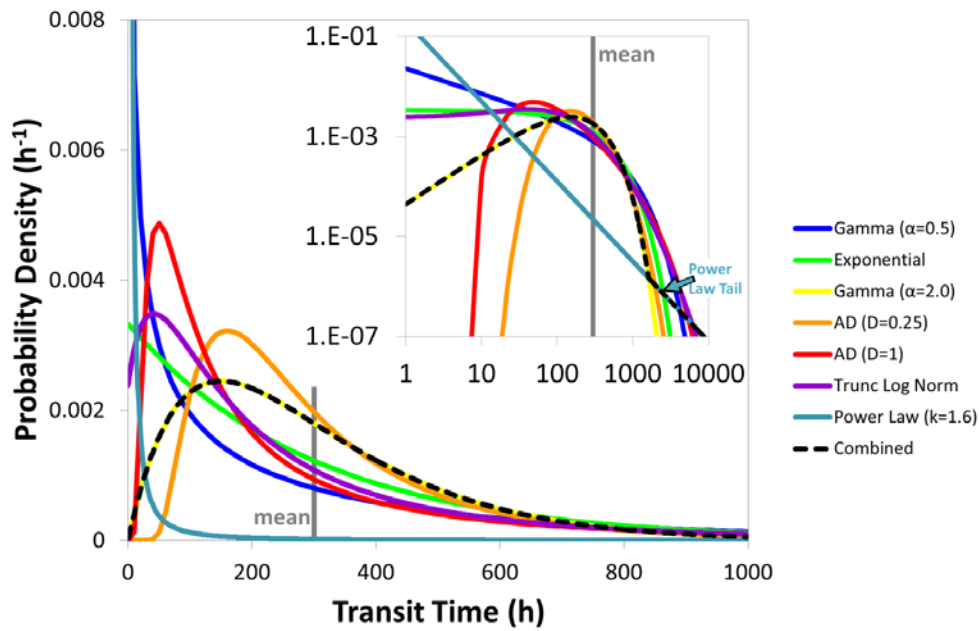
177

178

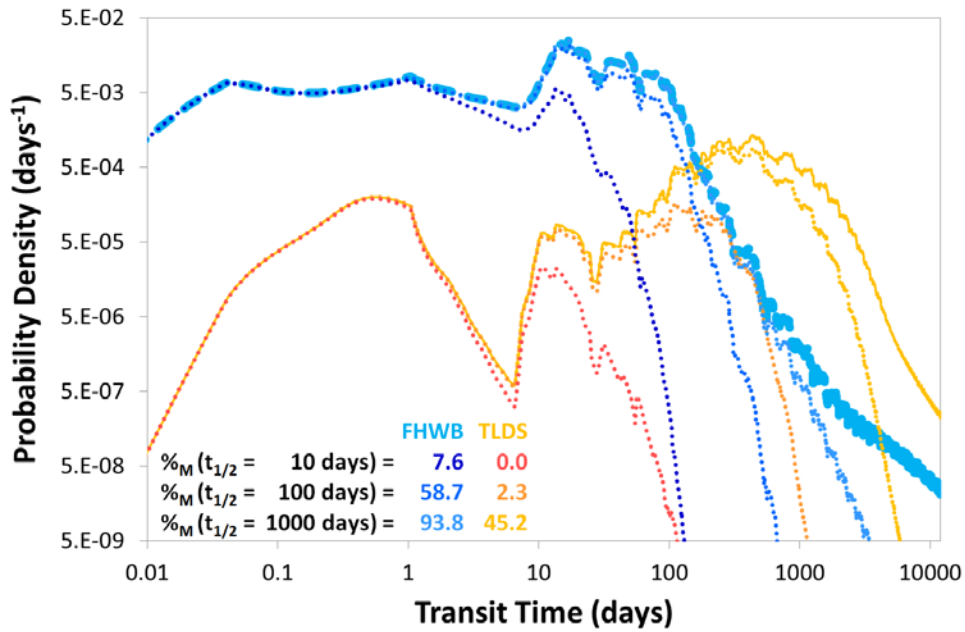
179

Figure S810: Similar to Fig. 7 except for the fact that outflow probability is plotted against cumulative outflow instead of transit time. Distributions are grouped by soil depth (upper panels a and b = deep (thick); lower panels c and d = shallow (flat)) and saturated hydraulic conductivity (left panels a and c = high; right panels b and d = low). Yellow colors indicate dry, green intermediate and blue wet antecedent moisture conditions θ_{ant} . Thick lines indicate big, large, mid-sized lines medium and thin lines small P_{sub} amounts of subsequent precipitation amounts. Insets show cumulative outflow probability distributions. Dashed black lines divide TTDs into four parts, each part controlled by different properties. Note the log-log axes.

180



181 Figure S9: A set of seven different common theoretical probability distributions (all but the power law having a mean value of 300
 182 h, grey line). The black dashed line is a distribution that is a combination of a Gamma distribution with the tail of a power law
 183 distribution. The inset has a log-log scale.
 184



186

187

188

189

190

Figure S101: Two TTDs from the FHWB (blue) and TLDS (yellow) scenarios. Each one modified by three functions of exponential decay (with half-lives $t_{1/2}$ of 10, 100 and 1000 days). The fraction of mass eventually leaving the system ($\%_M$) can differ greatly: for a half-life of 100 days, the FHWB TTD still delivers 59 % of the original input to discharge while the TLDS TTD only delivers 2 %.

D _{soil}	DEEP (THICK)																	
K _s	HIGH						WET						LOW					
θ _{ant}	DRY			INT			WET			DRY			INT			WET		
P _{sub}	SMALL	MED	BIG	SMALL	MED	BIG	SMALL	MED	BIG	SMALL	MED	BIG	SMALL	MED	BIG	SMALL	MED	BIG
Name	THDS	THDM	THDB	THIS	THIM	THIB	THWS	THWM	THWB	TLDS	TLDM	TLDB	TLIS	TLIM	TLIB	TLWS	TLWM	TLWB

Porosity:

Name	THDM	THIM	THWM
Porosity	Small Normal Large	Small Normal Large	Small Normal Large

Bedrock Conductivity:

VLow	Low	MLow	MHigh	High	VHigh
------	-----	------	-------	------	-------

Decay of Hydraulic Conductivity:

Name	THDB	THWB	TLDB	TLWB
Decay	No Yes	No Yes	No Yes	No Yes

Precipitation Frequency:

Arid	THDM	Humid
------	------	-------

Water Retention Curve:

Name	THDS	THDB	THWS	THWB	TLDS	TLDB	TLWS	TLWB
WRC	Silt Sand							

Extreme Precipitation after Full Saturation:

K _s	HIGH				LOW			
Name	THWB	THSB	THSB*	THSB***	TLWB	TLBS	TLBS*	TLBS***

D _{soil}	DEEP (THICK)																	
K _s	HIGH						WET						LOW					
θ _{ant}	DRY			INT			WET			DRY			INT			WET		
P _{sub}	SMALL	MED	BIG	SMALL	MED	BIG	SMALL	MED	BIG	SMALL	MED	BIG	SMALL	MED	BIG	SMALL	MED	BIG
Name	THDS	THDM	THDB	THIS	THIM	THIB	THWS	THWM	THWB	TLDS	TLDM	TLDB	TLIS	TLIM	TLIB	TLWS	TLWM	TLWB

Porosity:

Name	THDM	THIM	THWM
Porosity	Small Normal Large	Small Normal Large	Small Normal Large

Bedrock Conductivity:

VLow	Low	MLow	MHigh	High	VHigh
------	-----	------	-------	------	-------

Decay of Hydraulic Conductivity:

Name	THDB	THWB	TLDB	TLWB
Decay	No Yes	No Yes	No Yes	No Yes

Precipitation Frequency:

Arid	THDM	Humid
------	------	-------

Catchment Shape:

Name	THDM	THWM
Shape	Top Mid Bot	Top Mid Bot

Water Retention Curve:

Name	THDS	THDB	THWS	THWB	TLDS	TLDB	TLWS	TLWB
WRC	Silt Sand							

Extreme Precipitation after Full Saturation:

K _s	HIGH				LOW			
Name	THWB	THSB	THSB*	THSB***	TLWB	TLBS	TLBS*	TLBS***

Table S1: Information on which of the base-case scenarios (upper table) the other seven scenarios (porosity – blue; bedrock conductivity – orange; decay in hydraulic conductivity – red; precipitation frequency – green; catchment shape – bold; soil water retention curve – purple; extreme precipitation after full saturation – yellow) are based upon.

D _{50t} K _s θ _{best} P _{sub}		DEEP (THICK)												LOW					
		DRY			HIGH			WET			DRY			LOW			WET		
Name		SMALL	MED	BIG	SMALL	MED	BIG	SMALL	MED	BIG	SMALL	MED	BIG	SMALL	MED	BIG	SMALL	MED	BIG
F _{Yw Gam}		0.11	0.29	0.89	0.14	0.30	0.77	0.19	0.32	0.63	0.04	0.09	0.15	0.05	0.10	0.15	0.08	0.13	0.18
F _{Yw Mod}		0.01	0.03	0.11	0.05	0.11	0.26	0.18	0.25	0.40	0.00	0.01	0.08	0.01	0.03	0.12	0.05	0.12	0.20

D _{50t} Name		SHALLOW (FLAT)																	
		FHDS			FHMS			FHWs			FLDS			FLWS					
Name		FHDS	FHDM	FHDB	FHIS	FHIM	FHIB	FHWs	FHWM	FHWB	FLDS	FLOM	FLDB	FLIS	FLIM	FLIB	FLWS	FLWM	FLWB
F _{Yw Gam}		0.27	0.84	1.00	0.28	0.74	0.96	0.30	0.60	0.86	0.09	0.17	0.23	0.11	0.17	0.24	0.14	0.19	0.25
F _{Yw Mod}		0.03	0.11	0.40	0.10	0.25	0.51	0.25	0.39	0.61	0.01	0.05	0.20	0.02	0.10	0.23	0.09	0.17	0.25

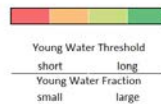


Table S2. Young water fractions (F_{Yw}) for the 36 different base-case scenarios. The young water fractions are determined from the best-fit Gamma distributions ($F_{Yw Gam}$) and from the modeled TTDs themselves ($F_{Yw Mod}$).

Name	THDM	1	2	3	4	5	6	7	8	9	10	11	12	13	14	15	μ	σ
1st Quartile	137	138	143	136	144	136	179	166	163	181	120	162	136	165	159	123	150	19
Median	207	220	208	245	241	227	250	251	239	246	207	244	236	242	244	204	234	16
Mean	280	277	280	286	291	280	306	300	300	302	262	296	285	298	296	265	288	13
3rd Quartile	366	357	339	358	367	360	368	363	361	366	349	362	358	355	365	351	359	8
Stand Dev	298	299	294	298	302	302	295	298	295	297	300	296	302	299	297	299	298	2.5
Skewness	14.8	15.7	15.6	15.4	15.3	15.5	15.6	15.6	15.7	15.6	15.4	15.6	15.5	15.9	15.5	15.4	15.5	0.16
Exc Kurtosis	407	433	434	423	416	422	432	432	436	433	421	433	424	439	429	422	429	6.5

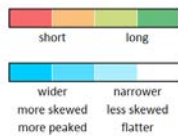


Table S3. Distribution metrics for the 15 TTDs resulting from different precipitation event sequences. For comparison we also show the metrics for the THDM scenario which uses an actually measured time series of precipitation and has a slightly different distribution of precipitation event amounts and interarrival times but otherwise similar catchment and climate properties. The means (μ) and standard deviations (σ) of the metrics of the 15 scenarios are also shown.

D _{50t} K _s θ _{best} P _{sub}		DEEP (THICK)												LOW					
		DRY			HIGH			WET			DRY			LOW			WET		
Name		SMALL	MED	BIG	SMALL	MED	BIG	SMALL	MED	BIG	SMALL	MED	BIG	SMALL	MED	BIG	SMALL	MED	BIG
InvGau		6	-4	-9	12	-2	-6	21	4	-1	31	25	22	102	44	32	60	35	18
Δ Mean		-282	-152	-109	-132	-94	-81	26	-25	-42	-423	-172	-10	-186	-74	40	-52	31	84
LogN		8	-3	-9	17	0	-6	30	6	0	38	32	32	115	56	44	75	49	32
InvGau		-32	7	6	-6	11	-1	1	-6	-8	-22	-19	-13	17	-44	-21	-28	-50	-37
Δ Median		-15	17	8	12	20	2	17	2	-4	18	10	8	59	-13	1	-6	-26	-20
LogN		-28	10	7	3	14	0	6	-3	-6	-13	-11	-6	27	-35	-14	-18	-43	-31
InvGau		0.44	0.32	0.33	0.68	0.22	0.19	1.20	0.31	0.30	0.51	0.92	1.10	1.78	1.80	1.65	2.63	2.40	2.10
FR		0.38	0.79	0.64	0.38	0.66	0.35	0.25	0.31	0.17	1.28	0.52	0.40	2.11	1.36	0.90	0.36	0.32	0.26
LogN		0.37	0.38	0.32	0.59	0.26	0.16	0.96	0.25	0.23	0.38	0.68	0.90	1.25	1.32	1.22	1.95	1.83	1.60

D _{50t} Name		SHALLOW (FLAT)																	
		FHDS			FHMS			FHWs			FLDS			FLWS					
Name		FHDS	FHDM	FHDB	FHIS	FHIM	FHIB	FHWs	FHWM	FHWB	FLDS	FLOM	FLDB	FLIS	FLIM	FLIB	FLWS	FLWM	FLWB
InvGau		-7	-11	-4	-7	-12	-7	1	-4	-1	13	10	9	34	16	10	79	15	8
Δ Mean		-156	-113	-67	-98	-89	-54	-23	-45	-29	-195	-56	11	-87	-17	40	1	35	57
LogN		-5	-11	-4	-5	-11	-7	4	-3	-1	19	15	15	45	26	19	42	26	18
InvGau		10	3	-4	10	-2	-2	-5	-10	-2	-33	-18	6	-41	-27	0	-32	3	1
Δ Median		21	6	-2	20	2	0	4	-6	1	-27	1	20	-12	-6	14	-7	20	13
LogN		13	4	-3	13	-1	0	-2	-8	1	-25	-12	11	-33	-21	4	-25	8	6
InvGau		0.38	0.41	0.14	0.36	0.30	0.20	0.36	0.25	0.29	0.68	0.53	0.44	2.13	1.40	0.98	1.71	1.21	0.92
FR		0.85	0.77	0.14	0.92	0.54	0.38	0.47	0.35	0.13	0.73	0.73	0.44	2.51	1.61	0.98	1.02	0.81	0.64
LogN		0.43	0.40	0.14	0.38	0.27	0.20	0.28	0.24	0.26	0.52	0.52	0.39	1.69	1.14	0.74	1.24	0.89	0.65



Table S4: Deviations of mean (green) and median (blue) transit times between the best-fit theoretical probability distributions and the modeled TTDs. Sum of the squared residuals (yellow) indicating goodness of fit between theoretical probability distribution and modeled TTDs.

Name	THDM			THIM			THWM		
	Small	Normal	Large	Small	Normal	Large	Small	Normal	Large
1st Quartile	97	137	178	76	105	135	46	67	91
Median	135	207	301	110	159	226	94	132	168
Mean	177	280	385	152	238	326	127	197	269
3rd Quartile	202	366	502	169	299	459	143	258	384
Stand Dev	248	298	349	239	285	336	239	275	323
Skewness	23	15	10	23	14	9	23	15	9
Exc Kurtosis	777	407	223	791	404	211	825	437	220

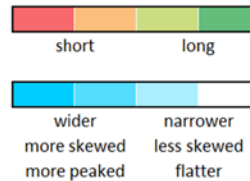


Table S5: Parameters of the TTDs derived from the simulations with different soil porosities: small = 0.24 m³ m⁻³, normal = 0.39 m³ m⁻³, large = 0.54 m³ m⁻³.

Name	VLow	Low	MLow	MHigh	High	VHigh	Equal
1st Quartile	89	89	90	93	105	102	96
Median	113	115	122	132	160	144	138
Mean	145	151	196	258	239	182	166
3rd Quartile	163	167	180	211	308	222	206
Stand Dev	138	189	497	520	211	129	116
Skewness	26	28	14	7	2	2	2
Exc Kurtosis	1472	1233	252	79	11	4	5



Table S6: Parameters of the TTDs derived from the simulations with different saturated bedrock hydraulic conductivity K_B . Very low = 10⁻⁷, low = 10⁻⁵, medium low = 10⁻³, medium high = 10⁻², high = 10⁻¹, very high = 1, equal = 2 m day⁻¹. The "low" scenario corresponds to THDB.

Name	THDB		THWB		TLDB		TLWB		H _{noDecay}	H _{Decay}
	No	Yes	No	Yes	No	Yes	No	Yes		
1st Quartile	89	84	45	37	126	128	91	81	88	82
Median	115	111	85	81	291	261	263	173	189	156
Mean	151	144	110	103	439	342	400	288	275	219
3rd Quartile	167	158	136	132	576	462	546	411	356	291
Stand Dev	189	182	173	173	505	354	519	401	347	278
Skewness	28	30	29	31	5	8	6	10	17	20
Exc Kurtosis	1233	1373	1426	1492	70	158	86	201	704	806

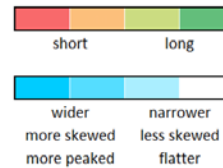


Table S7: Parameters of the TTDs for the simulations with a decay in saturated soil hydraulic conductivity K_s . Mean values of scenarios with and without decay are presented in the two columns on the right (μ).

Name	Arid					THDM	Humid					μ_{Arid}	μ_{Humid}	σ_{Arid}	σ_{Humid}
1st Quartile	134	162	173	180	193	137	138	143	136	144	136	168	139	20	3
Median	222	231	273	282	274	207	220	208	245	241	227	256	228	25	14
Mean	290	305	308	324	325	280	277	280	286	291	280	310	283	13	5
3rd Quartile	377	352	370	369	368	366	357	339	358	367	360	367	356	8	9
Stand Dev	293	281	288	285	286	298	299	294	298	302	302	287	299	4	3
Skewness	14	14	15	14	15	15	16	16	15	15	15	15	15	0	0
Exc Kurtosis	382	417	417	407	426	407	433	434	423	416	422	410	426	15	7

Table S8: Parameters of the TTDs derived from the model simulations with different precipitation frequencies (arid: low-frequency, 15 days interarrival time; humid: high-frequency, 3 days interarrival time). For comparison, the THDM scenario has a precipitation frequency (derived from a natural precipitation time series) which is quite similar to the humid case. Means (μ) and standard deviations (σ) of the arid and humid scenarios.

Name	THDS		THDB		THWS		THWB		TLDS		TLDB		TLWS		TLWB		μ_{Silt}	μ_{Sand}
	Silt	Sand																
1st Quartile	244	45	89	38	101	19	45	16	458	54	126	13	232	105	91	13	173	38
Median	441	142	115	81	218	50	85	42	785	160	291	16	565	393	263	76	345	120
Mean	515	175	151	87	354	98	110	58	1009	341	439	115	796	575	400	225	472	209
3rd Quartile	656	223	167	114	501	118	136	82	1308	491	576	100	1116	837	546	307	626	284
Stand Dev	455	325	189	171	443	245	173	142	880	455	505	250	816	665	519	378	497	329
Skewness	7	18	28	37	7	23	29	44	3	5	5	9	3	3	6	6	11	18
Exc Kurtosis	125	453	1233	1811	123	791	1426	2586	20	62	70	237	22	25	86	98	388	758

Table S9: Parameters of the TTDs derived from the modeling with silt-type and sand-type soil water retention curves (WRCs). The mean values for the silt μ_{Silt} and sand μ_{Sand} scenarios are given on the right side.

Name	THDM			THWM		
	Top	Mid	Bot	Top	Mid	Bot
1st Quartile	136	137	136	68	67	68
Median	203	207	205	133	132	132
Mean	277	280	279	196	197	198
3rd Quartile	351	366	368	254	258	259
Stand Dev	309	298	293	273	275	276
Skewness	15	15	14	15	15	15
Exc Kurtosis	407	407	391	444	437	431

Table S10: Parameters of the TTDs derived from the modeling with different catchment shapes (top-heavy, bottom-heavy). 'Mid' refers to the basic oval shape.

K _s Name	HIGH				LOW			
	THWB	THSB	THSB ⁺	THSB ⁺⁺⁺	TLWB	TLSB	TLSB ⁺	TLSB ⁺⁺⁺
% SOF ₁₀	0.5	8.9	9.3	64.2	75.7	91.3	92.1	99.3
1st Quartile	45	26	26	0	91	12	1	0
Median	85	77	77	0	263	96	44	0
Mean	110	96	96	22	400	258	206	7
3rd Quartile	136	124	124	0	546	380	271	0
Stand Dev	173	169	169	93	519	413	378	79
Skewness	29	31	31	45	6	5	6	28
Exc Kurtosis	1426	1526	1528	4099	86	81	91	1930

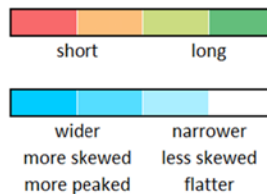


Table S11: Parameters of the TTDs derived from the modeling with wet (W) or fully saturated (S) antecedent conditions and very large (+: 10 mm h⁻¹) or extreme (+++: 100 mm h⁻¹) event precipitation.

References

- Jasechko, S., Kirchner, J. W., Welker, J. M., and McDonnell, J. J.: Substantial proportion of global streamflow less than three months old, *Nat. Geosci.*, 9(2), 126-129, <https://doi.org/10.1038/NGEO2636>, 2016.
- Kellison, S. G. and London, R. L.: *Risk Models and Their Estimation*, Actex Publications, Winsted, USA, 2011.
- Kirchner, J. W.: Aggregation in environmental systems—Part 1: Seasonal tracer cycles quantify young water fractions, but not mean transit times, in spatially heterogeneous catchments, *Hydrol. Earth Syst. Sc.*, 20(1), 279–297, <https://doi.org/10.5194/hess-20-279-2016>, 2016.
- Rolski, T., Schmidli, H., Schmidt, V., and Teugels, J. L.: *Stochastic processes for insurance and finance*, 505, John Wiley & Sons, Chichester, England, 2009.